To the Graduate Council:

I am submitting herewith a thesis written by Celeste Geron Shibata entitled "Purification and Characterization of Fully Deuterated Yeast Phosphoglycerate Kinase." I have examined the final copy of this thesis for form and content and recommend that it be accepted in partial fulfillment of the requirements for the degree of Master of Science, with a major in Biochemistry.

Engin Serpersu

Engin H. Serpersu, Major Professor

We have read this thesis
and recommend its acceptance:

Elizabeth E. Howell

Accepted for the Council:

Lew Minkel

Associate Vice Chancellor
and Dean of the Graduate School

STATEMENT OF PERMISSION TO USE

In presenting this thesis in partial fulfillment of the requirements for a Master's degree at The University of Tennessee, Knoxville, I agree that the Library shall make it available to borrowers under the rules of the Library. Brief quotations from this thesis are allowable without special permission, provided that accurate acknowledgment of the source is made.

Permission for extensive quotation from or reproduction of this thesis may be granted by my major professor, or in his absence, by the Head of Interlibrary Services when, in the opinion of either, the proposed use of the material is for scholarly purposes. Any copying or use of the material in this thesis for financial gain shall not be allowed without my written permission.

Signature Celeste Y. Shibata

Date Dec. 2, 1992

PURIFICATION AND CHARACTERIZATION OF FULLY DEUTERATED YEAST PHOSPHOGLYCERATE KINASE

A Thesis

Presented for the

Master of Science

Degree

The University of Tennessee, Knoxville

Celeste Geron Shibata

December, 1992

Dedicated to my husband

John H. Shibata

and to my children

Sarah Elizabeth Askew

and

David Benjamin Askew

With thanks for your love and support

ACKNOWLEDGMENTS

I would like to express my appreciation to my advisor, Dr. Engin H. Serpersu, for his guidance in this project. I would also like to thank my committee members, Dr. Elizabeth Howell and Dr. Jorge Churchich, for their interest, encouragement, and for many helpful comments and suggestions.

Special thanks to Jay Gregory and Patti Kreke for the many long hours they spent teaching and helping me with the NMR. Thanks also to Jack Perry of Dr. Jeffrey Becker's laboratory who transformed our yeast strain 20B-12 with the multi-copy plasmid pCGY219. Jack also helped me get started culturing yeast and then provided patient answers to my endless questions. I would also like to thank Brenda Gerhardt who purified the normal enzyme used in many of the experiments and prepared phosphoglycerate and dehydrogenase.

Finally, I would like to thank my family, without whose patience and support my work would not have been possible.

ABSTRACT

Fully deuterated yeast phosphoglycerate kinase was purified from yeast strain 20B-12, using plasmid pCGY219 to overproduce the enzyme. The yeast cells were grown in D_2O with deuterated algal hydrolysate as a source of amino acids and deuterated ethanol as a carbon source. The enzyme was ascertained to be fully deuterated by comparison of its one-dimensional ^1H NMR spectrum with that of a matched sample of the normal enzyme. The deuterated enzyme was then characterized by kinetic and binding studies to determine that its properties were not significantly different from those of the normal enzyme, and that the deuterated enzyme would thus be suitable for further structural studies. The deuterated enzyme was found to have K_M values of 162 μM for MgATP and 168 μM for phosphoglycerate; these are in good agreement with the K_M values of the normal enzyme. The V_{max} value of the deuterated enzyme, 373 μmol/mg.min, is also in good agreement with that of the normal enzyme. In binding studies, all binding properties of the deuterated enzyme with regard to the catalytically relevant ternary complex are similar to those of the normal enzyme.

One- and two-dimensional NMR studies were done on the complex formed by PGK and a substrate analogue, 2′-deoxy-ATP, using both the normal and deuterated enzymes.

It was expected that the deuteration of the protein would allow the substrate resonances to be more clearly visible and less ambiguous than would be the case in studies of Mg-2'-dATP bound to the normal enzyme, and this was seen to be the case. It is hoped that further experiments of a more quantitative nature aimed at deriving bound MgATP conformation from NOE constraints will be possible using the system worked out in this research.

TABLE OF CONTENTS

LIST OF FIGURES

FIGURE PAGE

LIST OF TABLES

LIST OF ABBREVIATIONS

A_{260}	Absorbance at 260 nm
A_{280}	Absorbance at 280 nm
ADP	Adenosine 5′-diphosphate
ATP	Adenosine 5′-triphosphate
COSY	Correlation spectroscopy
2′-dATP	2′-deoxyadenosine 5′-triphosphate
DNAse	Deoxyribonuclease
dPGK	Deuterated phosphoglycerate kinase
DSS	3-(Trimethylsilyl) propane sulfonic acid
EDTA	Ethylenediaminetetraacetic acid
G3P	Glycerol-3-phosphate
NADH	Nicotinamide adenine dinucleotide (reduced form)
NMR	Nuclear magnetic resonance
N.P.	Null point
PGA	3-Phospho-D-glycerate
PGK	Phosphoglycerate kinase
PMSF	Phenylmethylsulfonyl fluoride
RNAse	Ribonuclease
SDS-PAGE	Sodium dodecyl sulfate polyacrylamide gel electrophoresis
Tris-HCl	Tris(hydroxymethyl)aminomethane hydrochloride
trp	tryptophan
YEPD	Yeast extract, peptone, dextrose medium

CHAPTER I

INTRODUCTION

Phosphoglycerate kinase (PGK) or ATP:3-phospho-D-glycerate 1-phosphotransferase (EC2.7.2.3) catalyzes the reversible conversion of ADP + 1,3-bisphosphoglycerate to ATP + 3-phosphoglycerate (1). As one of the two ATP-generating enzymes of the glycolytic pathway, PGK is crucial to the metabolism of all living organisms. It is, as Mori *et al.* put it, "among the oldest housekeeping enzymes in nature." (2)

PGK is a monomeric enzyme of molecular weight about 46,000. Study of the three-dimensional structure and catalytic mechanism of PGK has been a complex process because of the difficulty of crystallizing the enzyme in any complexes with its substrates. Early crystallographic studies of the yeast enzyme at 3.5 Å resolution (3) determined that the molecule is divided into two domains of about equal size connected by a central "hinge" or "waist" region. PGK crystals were soaked in Mg- and Mn-ADP and phosphoglycerate (PGA), and 5 Å resolution x-ray data were collected for these crystals. Changes in x-ray diffraction intensity were seen in the crystals soaked in nucleotide substrate, but no such density change was observed for the PGA-soaked crystals. A somewhat later study of the horse muscle

enzyme at 3.5 Å resolution produced more information, most of which is thought to be applicable to the yeast enzyme as well (4). This study found that the two domains of PGK correspond to the C-terminal and N-terminal regions; that the two domains are almost exactly the same size and that each is composed of a central β-sheet of six parallel strands surrounded by helices. It was also found that although there is a "waist" region (residues 186-189) that connects the two domains, no feature of secondary structure crosses from one domain to the other. The probable binding site for ATP was located in the C-terminal domain; however, no binding site for PGA was found. In addition, the binding site for ATP was in a location which would seem to be unsuitable for possible PGA binding, the nearest functional groups which could assist with PGA binding being around 10 Å away. The only probable site for PGA binding which could be deduced from side-chain locations was on the face of the N-terminal domain opposite the ATP binding site on the C-terminal domain. This region makes up a cavity or "binding cleft." If this were the correct binding site, the γ-phosphorus of ATP would be at least 10 Å away from the carboxyl group of PGA, making direct phosphoryl transfer impossible. Banks *et al.* suggest a hinge-bending conformational change upon substrate binding, bringing the two domains and substrates into closer

proximity for the catalysis to occur. Other evidence of a large conformational change during catalysis was also obtained from NMR studies (5) and low-angle X-ray scattering (6).

The amino acid sequence and three-dimensional structure of yeast PGK were further elucidated by Watson *et al.* (7). The effects of sulfate, used in the enzyme crystallization process, were recognized as interfering with the crystallization of substrate-bound enzyme; since sulfate can act as a competitive inhibitor of either substrate, it was thought that substrate binding sites could be already occupied by sulfate. An alternative suggestion was that PGA, the more difficult of the two substrates to crystallize with the enzyme, could already be present as a copurified contaminant, accounting for the identical structure of enzyme crystallized with and without PGA. The data obtained by Watson *et al.* led them to agree with the idea of domain movement at catalysis, and to assert that both MgATP and PGA must be bound to the enzyme in order for this hinge-bending conformational change to occur.

Mori *et al.* (2) studied the DNA sequence of six different PGKs (mouse, human, horse, yeast, and two trypanosomes) and found that the "binding cleft" identified by previous crystallographic studies was highly conserved. Although yeast and mammalian PGK is

only 65% homologous in primary sequence overall, the homology of this inner loop region is 94%. The structural feature of six β-sheets found in the ATP binding site is a typical feature of nucleotide binding sites in kinases and NAD- or NADH-dependent dehydrogenases.

In 1990 Harlos, Vas, and Blake were successful in crystallizing pig muscle PGK in the presence of PGA (8). The PGA binding site for this enzyme was located in the "basic patch" earlier identified as a putative PGA binding site. This is a cluster of basic residues in the N-terminal domain in the region opposite the ATP binding site. Previous mutagenesis studies had shown that two basic patch residues (His-62 and Arg-170) were involved in PGA binding (9). Harlos *et al.* state that their finding on the pig muscle enzyme-PGA complex are likely to be applicable to the yeast enzyme as well, basing their opinion upon the high degree of conservation found among different PGKs and the fact that all residues known to be involved in PGA binding in the pig muscle enzyme are conserved in all known PGK sequences including that of yeast (9). However, their placement of the PGA binding site disagrees with earlier suggestions of its location; thus, the PGA binding site for the yeast enzyme is not conclusively known.

CHAPTER II

PURIFICATION OF FULLY DEUTERATED YEAST PHOSPHOGLYCERATE KINASE

A. Introduction

Deuterium (^2H), discovered in 1932 by Urey, Brickwedde, and Murphy (10), is a heavy, nonradioactive isotope of hydrogen. It has an atomic mass of 2, and is found in nature as 0.015% of all hydrogen. Because hydrogen is such a universal component of all biological compounds, and because the ^1H and ^2H isotopes differ in chemical properties to such a great extent, the incorporation of deuterium into biological systems provides a means of studying many aspects of the physical properties of these systems. However, these same characteristics make the deuteration of living organisms a rather complicated process. As Katz and Crespi point out, a deuterated organism is an artifact, and may differ from its normal counterpart in morphology, cytochemistry, and biosynthetic capacity (11). The deuterium isotope effect, related to differences in zero-point vibrational energy between C-H and C-D bonds, may cause large differences in the rates of many crucial enzymatic reactions involving the breaking of these bonds; in addition, the changes in the properties of

hydrogen bonding may affect conformation and helix-coil transitions in many cell proteins. For many years, until about 1960, biological experiments with deuterium indicated that substantial levels of deuteration in an organism were incompatible with life (11).

The first organisms to be successfully produced in fully deuterated form were unicellular green algae (12). In principle, their growth in a deuterated medium was fairly straightforward, since algae are autotrophic and require only water (in this case D_2O), inorganic salts, and CO_2 for growth. However, exposure to D_2O had an adverse effect upon growth and reproduction of the algal cells, and full adaptation to growth in D_2O required time periods of 10 days to a month. Morphological changes were reported in adapting cells, such as the appearance of "monster" cells of very large size and abnormally high nucleic acid content (12). Once the adaptation phase was completed, however, fully deuterated algae could be cultured at a steady rate. This algae was useful in two ways: first, studies could be made of its own enzymes, proteins, and other cell components (13); and second, extracts prepared from it could be used as a nutrient medium for the cultivation of heterotrophic organisms such as yeast and bacteria in deuterated form. In addition to providing amino acids and some sugars as nutrients, the extracts made from

deuterated algae were found to supply a variety of vitamins and "nutritional factors" essential to the growth of heterotrophs in deuterated media (14).

Mohan and coworkers found that *S. cerevisiae* could be grown quite well in fully deuterated form using D_2O, inorganic salts, vitamin supplements, and deuterated glucose (15). This being the case, it seems reasonable to suppose that the glycolytic enzymes, such as phosphoglycerate kinase, would be produced in active form in the deuterated yeast. Thus, the purification of fully deuterated phosphoglycerate kinase from yeast grown in deuterated media would seem feasible. A fully deuterated enzyme, in which all protons would be replaced by deuterons, would be "invisible" in ^1H NMR and would enable one to carry out studies of enzyme-bound substrates without interference from the protein resonances.

B. **Experimental Procedures**

1. *Materials*

Saccharomyces cerevisiae strain 20B-12 and plasmid pCGY219 were obtained from Ronald Hitzeman of Genentech. Yeast nitrogen base and casein amino acids were obtained from Difco; glucose, adenine sulfate, uracil, inositol, pyridoxine, and thiamine were obtained from Sigma.

Deuterated algal hydrolysate, deuterated algal lyophilized cells, ^2HCl, NaO^2H, deuterated ethanol, ^2H_2O, and deuterated Tris were obtained from MSD Isotopes, Cambridge Isotope Laboratories, and Isotech.

All reagents used in protein purification were of the highest commercially available purity. Column chromatography was carried out using Sephacryl HR-200S resin; all column buffers were passed over Chelex 100 prior to use to remove any contaminating metals. A Filtron Omegacell stirred cell was used to concentrate column fractions containing protein. PGK activity was assayed spectrophotometrically using a Beckman DU-70 spectrophotometer. Rabbit muscle glyceraldehyde phosphate dehydrogenase used in PGK activity assays was obtained from Boehringer as an ammonium sulfate precipitate; ammonium sulfate was removed by dialysis against 2 mM Tris at pH 7.5. ATP (sodium salt), D- 3-phosphoglycerate (barium salt), and NADH were obtained from Sigma.

2. *Preparation of Deuterated Algal Hydrolysate*

Several preparations of deuterated PGK have been done in the course of this research. For some preparations, deuterated algal hydrolysate was purchased and required only neutralization and sterilization for use. For other preparations, deuterated algal

lyophilized cells were obtained. Cells were hydrolyzed in 5N ^{2}HCl at approximately 110°C with refluxing. The extract thus obtained was brought to pH 5.5 with 6N NaO^{2}H and filter sterilized. The optimal concentration of algal hydrolysate for yeast growth was determined by test cultures containing varying concentrations of algal hydrolysate. Concentrations of 5-8% were usually found to be optimal.

3. *Yeast Growth in Deuterated Medium*

S. cerevisiae strain 20B-12 was transformed with plasmid pCGY219, a multicopy plasmid which overproduces PGK to up to 30% of total cell protein. The yeast strain is a *trp 1* mutant, and the plasmid contains the *trp 1* gene; thus growth in medium lacking tryptophan is used to select for cells containing the plasmid. In both normal and deuterated media, the use of acid hydrolyzed protein assures the absence of tryptophan.

Initial yeast cultures were grown in medium containing 0.67% yeast nitrogen base without amino acids, 0.5% casein amino acids, 2% glucose, and 0.01 mg/ml adenine and uracil. This yeast was grown overnight, centrifuged, washed in sterile water, centrifuged again, and resuspended in sterile ^2H_2O. A quantity of this yeast culture adequate to give about 4 x 10^6 cells/ml was diluted into 25 ml of medium containing

^2H_2O, 0.67% yeast nitrogen base without amino acids, 5--8% deuterated algal hydrolysate, 2% deuterated ethanol, 0.01mg/ml adenine and uracil, and 0.5 mg/ml thiamine, pyrodoxine, and inositol. This culture was allowed to grow to about 7 x 10^7 cells/ml and was then diluted into a further 475 ml of deuterated medium. The growth of this culture was closely monitored to allow the cells to attain their maximum density while still being harvested in the exponential growth phase. Cells were harvested by centrifugation, washed in sterile water, recentrifuged, and frozen at -80°C.

4. *Purification of Fully Deuterated PGK*

The procedure used for the purification of deuterated PGK was essentially that described by Scopes, with modifications based upon recent work using a PGK overexpression vector by Minard *et al.* (16), (17). Other adaptations of these procedures were made to accommodate our conditions of the small-scale preparation necessitated by the use of deuterated medium.

Frozen deuterated yeast cells were thawed and then refrozen with dry ice and thawed twice more. The thawed cells were placed in a lysis solution of volume equal to that of the cells, containing 0.5M ammonia, 1 mg/ml EDTA, and 1mM PMSF. The cells were stirred in this solution at room temperature for several hours and then allowed to

sit overnight at room temperature without stirring. Stirring was restarted and sufficient 0.5M lactic acid was added to bring the pH to approximately 7.5. This solution was centrifuged at 30,000 x *g* for one hour and the pellet discarded. 1 mg solid protamine sulfate per ml of supernatant was added to precipitate contaminating nucleic acids. This solution was stirred for 30 minutes and then centrifuged at 20,000 x *g* for one hour. The resulting pellet was again discarded. 15 μg DNAse and 20 μg RNAse per ml of supernatant was added and allowed to incubate for 15 minutes at room temperature. At the end of the incubation period, 30 g ammonium sulfate per 100 ml supernatant was added over 15 minutes, the solution was stirred for a further 30 minutes and centrifuged at 20,000 x *g* for 15 minutes, and the pellet was discarded. A second addition of ammonium sulfate (13 g/100 ml supernatant) was made as above and the solution centrifuged. The supernatant from this step was treated with 5M ammonium lactate, pH 3.5, to bring the pH of the supernatant to 4.3, resulting in the precipitation of the PGK. The solution was centrifuged as above and the pellet was dissolved in 1 ml of either 10 mM Tris-HCl, pH 7.5, or 2 mM deuterated Tris-^{2}HCl, pH 7.5. This solution was loaded onto a Sephacryl HR-200S column (0.9 cm x 95 cm). The column was equilibrated and run in either 10 mM Tris-HCl, pH 7.5, or 2 mM deuterated Tris-^{2}HCl, pH 7.5.

Fractions of 1.5 ml were collected and assayed for protein content and PGK activity.

The protein content of the column fractions was determined spectrophotometrically using an extinction coefficient $A_{280\,nm}$ = 0.5 $mg^{-1}.ml.cm^{-1}$ (18). PGK activity was assayed using a coupled-enzyme system with glyceraldehyde phosphate dehydrogenase as the coupling enzyme (18). Decrease in A_{340} was measured as NADH was oxidized in the assay reaction. The assay solution contained 50 mM Tris-HCl, pH 7.5, 100 mM NaCl, 0.2 mM NADH, 4 mM ATP, 5 mM $MgCl_2$, and 7 mM 3-Phosphoglycerate. At least 150 μg dehydrogenase was used per assay. $A_{280/260}$ of fractions containing PGK activity was also determined; ratios $\geq$ 1.5 indicate an acceptably low level of contaminating nucleotides. Purity of the enzyme was ascertained by SDS-PAGE. Fractions containing the enzyme were pooled, concentrated, and stored at -80 °C for further use in kinetic or NMR studies. The enzyme was found to be fully deuterated by comparison of its ^1H NMR spectrum with that of normal PGK.

C. **Results and Discussion**

Figure 1* shows a denaturing SDS-polyacrylamide gel of cell lysates prepared from four sources. Lane A is pure PGK obtained from Boehringer. Lane B is lysate from the untransformed yeast strain 20B-12 grown in normal YEPD medium. Lane C is lysate from yeast strain 20B-12 transformed with plasmid pCGY219 and grown in the casein amino acid/glucose medium described above. Lane D is lysate from the same transformed yeast strain grown in normal (undeuterated) algal hydrolysate/ethanol medium. Lane E is lysate from the same transformed yeast strain grown in deuterated algal hydrolysate/deuterated ethanol medium. This gel demonstrates that the plasmid does cause the yeast strain to overproduce PGK, since the heavy protein band which migrates to the same position as the PGK standard in the lanes containing transformed yeast lysates is absent in the untransformed yeast lysate. The gel also shows that PGK is still overproduced in the cells grown in deuterated medium. The cultures used to prepare these lysates were grown for

---

* All tables and figures may be found in the Appendix.

the same amount of time; since the yeast grows more slowly in deuterated medium (*vide infra*), less protein was produced, but PGK still appears as a proportionately heavy band in this lane.

Figure 2 shows a typical plot of test cultures grown to ascertain the optimal concentration of deuterated algal hydrolysate prepared from lyophilized algal cells. The -fold increase in cell concentration after 50 hours growth is plotted against the percentage of hydrolysate in the medium; in this case optimal growth was obtained at about 4.5%. The sharp decline in cell growth at higher concentrations of hydrolysate may indicate the presence of some unknown toxic compounds. This would seem likely since the hydrolysate is a crude mixture of all algal cell components. At any rate, the plot demonstrates that more nutrient solution is not necessarily better, and that each preparation of hydrolysate must be individually tested.

Figure 3 shows growth curves of yeast strain 20B-12 transformed with plasmid pCGY219, grown under three different conditions: in casein amino acid/glucose medium, in normal algal hydrolysate/ethanol medium, and in deuterated algal hydrolysate/deuterated ethanol medium. In each of the three media, the yeast attains a maximal concentration of about 2×10^8 cells/ml, but the rate of growth is markedly slower in the deuterated

medium. Each culture was started at approximately the same cell concentration (about 5.5 x 10^6 cells/ml); the culture grown in glucose medium attained its maximal concentration in about 15 hours, the culture grown in normal algal hydrolysate in about 30 hours, and the culture grown in deuterated algal hydrolysate in about 80 hours. The somewhat slower growth rate of the culture in normal algal hydrolysate may be attributed to the use of ethanol rather than glucose as a carbon source; however, in some cultures grown in this medium the growth rate was much closer to that of the cells grown in glucose. The slow growth rate in deuterated medium is unsurprising when one considers the many changes in cell chemistry and biosynthetic capabilities that may be brought about by the incorporation of deuterium into the organisms. The deuterated cells, however, when viewed under a phase-contrast microscope, appeared similar to normal cells in size and visible morphology; thus it is reasonable to suppose that despite the slow rate of growth, the deuterated cells were capable of carrying on the processes necessary for life and health.

Figure 4 shows several typical growth curves of deuterated yeast cultures grown for PGK preparations. Although the time required for maximal growth is similar from one culture to another, each culture was watched carefully in order to obtain the largest possible

quantity of healthy cells. It was sometimes found that if cell growth were slowing down while concentration was still fairly low, the addition of further deuterated ethanol to the culture medium would allow growth to continue at a good rate.

Figure 5 shows a denaturing SDS-polyacrylamide gel of samples taken from each step of the PGK purification procedure. Lane A is normal PGK purified in our laboratory; this purification included a further step of affinity chromatography which was omitted from the deuterated purification procedure because it entailed a large loss of active enzyme. Lane B shows a sample of the original cell extract after the addition of protamine sulfate. Lanes C and D show the supernatant and pellet, respectively, of the first ammonium sulfate precipitation. One may see that almost no PGK precipitated at this concentration of ammonium sulfate but that many other proteins were removed. Lanes E and F show the supernatant and pellet of the second ammonium sulfate precipitation. A larger quantity of PGK is precipitated along with other proteins in this step; active enzyme from this fraction could be further purified by ion-exchange chromatography and gel filtration, and this fraction of each purification has been saved frozen at -80°C. Lane G shows the pellet which resulted from lowering the pH of the previous

supernatant to 4.3. Virtually all the PGK was precipitated at this step. Lane H shows a sample of the fraction applied to the Sephacryl HR200-S column; Lanes I, J, and K show column fractions containing deuterated PGK. These fractions were later pooled and concentrated for further use.

Table 1 shows the purification data from the PGK preparation for which the gel was shown in Figure 5. Each protein purification is, of course, slightly different both in the quantity of enzyme produced and in the relative loss of enzyme activity at the various steps of the process; however, this example may be considered typical. The apparent increase in total activity after the first ammonium sulfate precipitation may be attributed to reasonable experimental error in the assay procedure since the assay requires large dilutions of the enzyme solution. There is a much larger discrepancy between the apparently small quantity of activity recovered after the pH of the ammonium sulfate supernatant was dropped and the much larger activity found in the fractions taken from the Sephacryl column. It is possible that some of the PGK may have become partially unfolded as the pH was decreased, and have refolded to an active conformation when it was placed in buffer at pH 7.5 prior to being loaded onto the column.

Figure 6 shows the elution profile of deuterated PGK from the Sephacryl HR-200S column. It may be seen that the large protein peak and the enzyme activity coincide, and that there is a smaller peak, fairly well separated from the active enzyme. Samples from these fractions were analyzed by denaturing SDS-PAGE and were found to contain little or no protein; they are thought to contain contaminating nucleic acids.

Table 2 shows a detailed analysis of the Sephacryl fractions. A total of 30.18 mg deuterated PGK was obtained, with an average specific activity of 430. Different specific activities for the enzyme have been reported in the literature (16), (19), based upon different assay conditions. The specific activity of deuterated PGK represents 95% and 80% with respect to commerical (450 units/mg) and laboratory prepared enzyme (550 units/mg).

Figure 7 shows the ^{1}H NMR spectra of normal PGK (A) and deuterated PGK (B). These spectra were obtained from samples of identical concentration, and the same number of scans was accumulated for each spectrum. The only difference in acquisition parameters between the two spectra is that it was possible to set the receiver gain 10-fold higher for the deuterated sample, which, of course, amplifies the residual proton signals of the deuterated enzyme. In spite of this amplification,

examination of the spectra shown in Figure 7 indicates that a very high level of deuteration has been achieved.

Chapter III

KINETIC STUDIES

A. Introduction

The kinetic behavior of phosphoglycerate kinase has been extensively analyzed, but the mechanistic picture which emerges is a complex and confusing one. In 1964, Larsson-Raznikiewicz presented evidence that the activating metal ion (Mg^{2+}) forms a complex with ATP^{4-} which is the true substrate of the enzyme according to the following scheme:

$$Mg^{2+} + ATP^{4-} \rightleftharpoons MgATP^{2-}$$

$$MgATP^{2-} + PGK \rightleftharpoons PGK\text{-}MgATP$$

She also observed that high concentrations of either free Mg^{2+} or ATP^{4-} inhibit enzyme activity (20). Metal-ion specificity of the enzyme has been examined, and it was found that $MgATP^{2-}$ can be replaced with $MnATP^{2-}$, which is 90% as good a substrate; by $CaATP^{2-}$, $ZnATP^{2-}$, and $CoATP^{2-}$, which are 70% as good substrates, and by $NiATP^{2-}$, which is 15% as good a substrate (21). Further work demonstrated that neither $MgATP^{2-}$ nor 3-phosphoglycerate affects the binding of the other substrate to the enzyme; studies of varied concentration of each substrate at fixed concentrations of the other gave plots which showed identical K_M values for each fixed concentration. In

addition, at high Mg^{2+} concentrations, double-reciprocal plots for both substrates were found to become nonlinear, exhibiting downward curvature at high substrate concentrations. It was suggested that this behavior could be explained by the presence of more than one binding site for each substrate (22). Larsson-Raznikiewicz originally proposed that there could be two catalytically active sites on the enzyme molecule, and that the second site's conformation is changed sufficiently at high Mg^{2+} concentrations to give the nonlinear plots that were seen; alternatively, she suggested that there could be one catalytic site and another regulatory binding site. In further work concerning product inhibition studies (23), (24), it was found that there are two binding sites for each substrate but only one catalytic center per enzyme molecule. The active site corresponds to the "high-affinity" site for each substrate, while the "low-affinity" site serves a regulatory function. Reaction products, 1,3-bisphosphoglycerate and adenosine diphosphate, were found to bind preferentially to this regulatory site.

Further perplexities are introduced into the study of PGK kinetics by the presence of both activation and inhibition by a variety of monovalent and divalent ions. It was found that salts of monovalent cations activate

the enzyme at low concentrations (up to about 100 mM) and inhibit activity at higher concentrations (25). These effects were also observed for divalent anions, sulfate being the most extensively studied. Sulfate was found to activate the enzyme at low concentrations; optimal sulfate concentration for activation was dependent upon substrate concentration but ranged from 5-40 mM. At higher sulfate concentrations, the anion acted as a competitive inhibitor of both substrates. These results led to the proposal that there is a specific sulfate binding site on the enzyme outside the catalytic center, and that there may be separate anion binding sites for the activating and inhibiting sulfates (26).

An exhaustive re-examination of yeast PGK kinetics, covering 1000-fold range in substrate concentrations, using ten different assay systems employing a variety of coupling enzymes, and utilizing fluorimetric and stopped-flow assay procedures, was carried out by Scopes (27). Further work was done specifically to investigate ligand binding to the enzyme (28). Scopes' studies confirmed the anomalous nonlinear plots for each substrate and the effects of sulfate at low and high concentrations. Evidence was found for two binding sites for each nucleotide substrate (i.e. MgATP and MgADP), but for only one binding site for the

phosphoglycerate substrates (i.e. 3-phosphoglycerate and 1,3-bisphosphoglycerate). Scopes interprets the kinetic data as supporting a rapid-equilibrium random mechanism in which the binding of either substrate does not affect the other. He accounts for the observed substrate activation by 3-phosphoglycerate despite there being only one binding site for that substrate by proposing a two-step dissociation process for the 1,3-bisphosphoglycerate product as the rate-limiting step of the PGK reaction.

B. **Experimental Procedures**

1. *Materials*

Rabbit muscle glyceraldehyde phosphate dehydrogenase was obtained from Boehringer as an ammonium sulfate precipitate. Ammonium sulfate was removed by dialysis against 2 mM Tris-HCl, pH 7.5. At least 100 μg of dehydrogenase was used per assay, and the concentration used was ascertained to be non-limiting for each experiment. 5′-adenosine triphosphate and 2′-deoxyadenosine 5′-triphosphate were obtained from Sigma as the disodium salts. Before use they were put over Chelex-100 to remove any contaminating metal ions; their concentration was determined spectrophotometrically using a molar extinction coefficient for the adenine ring of ϵ_{260} = 15,400 M^{-1} cm^{-1}. D-3-phosphoglycerate and D,L-

glycerol-3-phosphate were obtained from Sigma. D-3-phosphoglycerate was obtained as the barium salt; before use it was dissolved in HCl, treated with Na_2SO_4 to precipitate the barium, and put over a Chelex-100 column to remove trace metals. All other reagents used in the assays were of the highest commercially available purity.

2. *Assay Method*

Kinetic measurements were made using a coupled enzyme system with glyceraldehyde phosphate dehydrogenase as the coupling enzyme. The enzymatic reactions are measured in the direction of gluconeogenesis:

$$\text{3-Phosphoglycerate} + \text{ATP} \xrightleftharpoons{\text{PGK}} \text{1,3-Bisphosphoglycerate} + \text{ADP}$$

$$\text{1,3-Bisphosphoglycerate} + \text{NADH} + \text{H}^+ \xrightleftharpoons{\text{GAPDH}} \text{Glyceraldehyde 3-phosphate} + \text{NAD}^+ + \text{P}_i$$

Since one molecule of NADH is reduced for each molecule of substrate utilized, the rate of the reaction is measured as the rate of disappearance of NADH, using a molar extinction coefficient for NADH of $\epsilon_{340} = 6220\ M^{-1}\ cm^{-1}$. The measurements were carried out in a 1-cm quartz cuvette using a Beckman DU-70 spectrophotometer.

All reactions were done in a volume of one milliliter. Each reagent was mixed separately in the cuvette for each assay. All assays used 150 mM NaCl, 50 mM Tris-HCl, pH 7.5, and 0.2 mM NADH. The concentration of MgATP was calculated using a K_D of 80 μM; free ATP and $MgCl_2$ were included in the reaction mixtures with $MgCl_2$ at a 1 mM excess of ATP. Concentrations of substrates were varied according to the individual experiments, as explained below. Approximately 0.25 μg of normal PGK or 0.69 μg of deuterated PGK was used for each assay. All reactions were carried out at 25°C. Initial rates were calculated based upon the linear portion of the ΔA_{340} *vs* time curve. The data obtained were fit to the Michaelis-Menten equation by use of the Enzfitter computer program.

3. *Kinetics of Deuterated Phosphoglycerate Kinase*

Kinetic studies were carried out with the deuterated enzyme to determine the V_{max} and the K_M for each of the two substrates. In each experiment, one substrate was varied at four subsaturating concentrations of the other to give four curves. K_M of the enzyme for the varied substrate may be determined from the x-intercept of Lineweaver-Burk plots of these curves; V_{max} may be obtained by plotting $1/V_{max\ apparent}$ for each curve *vs* the inverse of the concentration of the constant substrate for that curve.

With 3-phosphoglycerate as the variable substrate, PGA concentration was varied between 0.10 mM and 5.15 mM at MgATP concentrations of 0.089 mM, 0.18 mM, 0.42 mM, and 1.21 mM. A second experiment was done with PGA as the variable substrate in the presence of 10 mM Na_2SO_4; PGA was varied between 0.10 mM and 5.15 mM at MgATP concentrations of 0.087 mM, 0.21 mM, and 0.44 mM. With MgATP as the variable substrate, MgATP concentration was varied between 0.047 mM and 1.21 mM at PGA concentrations of 0.31 mM, 0.52 mM, 1.0 mM, and 5.15 mM.

4. *Kinetics of Normal Phosphoglycerate Kinase*

A control experiment was done using normal PGK to determine its V_{max} and its K_M for each substrate at our conditions. Each substrate was varied at saturating concentration of the other. Using MgATP as the variable substrate, MgATP concentration was varied between 0.048 mM and 2.41 mM at PGA concentration of 6.87 mM. With PGA as the variable substrate, PGA concentration was varied between 0.098 mM and 4.91 mM at MgATP concentration of 4.11 mM.

5. *Kinetics of Normal PGK With Substrate Analogues*

Experiments were done using normal PGK and the substrate analogues glycerol-3-phosphate (G3P) and 2′-deoxyadenosine 5′-triphosphate (2′-dATP). Inhibition

kinetics were done with glycerol-3-phosphate; PGA concentration was varied at a constant subsaturating concentration of MgATP in the presence of three different concentrations of glycerol-3-phosphate. PGA concentration was varied between 0.12 mM and 1.08 mM at MgATP concentration of 0.25 mM and glycerol-3-phosphate concentrations of 0.42 mM, 1.56 mM, and 3.64 mM. The slope of each of these curves was plotted against the glycerol-3-phosphate concentration to give the K_i. Mg-2′-dATP is a substrate of PGK which gives slower rates than Mg-ATP; its concentration was varied at saturating PGA concentration to give V_{max} and K_M of the enzyme for this substrate. Mg-2′-dATP was varied between 0.029 mM and 1.17 at PGA concentration of 7.37 mM.

C. Results and Discussion

The results of these experiments are summarized in Table 3.

Figure 8 shows Lineweaver-Burk plots of deuterated PGK kinetics with MgATP as the variable substrate. The y-intercept of each curve is $1/V_{max\ apparent}$ for that curve; the inset plots are secondary plots of $1/V_{max\ apparent}$ *vs* 1/[S] for each curve. Just as the y-intercept of each curve in the primary plot represents the extrapolation of velocity to infinite concentration of the variable

substrate at a given concentration of the fixed substrate, so the y-intercept of the secondary plot is a further extrapolation to infinite concentration of the fixed substrate. This y-intercept gives the inverse of the true V_{max}. K_M may be determined directly from the primary plot; $-1/K_M$ is the x-intercept of each curve, and the value for K_M given in Table 3 is the average of the four values found in the plot.

Figure 9 is a Lineweaver-Burk plot of normal PGK kinetics at pH 7.5 with MgATP as the variable substrate. Extensive work on normal PGK kinetics at pH 5.9 has been done by others in this laboratory (29), and data have been reported in the literature on normal PGK kinetics at pH 7.5-7.8 (20-23, 27). The purpose of experiments with normal PGK at pH 7.5 is only to ascertain whether the kinetic values obtained for the deuterated enzyme are in reasonable agreement with those obtained for the normal enzyme. It thus did not seem necessary to undertake as detailed a study of the normal enzyme kinetics as that done for the deuterated enzyme. It is rather difficult to compare one's kinetic values with those found in the literature, because virtually all PGK kinetics have been done in the presence of 20-50 mM sulfate, which is known to affect activity. However, results obtained from these experiments are in good agreement with those reported in two papers which examined normal PGK kinetics in the

absence of sulfate (26), (30). K_M^{MgATP} is reported by Mas *et al.* as 0.16 mM (30), and by Larsson-Raznikiewicz as 0.425 mM (26). In these experiments, K_M^{MgATP} for the normal enzyme was found to be 0.409 mM, and for the deuterated enzyme to be 0.162 mM. Thus the agreement between the K_M values of the deuterated and normal enzyme is reasonable.

Figure 10 shows Lineweaver-Burk plots of deuterated PGK kinetics using PGA as the variable substrate. These plots show downward curvature at high substrate levels, as observed in the kinetic studies of normal PGK, which is indicative of a second, "low-affinity" binding site for the substrate (22, 27). The curves shown in the primary plot were fitted by the Enzfitter program to the linear portion of each set of data, representing the high affinity site. The top inset plot shows curves fit by the Enzfitter program to the low affinity portion of each set of data. V_{max} values from these curves were plotted against 1/[MgATP] in the lower inset plot to give V_{max}, as explained for Figure 8. The V_{max} value calculated from the data using PGA as the variable substrate (371 ± 59 μmol/min.mg) is nearly identical to that calculated using MgATP as the variable substrate (373 ± 60 μmol/min.mg).

Figure 11 is a Lineweaver-Burk plot of normal PGK kinetics at pH 7.5 using PGA as the variable substrate at saturating MgATP concentration. As was the case with the

deuterated enzyme, the plot shows downward curvature at high PGA levels. The low affinity region was used to calculate V_{max}, and K_M values for both high- and low-affinity sites were calculated. V_{max} for normal PGK using PGA as the variable substrate (588 ± 29 μmol/min.mg) is in good agreement with the value obtained using MgATP as the variable substrate (623 ± 16 μmol/min.mg). K_M^{PGA} at pH 7.5-7.8 is reported by Larsson-Raznikiewicz as 0.188 mM (26), and by Mas *et al.* as 0.19 mM (30). These experiments found the high-affinity K_M^{PGA} to be 0.152 mM for normal PGK and 0.168 mM for deuterated PGK.

V_{max} values for the deuterated enzyme (av. 372 μmol/min.mg) are somewhat lower than those for the normal enzyme (av. 606 μmol/min.mg); it has also been observed that specific activities of deuterated PGK prepared in this laboratory are somewhat lower than those of normal PGK likewise prepared in this laboratory. This lower velocity cannot be attributed to the kinetic isotope effect, as no C-H (or C-D) bond is broken by the reaction catalyzed by PGK. It is possible that changes in the hydrogen bonding properties of the deuterated enzyme may account for the decrease in activity.

Figure 12 shows kinetics of deuterated PGK with PGA as the variable substrate in the presence of 10 mM Na_2SO_4. The effects of sulfate upon PGK are very complex: it activates at low concentrations and inhibits at higher

concentrations, and the activating/inhibiting concentrations vary with substrate concentration. In addition, sulfate eliminates the downward curvature of kinetic plots at high substrate concentrations (27). The present experiment is not detailed enough to elucidate the effect of sulfate upon the deuterated enzyme; it is intended as a qualitative demonstration that, like the normal enzyme, deuterated PGK is affected by the presence of sulfate. K_M^{PGA} is much higher in the presence of sulfate (385 μM) than in its absence (168 μM), and V_{max} is reduced (199 μmol/min.mg from 372 μmol/min.mg without sulfate). In addition, the downward curvature indicating activation at high PGA concentration has been eliminated in these plots.

In addition to these experiments intended to demonstrate the relationship between deuterated PGK and its normal counterpart, two kinetic experiments were done with the normal enzyme to verify the usefulness for future NMR experiments of two substrate analogues, 2′-deoxyadenosine 5′-triphosphate (2′-dATP) and glycerol-3-phosphate (G3P).

Glycerol-3-phosphate is reported in the literature to be a competitive inhibitor of pig muscle phosphoglycerate kinase against 3-phosphoglycerate (31). Figure 13 shows the results of inhibition kinetics of normal yeast PGK in the presence of G3P. The

slope of each curve is plotted against the G3P concentration to give a K_i for D-G3P of 249 μM. This agrees well with the K_i value of 350 μM reported by Vas *et al.* for D-G3P with the pig muscle enzyme. Since G3P is not a substrate of PGK, it can be used with MgATP to form ternary enzyme-substrate complexes for NMR studies.

2'deoxyadenosine 5'triphosphate will be used in both binary and ternary complexes with PGK and G3P for NMR studies because the 2' and 2" protons of its ribose ring resonate at approximately 2.5 and 2.8 ppm respectively; in contrast, the 2' proton of the ribose ring of ATP is obscured by the $^{2}HO^{1}H$ signal. Since 2'-dATP is a substrate of PGK, it was necessary to ascertain its kinetic values. Figure 14 shows a Lineweaver-Burk plot of normal PGK using 2'-dATP as the variable substrate at saturating PGA concentration. Kinetic values obtained are as reported in Table 3.

CHAPTER IV

WATER PROTON RELAXATION RATE STUDIES

A. Introduction

The measurement of the longitudinal relaxation rates ($1/T_1$) of water protons in the coordination sphere of paramagnetic metal ions in enzyme-metal-substrate complexes can provide a great deal of thermodynamic and structural information about the environment of the metal in these complexes (32). Stoichiometry and dissociation constants for binary and ternary enzyme-substrate complexes may be determined by this method.

Proton relaxation rate studies are based upon the effects of enhancement observed when a water proton is immobilized upon a macromolecule (in this case, an enzyme molecule), or co-ordinated in the inner sphere of a paramagnetic ion, or both. Protons undergo longitudinal relaxation as they exchange magnetic energy with the lattice. In order for this exchange of energy to occur, the lattice or magnetic environment must be capable of absorbing energy at the Larmor frequency of the proton, that is, the frequency at which the magnetic moments of the nuclei precess about the applied magnetic field. In the case of water protons, exchange of magnetic energy leading to relaxation occurs at a slow rate because of

the molecular tumbling (rotation) of the water molecules. Tumbling is a very rapid process for small molecules such as water (about 10^{11} sec^{-1}); the Larmor frequency of protons at the magnetic field strength used in these experiments is 2.43×10^7 sec^{-1}. Because of the large difference in frequency between these two processes, energy exchange is inefficient and relaxation is slow for water protons in an environment of aqueous diamagnetic salts and buffers. However, when a water molecule is bound to a macromolecule, it interacts with the lattice at the slower tumbling frequency of the macromolecule (about 10^8 sec^{-1}), which is much closer to the Larmor frequency of the proton; thus transfer of energy becomes efficient and relaxation can occur at a faster rate. The relaxation rate of a water proton in a molecule co-ordinated to a paramagnetic ion is further enhanced by the much stronger magnetic character of the ion.

The experimentally measured value of observed enhancement in proton relaxation rates is called ϵ^* and is defined as the enhancement of the paramagnetic relaxation rate in the presence of a macromolecule. ϵ^* is determined as a ratio of the paramagnetic effect on the relaxation rates of water protons in the presence and absence of the macromolecule:

* indicates the presence of the macromolecule (in this case, the enzyme phosphoglycerate kinase).

$$\epsilon^* = \frac{1/T_{1p}^*}{1/T_{1p}} = \frac{1/T_{1obs}^* - 1/T_{1d}^*}{1/T_{1obs} - 1/T_{1d}}$$

$\mathbf{1/T_{1p}}$ is the contribution of the paramagnetic ion (in this case, Mn^{2+}) to the relaxation rate.

$\mathbf{1/T_{1d}}$ is the diamagnetic relaxation rate, or the relaxation rate in the absence of a paramagnetic ion.

$\mathbf{1/T_{1obs}}$ is the observed relaxation rate in the presence of the paramagnet.

B. **Experimental Procedures**

1. *Materials*

Normal and deuterated phosphoglycerate kinase were purified from *S. cerevisiae* in this laboratory as described in Chapter II. Enzyme activity was assayed (as described in Chapter II) at the beginning and end of each experiment. All experiments were done in 50-75 mM Tris-HCl, pH 7.5, with 100 mM NaCl. Nucleotide substrate solutions were prepared as described in Chapter III. $MnCl_2$ solutions were prepared from ultrapure $MnCl_2$ obtained from Johnson-Matthew. Titrations were carried out at 24.3 MHz with a Seimco pulsed NMR instrument using the 180°-τ-90° pulse sequence of Carr and Purcell

(33). Null points (N.P.) obtained by this method were used to calculate observed relaxation rates ($1/T_{1obs}$):

$$1/T_{1obs} = \frac{\ln 2}{N.P.}$$

Titration volumes were from 40-75 μl and were contained in acetate Beckman Airfuge tubes.

2. *Binary Complex Studies*

In any solution, ϵ^* is a weighted average of the enhancements due to each species of manganese complex, and there is a characteristic enhancement value (ϵ) associated with each manganese species (34). In the binary enzyme-metal complex PGK-Mn^{2+}, ϵ^* may be expressed as:

$$\epsilon^* = \left(\frac{[Mn]_f}{[Mn]_T}\right)\epsilon_f + \left(\frac{[Mn]_b}{[Mn]_T}\right)\epsilon_b$$

ϵ_f is the enhancement due to free manganese, and is **1** by definition.

ϵ_b is the enhancement due to manganese bound in the binary complex with the enzyme.

ϵ_b can be obtained graphically. One titrates manganese solutions at various concentrations with the enzyme.

Double-reciprocal plots of $1/\epsilon^*$ *vs* 1/[PGK] are made, and the y-intercepts, which are the extrapolations of enhancement to infinite enzyme concentration at each manganese concentration used, give ϵ_b. Once ϵ_b has been determined, bound and free Mn^{2+} concentrations can be calculated by a re-arrangement of the above equation:

$$[Mn]_f = [Mn]_T \left(\frac{\epsilon^* - \epsilon_b}{1 - \epsilon_b} \right)$$

Free and bound manganese concentrations can be used to obtain a Scatchard plot showing $[Mn]_b/[PGK][Mn]_f$ *vs* $[Mn]_b/[PGK]$, which will indicate the number of Mn^{2+} binding sites per enzyme molecule and the K_D of the PGK-Mn^{2+} complex.

For binding studies with normal PGK, Mn^{2+} concentrations of 50.3 μM, 75.3 μM, 150.5 μM, and 224.7 μM were used. PGK was titrated into these solutions up to a concentration of 513 μM. Additional points using $[Mn^{2+}]$ of 0.301 mM-3.5 mM at a PGK concentration of 272.5 μM were obtained to complete data required for the Scatchard plot. For binding studies with deuterated PGK, Mn^{2+} concentration of 150.5 μM was used, titrated with deuterated PGK up to a concentration of 311 μM. Additional points with a deuterated PGK concentration of 249 μM and Mn^{2+} concentrations from 1.3 mM-3.1 mM were

obtained to complete data required for the Scatchard plot (See Figures 15-16).

3. *Ternary Complex Studies*

The analysis of the ternary enzyme-metal-substrate complex (in this case, PGK-ATP-Mn^{2+}) is similar to that of the binary complex, but the additional component increases the complexity of the calculations which must be done. ϵ^* is again presented as the weighted average of the enhancements due to all Mn^{2+} species present in the complex:

$$\epsilon^* = \left(\frac{[Mn]_f}{[Mn]_T}\right)\epsilon_f + \left(\frac{[PGK\text{-}Mn]}{[Mn]_T}\right)\epsilon_b + \left(\frac{[ATP\text{-}Mn]}{[Mn]_T}\right)\epsilon_a + \left(\frac{[PGK\text{-}ATP\text{-}Mn]}{[Mn]_T}\right)\epsilon_T$$

ϵ_a is the enhancement due to manganese bound in a binary complex with ATP.

ϵ_T is the enhancement due to manganese bound in the ternary complex with PGK and ATP.

ϵ_a is available from the literature (35) or it can easily be determined by binary titrations; it is necessary to obtain ϵ_T graphically. One first titrates ATP into PGK-Mn^{2+} at a fixed Mn^{2+} concentration for several PGK concentrations. Double-reciprocal plots of $1/\epsilon^*$ *vs* 1/[ATP] are done, extrapolating enhancement to infinite substrate concentration for each enzyme concentration. Each extrapolated enhancement is called

ϵ_c^*. A secondary plot is made of $1/\epsilon_c^*$ *vs* 1/[PGK]; this extrapolates enhancement at infinite substrate concentration to infinite enzyme concentration and thus gives ϵ_T.

One may also obtain ϵ_T and additional information from a titration of substrate (ATP) into PGK-Mn^{2+} at different Mn^{2+} concentrations. One plots ϵ^* *vs* [ATP] and fits the data obtained to an equation based upon the equilibria which define the ternary system: (36), (37)

$$K_D = \frac{[PGK]\,[Mn]}{[PGK\text{-}Mn]}$$

$$K_1 = \frac{[ATP]\,[Mn]}{[ATP\text{-}Mn]}$$

$$K_2 = \frac{[PGK]\,[ATP\text{-}Mn]}{[PGK\text{-}ATP\text{-}Mn]}$$

$$K_3 = \frac{[PGK\text{-}Mn]\,[ATP]}{PGK\text{-}ATP\text{-}Mn]}$$

$$K_{A'} = \frac{[PGK\text{-}ATP]\,[Mn]}{[PGK\text{-}ATP\text{-}Mn]}$$

$$K_S = \frac{[PGK]\,[ATP]}{[PGK\text{-}ATP]}$$

From these equilibrium relationships it may be seen that:

$$K_1 K_2 = K_3 K_D = K_{A'} K_S$$

By inserting equilibrium constants into the equation defining ϵ* above, one may obtain the following relationship:

Fitting the data to this equation is an iterative process using the computer program EPS7A (32),(37),(38). One

$$\epsilon^* = \frac{\frac{K_D K_3}{[PGK]\,[ATP]} + \frac{K_2}{[PGK]}\epsilon_a + \frac{K_3}{[ATP]}\epsilon_b + \epsilon_T}{\frac{K_D K_3}{[PGK]\,[ATP]} + \frac{K_2}{[PGK]} + \frac{K_3}{[ATP]} + 1}$$

inserts dissociation constants together with ϵ_b and ϵ_a values and obtains fitted values for the other constants and ϵ_T. Based on the given dissociation constants, the computer program determines the remaining constants and fits the values into the equation given above by incrementing the K_S value. The fit involves the determination of the contribution of each species to the observed ϵ^* based on its concentration and known ϵ_a and ϵ_b values for the binary complexes. Thus one obtains ϵ_T for each titration curve. Such fittings of multiple experiments with different enzyme-substrate ratios allow one to compare the resulting ϵ_T values, since ϵ_T should be constant for a given ternary complex.

ϵ_T titrations were done with normal PGK using 50.3 μM Mn^{2+}, PGK concentrations of 131.7 μM, 199.3 μM, 313.2 μM, 398.7 μM, and 512.6 μM, and ATP concentrations up to 470 μM. These titrations were not done with deuterated PGK because the quantity of enzyme required was prohibitive.

Ternary complex (PGK-ATP-Mn^{2+}) titrations were done with normal PGK using Mn^{2+} concentrations of 50.3 μM, 100.6 μM, and 150.9 μM, PGK concentration of 131.7 μM,

and ATP concentrations up to 490 μM. Ternary complex titrations were done with deuterated PGK using Mn^{2+} concentration of 100.9 μM, dPGK concentration of 124.4 μM, and ATP concentrations up to 2.2 mM.

4. *Quaternary Complex Studies*

Quaternary complex titrations were carried out by titrating glycerol-3-phosphate, a 3-phosphoglycerate analogue, into the PGK-ATP-Mn^{2+} complex using both the normal and the deuterated enzyme. These experiments were qualitative in nature, seeking only to observe complex formation. The analysis of quaternary complexes by the methods detailed above are theoretically possible but not practically feasible given the larger number of equilibrium constants and simultaneous equation solution this would entail. The computer program used to analyze the ternary complex cannot be used for the quaternary system. Titrations were carried out with the normal enzyme using Mn^{2+} concentrations of 50.5 μM, 100.9 μM, and 151.4 μM, PGK concentration of 120.2 μM, ATP concentration of 181.3 μM, and glycerol-3-phosphate concentrations up to 10.0 mM. Titrations were done with the deuterated enzyme using Mn^{2+} concentration of 100.6 μM, dPGK concentration of 132.6 μM, ATP concentration of 181.3 μM, and glycerol-3-phosphate concentrations up to 10.7 mM.

C. Results and Discussion

The results of these experiments are summarized in Table 4. The purpose of these experiments was both to complete the characterization of the deuterated enzyme and to ascertain that its thermodynamic parameters are sufficiently similar to those of the normal enzyme to be useful for further NMR studies. Table 4 indicates that, with the exception of K_D^{Mn2+} as obtained from the Scatchard analysis, and ϵ_b, the values obtained for the two enzymes are close. The difference in metal binding properties indicated by the large difference in K_D^{Mn2+} and ϵ_b between the normal and deuterated enzymes, however, only relate to the binary metal-enzyme complex which is not the catalytically relevant complex. It is clear from this data that the binding properties of the deuterated enzyme with regard to the active ternary complex are similar to those of the normal enzyme, so that the apparent differences in binary metal-enzyme complex formation do not seem to affect the catalytically more important ternary complex formation.

Figure 15 (A) shows the double-reciprocal plots of $1/\epsilon^*$ *vs* 1/[PGK] obtained from titrations of Mn^{2+}solutions with normal PGK. Although the y-intercepts (extrapolation of ϵ^* to infinite enzyme concentration at each Mn^{2+} concentration) do not converge, an average

value of 7.31 was obtained for ϵ_b. (B) shows a Scatchard plot from data collected by titration of Mn^{2+} with normal PGK. The x-intercept of the plot indicates the number of Mn^{2+} binding sites per enzyme molecule (1.11 in this case), and the slope of the curve indicates the K_D^{Mn2+} (1.16 mM) for the normal enzyme. This value is in good agreement with the K_D^{Mn2+} value of 1.0 mM reported by Chapman *et al* (34).

Figure 16 (A) shows the $1/\epsilon^*$ *vs* 1/[dPGK] plot obtained from titration of Mn^{2+} with deuterated PGK. An ϵ_b value of 2.91 was obtained from this data. (B) shows a Scatchard plot from data collected by titration of Mn^{2+} with deuterated PGK. This plot indicates 0.923 Mn^{2+} binding sites per enzyme molecule, and a K_D^{Mn2+} of 160.3 μM for the deuterated enzyme.

Figure 17 (A) shows double-reciprocal plots of data obtained by titration of five different PGK-Mn^{2+} complexes with ATP. The upward curvature of each plot at high ATP concentration is due to the formation of large amounts of binary complex (Mn^{2+}-ATP) in the solution at these high ATP concentrations. Therefore, each curve is fit only to the linear portion of the data. The y-intercept of each curve gives $1/\epsilon_c^*$ for that PGK concentration. (B) shows the secondary plot $1/\epsilon_c^*$ *vs* 1/[PGK] from which ϵ_T is obtained. The value of ϵ_T given by this method is 13.38.

Figure 18 shows curves obtained by titration of PGK-Mn^{2+} complex with ATP. Data from the titration of the normal and deuterated enzymes are included. These curves were fit iteratively by the EPS7A computer program.

Values of ϵ_b for both the normal and the deuterated enzyme found by titration and by the curve fit are quite consistent with each other, although ϵ_b for deuterated PGK is much smaller than it is for normal PGK. Values of ϵ_T for the normal enzyme are likewise consistent as obtained by the two different methods. It was not possible to carry out more than one ternary titration for deuterated PGK as this experiment requires a very large quantity of enzyme; however, the ϵ_T value obtained for the deuterated enzyme by the curve fit is reasonably consistent with that of the normal enzyme. K_S, K_2, and K_A' values are also in good agreement for the normal and deuterated enzymes. K_D^{Mn2+} values for both the normal and deuterated enzyme obtained by the two methods are within a factor of two, and the values obtained for the deuterated enzyme are smaller than those obtained for normal PGK. This taken together with the smaller ϵ_b value obtained for the deuterated enzyme may indicate a genuine difference in Mn^{2+} binding properties. One should also realize that this method yields information about the immediate environment of the paramagnetic probe by determining the relaxation rates of protons. Clearly,

in the case of deuterated enzyme, there will be deuterium atoms close to the metal; thus some differences in the enhancement values are expected.

Figure 19 shows the titration curves for the quaternary complexes PGK-Mn^{2+}-ATP-Glycerol-3-phosphate. Although these curves were not fit to specific thermodynamic parameters, the decline in ϵ^* as glycerol-3-phosphate concentration increases indicates that the quaternary complex does form. The similarity in the shape of the curve as well as the concentration of G3P at which half maximal effect was observed for the deuterated enzyme and the normal enzyme would seem to indicate that the process of complex formation is similar for the two enzymes.

CHAPTER V

NUCLEAR MAGNETIC RESONANCE STUDIES

A. Introduction

The essential purpose in the purification of a fully deuterated enzyme is its usefulness for NMR studies. The magnetic moment of the deuteron is much smaller (one-third) than that of the proton, and its resonance occurs at a frequency very far removed from that of the proton at a particular magnetic field strength. Thus if one is observing proton resonances, one does not observe deuterium resonances at the same time (39). Because deuterium is "invisible" to ^{1}H-NMR, a deuterated enzyme should have fewer visible proton peaks in comparison with the vast, overlapping peaks seen in a normal enzyme spectrum. Both complete and selective deuteration have been used since the late 1960's as a means of enhancing the resolution of protein NMR spectra and of simplifying the spectra in order to facilitate resonance assignment (4), (40), (41). Some NMR studies have also been done using deuterated enzymes to examine the binding interaction between the enzymes and small molecules (38), (39). Other deuterated protein-ligand studies have

been done with deuterated monoclonal immunoglobulin Fab and spin-labeled haptens (42).

In addition to simplifying resonance assignment and resolution by eliminating the large proton "envelope" that makes up the large part of most protein spectra, deuteration of proteins can help solve other difficulties inherent in NMR studies. One of these difficulties is spin diffusion, a phenomenon that besets the study of dipolar coupling relations, as for example in experiments measuring the nuclear Overhauser effect of dipolar coupling between nuclei. As magnetization is transferred from one nucleus to another, one sees this effect; however, if enough transferred magnetization is built up on the second nucleus, it may in turn transfer magnetization to a third nucleus. Eventually the magnetization is diffused into the system such that the spatial relationships which one studies by these methods are impossible to perceive. ^{1}H-^{2}H dipolar interactions, however, are only 1/16 as efficient as ^{1}H-^{1}H interactions, and thus the introduction of deuterium into the system could be expected to reduce spin diffusion significantly. This has in fact proved to be the case in many studies reviewed by D. M. LeMaster (41).

The deuterated PGK purified and characterized in this research has been used in preliminary NMR experiments designed to examine the conformation of MgATP

bound to the enzyme. It was expected that the deuteration of the protein would allow the substrate resonances to be more clearly visible and less ambiguous than would be the case in studies of MgATP bound to the normal enzyme. It is hoped that further experiments of a more quantitative nature aimed at deriving bound MgATP conformation from NOE constraints will be possible using the system worked out in this research.

B. **Experimental Procedures**

1. *Materials*

Normal and deuterated PGK were purified from *S. cerevisiae* in this laboratory as described in Chapter II. 2′-deoxyadenosine 5′-triphosphate was obtained from Sigma and prepared as described in Chapter III. Enzymes and nucleotide substrates were further prepared for NMR experiments by lyophilization to remove ^1H_2O. They were then dissolved two times in ^2H_2O (99.9 atom %) and lyophilized, dissolved in ^2H_2O (99.96 atom %) and lyophilized a final time before being taken up in ^2H_2O (99.96 atom %) to a final sample volume of 500 μl. $MgCl_2$ and NaCl solutions were prepared in ^2H_2O (99.9 atom %).

The concentration of the NMR sample of deuterated PGK was 30.5 mg/ml. One may assume that the molecular weight of the fully deuterated enzyme is approximately 3

kD greater than that of the normal enzyme, and thus the deuterated sample's concentration was estimated to be 622 μM. A sample of normal PGK of matching concentration was prepared. Prior to lyophilization, this sample was put over a Sephadex G-25 column equilibrated in 2 mM deuterated Tris-^{2}HCl, pH 7.5 in order to remove the protiated buffer in which the normal enzyme was purified.

NMR samples of normal and deuterated PGK with Mg-2'-dATP were prepared. All samples were either purified in deuterated Tris-^{2}HCl, pH 7.5, or were transferred into this buffer as described above. All samples contained 100 mM NaCl. PGK with Mg-2'-dATP contained 458.5 μM PGK, 4.78 2'-dATP, and 5.73 mM $MgCl_2$. Deuterated PGK with Mg-2'-dATP contained 452.2 μM deuterated PGK, 4.78 mM 2'-dATP, and 5.73 mM $MgCl_2$. A second set of samples with enzyme and 2'-dATP contained 4.78 mM 2'-dATP, 5.73 mM $MgCl_2$, and 400.7 μM and 399.7 μM PGK and deuterated PGK respectively. A sample of free nucleotide solution was also prepared containing 19.14 mM 2'-dATP in ^2H_2O.

Ultra-thin-walled 5mm NMR sample tubes were obtained from Wilmad.

2. *One-dimensional NMR Spectra*

Spectra were recorded on a Bruker AMX400 spectrometer at a temperature of 27°C. Quadrature phase detection and a 60° observation pulse were used. 32K

data points were collected over a spectral width of 6024 Hz, with an acquisition time of 2.72 s. For samples containing nucleotide substrates, 128 transients were collected; for samples containing free enzyme, 2300 transients were collected. A relaxation delay of 12 s was used for all samples containing enzyme; a 6 s delay was used for the free substrate sample. Chemical shift values were determined relative to external DSS. Prior to Fourier transformation, an exponential multiplication function with a linebroadening factor of 1.0 Hz was applied to the free induction decays.

3. *Two-dimensional NMR Experiments*

Nuclear Overhauser enhancement spectroscopy (NOESY) experiments were carried out on the enzyme-substrate samples described above. These experiments were done on a Bruker AMX400 spectrometer at 30°C. Data were collected in the phase-sensitive mode using the time-proportional phase increment method (43). The transmitter offset was placed on the HO^2H resonance peak, which was irradiated during the relaxation delay of 1.0 s in order to suppress the water signal. NOESY spectra for the normal PGK-substrate complex were recorded with mixing times of 15, 30, 60, 90, and 200 ms; for the deuterated PGK-substrate complex spectra were recorded with mixing times of 15, 30, 60, 90, 120, 150, and 200

ms. All mixing times were varied randomly up to ± 5% in order to eliminate COSY cross-peaks. All experiments were carried out using a spectral width of 4032.26 Hz. For each experiment, 2K data points were recorded in t_2 for each of 250-350 t_1 values, with 128 transients per free induction decay. The data were zero-filled to 2K points in t_1 and were multiplied by a $(\text{sine})^2$ window function in both dimensions before Fourier transformation. Phase corrections and baseline corrections were performed in both dimensions.

NOESY (two-dimensional NOE) experiments allow one to observe all the spatial correlations within a system without going through the repetitive process of selective peak irradiation which is the basis for one-dimensional NOE studies (44), (45), (46). The basic pulse sequence for a NOESY experiment is:

Relaxation Delay → 90° → t_1 → 90° → τ_m → 90° → t_2

in which t_1 is the evolution period, τ_m is the mixing time, and t_2 is the acquisition period. Spectra are collected during t_2 for each incrementally varied value of t_1. The first 90° pulse perturbs the equilibrium of the nuclei in the system; during the evolution period (t_1) each nucleus is frequency-labeled by its chemical shift precession. The second 90° pulse rotates the magnetization back to the **z** axis. During the mixing time magnetization is transferred between nuclei through

dipolar interaction, and the chemical shifts of these nuclei are correlated. The third 90° pulse rotates the magnetization into the **xy** plane where it can be detected during acquisition. For each nucleus in the system, there is an optimal value for t_1 at which the magnetization of the nucleus can be observed during acquisition. If one examines the one-dimensional spectrum acquired in t_2 for that evolution time, one sees a large peak at the resonance of that nucleus and smaller peaks at the resonances of those nuclei which exchange magnetization with it through the dipolar mechanism. When the data acquired in t_2 for all values of t_1 is Fourier transformed in both dimensions, one sees cross-peaks which correlate the chemical shifts of those nuclei which exchange magnetization.

C. Results and Discussion

Figure 20 shows a one-dimensional spectrum of 2′-deoxyadenosine 5′-triphosphate, the nucleotide substrate analogue used for these experiments. Deoxy-ATP was chosen for these preliminary investigations because its 2′ and 2″ protons resonances, unlike the 2′ resonance of ATP, are upfield shifted and are not obscured by the residual $^2HO^1H$ signal. Their NOE crosspeaks with the 3′ proton should be visible even though in the one-

dimensional spectrum the 3′ resonance is obscured beneath the water peak.

Figure 21 shows a one-dimensional spectrum of 2′-dATP bound to normal PGK. One can see that the substrate resonances are virtually buried beneath the proton "envelope," particularly in the region upfield of the water peak. Substrate resonances are clearly visible in the region downfield of the water peak, but one may still observe the large mass of overlapped aromatic resonances between 6.6-7.8 ppm. (A) shows the region of the spectrum upfield of the water peak, while (B) shows the region of the spectrum downfield of the water peak.

Figure 22 shows a one-dimensional spectrum of 2′-dATP bound to deuterated PGK, and the contrast between it and Figure 21 is clear. (A) In the region upfield of the water peak only a few residual proton peaks are visible, but they are much more clearly resolved and do not form the mass observed in the spectrum of the normal protein. (B) In the region downfield of the water peak, the envelope of aromatic resonances has likewise been almost eliminated, a feature of the deuterated enzyme which could prove useful in studies of the aromatic residues of PGK. Substrate resonances are clearly visible in this spectrum.

Figures 23 and 24 are a pair of contour plots obtained from NOESY experiments using matched samples of

normal (Figure 23) and deuterated (Figure 24) PGK with Mg-2′-dATP. Both spectra were acquired with a mixing time of 30 ms. In the NOESY spectrum with deuterated enzyme, one may easily observe the substrate crosspeaks between 2′→3′ and 2″→3′, as well as those between 2′→1′ and 2″→1′. The strong crosspeaks at (F_2≈2.7 ppm, F_1≈3.8 ppm) are observed between two protein resonances. The spectrum of the normal PGK-substrate complex is ambiguous. The substrate crosspeaks between 2′→1′ and 2″→1′ are visible, but the crosspeaks between 2′→3′ and 2″→3′ are obscured in the large mass of crosspeaks between enzyme protons. Even in the cleaner region of the spectrum there are several protein-protein and protein-substrate crosspeaks visible which could confuse the identification of substrate-substrate crosspeaks. One substrate crosspeak is visible on this spectrum which has not appeared at this mixing time on the deuterated spectrum: 2′→8. This crosspeak appears in the deuterated spectrum at a mixing time between 60-90 ms. Therefore, in a quantitative study the H-2′→ H-8 distance would have been significantly underestimated with the normal enzyme.

Figures 25 and 26 show a pair of contour plots obtained from NOESY experiments using a mixing time of 200 ms. Substrate-substrate crosspeaks are visible on both spectra. In addition to the crosspeaks seen at 30 ms, a 4′→1′ crosspeak is now visible on both spectra.

The spectrum of the normal PGK-substrate complex, however, is much more obscured by noise and t_1 ridges than the spectrum of the deuterated PGK-substrate complex. The NOESY spectrum with deuterated enzyme becomes even clearer when a processing operation, symmetrization, is applied to it. A feature of true NOESY crosspeaks (as opposed to artifacts or noise) is that they are symmetrical about the diagonal. Symmetrization removes non-symmetrical points and thus rids the spectrum of extraneous features. Unfortunately, symmetrization also decreases the intensity of true NOE crosspeaks, and so it cannot be applied indiscriminately when quantitative volume integrations of peaks are desired.

These experiments, both one- and two-dimensional, indicate that the substrate resonances are indeed more clearly visible and less ambiguous when bound to the deuterated enzyme than when bound to the normal. It is hoped that further experiments using deuterated PGK-substrate systems will further elucidate the binding conformations of the substrates.

LIST OF REFERENCES

LIST OF REFERENCES

1. Scopes, R. K. (1973) in *The Enzymes*, 3rd ed. (Boyer, P.D., ed.) vol 8, pp. 335-351. Academic Press, New York.

2. Mori, N., Singer-Sam, J., and Riggs, A. D. (1986). Evolutionary conservation of the substrate-binding cleft of phosphoglycerate kinase. *FEBS Lett.* **204**, 313-316.

3. Bryant, T. N., Watson, H. C., and Wendell, P.L. (1974). Structure of yeast phosphoglycerate kinase. *Nature* **246**, 14-17.

4. Banks, R. D., Blake, C. C. F., Evans, P. R., Haser, R., Rice, D. W., Hardy, G. W., Merrett, M., and Phillips, A. W. (1979). Sequence, structure and activity of phosphoglycerate kinase: a possible hinge-bending enzyme. *Nature* **279**, 773-777.

5. Tanswell, P., Westhead, E. W., and Williams, R. J. P. (1976). Nuclear-magnetic-resonance study of the active-site structure of yeast phosphoglycerate kinase. *Eur. J. Biochem.* **63**, 249-262.

6. Pickover, C. A., McKay, D. B., Engleman, D. B., and Steitz, T.A. (1979). *J. Biol. Chem.* **254**, 11323-11329.

7. Watson, H. C., Walker, N. P. C., Shaw, P.J., Bryant, T. N., Wendell, P. L., Fothergill, L. A., Perkins, R. E., Conroy, S.C., Dobson, M. J., Tuite, M. F., Kingsman, A. J., and Kingsman, S. M. (1982). Sequence and structure of yeast phosphoglycerate kinase. *EMBO J.* **1**, 1635-1640.

8. Harlos, K., Vas, M., and Blake, C. F. (1992). Crystal structure of the binary complex of pig muscle pphosphoglycerate kinase and its substrate 3-phospho-D-glycerate. *Proteins: Structure, Function, and Genetics* **12**, 133-144.

9. Fairbrother, W. J., Walker, P. A., Minard, P., Littlechild, J.A., Watson, H. C., and Williams, R. J. P. (1989). Site-directed mutagenesis of histidine-62 in the basic patch region of yeast phosphoglycerate kinase. *FEBS Lett.* **258**, 247-250.

10. Urey, H. C., Brickwedde, F. G., and Murphy, G. M. (1932). A hydrogen isotope of mass 2. *Phys. Rev* 39, 164-165.

11. Katz, J. J., and Crespi, H. L. (1966). Deuterated organisms: cultivation and uses. *Science* **151**, 1187-1194.

12. Crespi, H. L., Conrad, S. M., Uphaus, R. A., and Katz, J. J. (1960). Cultivation of microorganisms in heavy water. *Ann. N.Y. Acad. Sci.* **84**, 648-666.

13. Crespi, H. L., and Katz, J. J. (1972). Preparation of deuterated proteins and enzymes. *Methods Enzymol.* **26**, 627-637.

14. Crespi, H. L., Marmur, J., and Katz, J. J. (1962). Use of fully deuterated algae extracts for the isolation of nucleic acids. *J. Amer. Chem. Soc.* **84**, 3489-3491.

15. Mohan, V. S., Crespi, H. L., and Katz, J. J. (1962). Nutritional requirements for the cultivation of fully deuterated yeasts *Torulopsis utilis* and *Saccharomyces cerevisiae*. *Nature* **193**, 189-190.

16. Scopes, R.K. (1971). An improved procedure for the isolation of 3-phosphoglycerate kinase from yeast. *Biochem. J.* **122**, 89-92.

17. Minard, P., Bowen, D.J., Hall, L., Littlechild, J.A., and Watson, H.C. (1990). Site-directed mutagenesis of aspartic acid 372 at the ATP binding site of yeast phosphoglycerate kinase: over-expression and characterization of the mutant enzyme. *Protein Engineering* **3**, 515-521.

18. Bucher, T. (1942). Uber ein phosphatubertragendes garungsferment. *Biochim. Biophys. Acta* **1**, 292-314.

19. Kuntz, G. W. K., and Krietsch, W. K. G. (1982). Phosphoglycerate kinase from spinach, blue-green algae, and yeast. *Methods Enzymol.*, **90**, 110-114.

20. Larsson-Raznikiewicz, M. (1964). Kinetic studies on the reaction catalyzed by phosphoglycerate kinase. I. The effect of Mg^{2+} and adenosine 5′-triphosphate. *Biochim. Biophys. Acta* **85**, 60-68.

21. Larsson-Raznikiewicz, M. (1970). The phosphoglycerate kinase reaction and its metal ion specificity. *Eur. J. Biochem.* **17**, 183-192.

22. Larsson-Raznikiewicz, M. (1967). Kinetic Studies of the reaction catalyzed by phosphoglycerate kinase. II. The kinetic relationships between 3-phosphoglycerate, $MgATP^{2-}$ and activating metal ion. *Biochim. Biophys. Acta* **132**, 33-40.

23. Schierbeck, B., and Larsson-Raznikiewicz, M. (1979). Product inhibition studies of yeast phosphoglycerate kinase evaluating properties of multiple substrate binding sites. *Biochim. Biophys. Acta* **568**, 195-204.

24. Larsson-Raznikiewicz, M., and Arvidsson, L. (1971). Inhibition of phosphoglycerate kinase by products and product homologues. *Eur. J. Biochem.* **22**, 506-512.

25. Larsson-Raznikiewicz, M., and Jansson, J. R. (1973). Activation of yeast phosphoglycerate kinase by salts of monovalent cations. *FEBS Lett.* **29**, 345-347.

26. Khamis, M. M., and Larsson-Raznikiewicz, M. (1981). Activation and inhibition of phosphoglycerate kinase by sulphate ion. *Biochim. Biophys. Acta* **657**, 190-194.

27. Scopes, R. K. (1978). The steady-state kinetics of yeast phosphoglycerate kinase: anomalous kinetic plots and the effects of salts on activity. *Eur. J. Biochem* **85**, 503-516.

28. Scopes, R. K. (1978). Binding of substrates and other anions to yeast phosphoglycerate kinase. *Eur. J. Biochem.* **91**, 119-129.

29. Gregory, J. D., and Serpersu, E. H. Arrangement of substrates at the active site of yeast phosphoglycerate kinase: the effect of sulfate ion. *J. Biol. Chem*, "accepted for publication."

30. Sherman, M. A., Szpikowska, B. K., Dean, S. A., Mathiowetz, A. M., McQueen, N. L., and Mas, M. T. (1990). Probing the role of arginines and histidines in the catalytic function and activation of yeast 3-phosphoglycerate kinase by site-directed mutagenesis. *J. Biol. Chem.* **265**, 10659-10665.

31. Tompa, P., Hong, P. T., and Vas, M. (1986). The phosphate group of 3-phosphoglycerate accounts for conformational changes occuring on binding to 3-phosphoglycerate kinase: enzyme inhibition and thiol reactivity studies. *Eur. J. Biochem.* **154**, 643-649.

32. Mildvan, A.S., and Engle, J. L. (1972). Nuclear relaxation measurements of water protons and other ligands. *Methods Enzymol.* **260**, 654-683.

33. Carr, H. J., and Purcell, E. M. (1954). *Phys. Rev.* **94**, 630-638.

34. Mildvan, A. S., and Cohn, M. (1966). Kinetic and magnetic resonance studies of the pyruvate kinase reaction. *J. Biol. Chem* **241**, 1178-1193.

35. Chapman, B. E., O'Sullivan, W. J., Scopes, R. K., and Reed, G. H. (1977). Magnetic resonance studies on manganese-nucleotide complexes of phosphoglycerate kinase. *Biochemistry* **16**, 1005-1010 .

36. Mildvan and Cohn, 1966. See especially discussion on p. 1180 and equations 2a-4.

37. Serpersu, E. H., Shortle, D., and Mildvan, A. S. (1986) Kinetic and resonance studies of effects of genetic substitution of a Ca^{2+}-liganding amino acid in Staphylococcal nuclease. *Biochemistry* 25, 68-77.

38. Reed, G. H., Cohn, M., and O'Sullivan, W.J. (1970). *J. Biol. Chem.* **245**, 6547-6552.

39. Markley, J. L. (1972). High-resolution proton magnetic resonance spectroscopy of selectively deuterated enzymes. *Methods Enzymol.* **26**, 605-627.

40. LeMaster, D. M. (1989). Deuteration in protein proton magnetic resonance. *Methods Enzymol.* **177**, 23-43.

41. LeMaster, D. L. (1990). Uniform and selective deuteration in two-dimensional NMR of proteins. *Ann. Rev. Biophys. Biophys. Chem.* **19**, 243-266.

42. Anglister, J., Frey, T., McConnell, H. M. (1984) *Biochemistry* **23**, 5372.

43. Redfield, A. G., and Kunz, S. D. (1975). *J. Magn. Reson.* **19**, 250-254.

44. Bruch, M. D. (1987). Two-dimensional NMR spectroscopy of liquids. Chapter 3 in *NMR Spectroscopy Techniques*, ed. C. Dybowski & R. L. Lichter (New York: Marcel-Dekker).

45. Derome, A. E. (1987). *Modern NMR Techniques for Chemistry Research* (Oxford: Pergamon Press). See especially Chapter 5, "The Nuclear Overhauser Effect," and Chapter 8, "Homonuclear Shift Correlation."

46. Williams, K. R., and King, R. W. (1990). The Fourier transform in chemistry--NMR. Part 4. Two-dimensional methods. *J. Chem. Ed.* **67**, 125-137.

APPENDIX

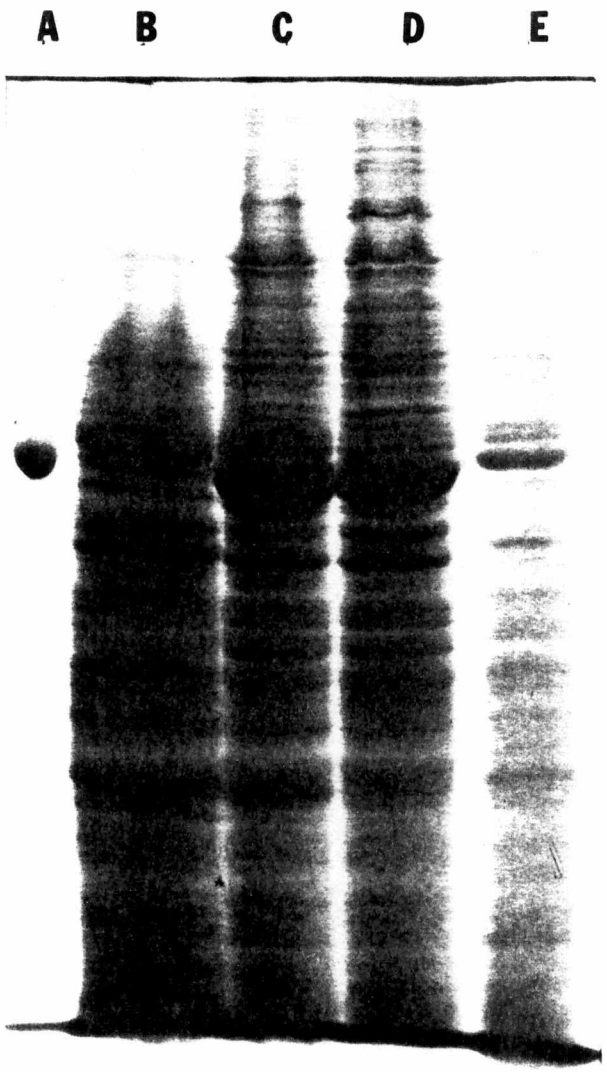

Figure 1. PGK overexpression in yeast cells. Denaturing 10% polyacrylamide gel of cell lysates prepared from transformed and untransformed yeast to demonstrate overproduction of PGK by tranformed yeast grown in deuterated medium. (A) PGK, 1μg. (B) Lysate from untransformed yeast strain 20B-12 grown in normal YEPD medium. (C) Lysate from yeast strain 20B-12 transformed with plasmid pCGY219, grown in selective medium for retention of the plasmid. (D) Lysate from the tranformed yeast strain grown in a medium containing algal hydrolysate with ethanol as the carbon source. (E) Lysate from the transformed yeast strain grown in medium containing $^{2}H_{2}O$, deuterated algal hydrolysate, and deuterated ethanol.

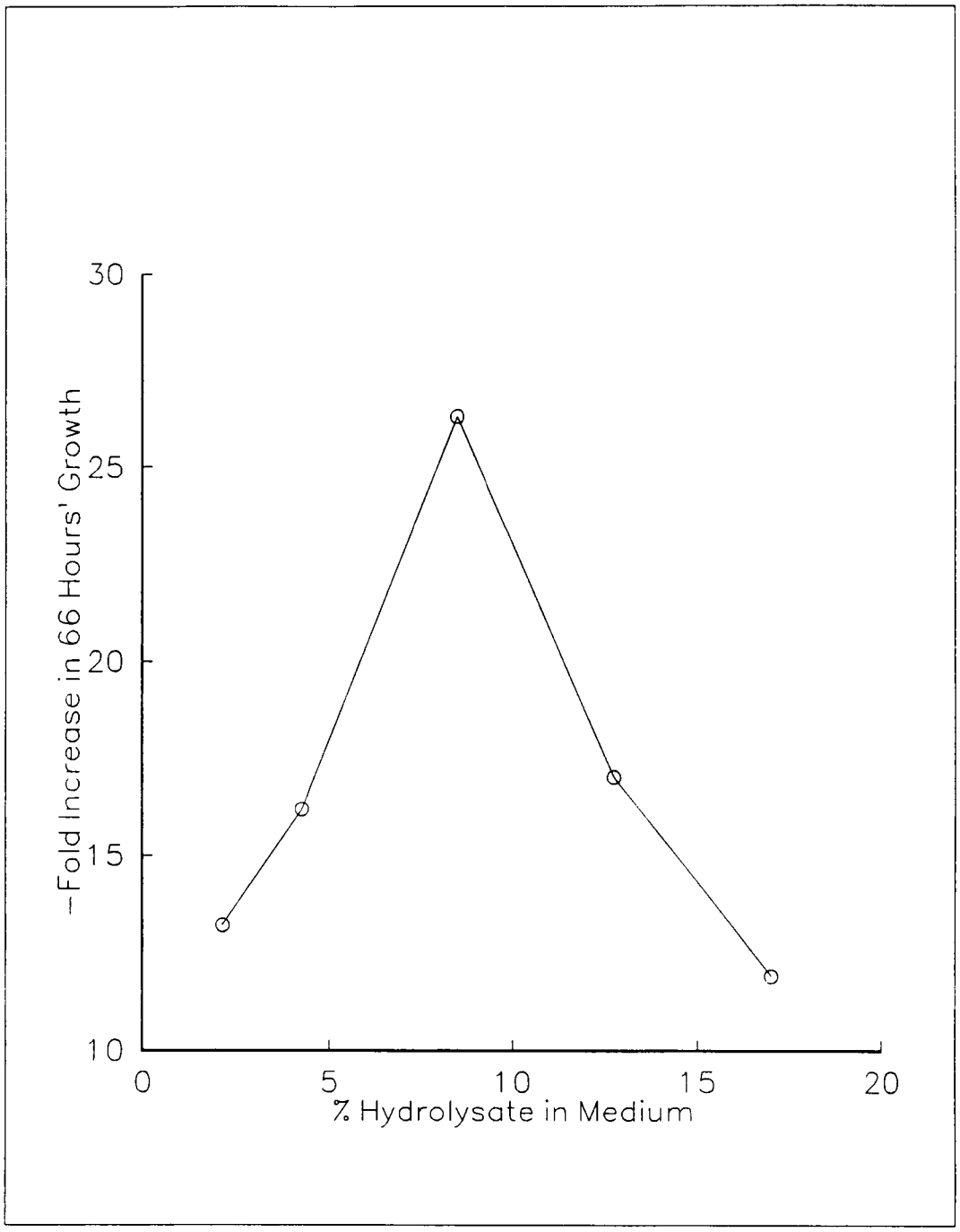

Figure 2. Test Cultures for Deuterated Algal Hydrolysate. Test cultures were grown to ascertain the optimal concentration in yeast growth medium of deuterated algal hydrolysate prepared from lyophilized algal cells.

Figure 3. Yeast growth in normal and deuterated medium. Yeast strain 20B-12, transformed with plasmid pCGY21, grown under three different conditions. Curve labeled "Glucose" shows growth in medium containing 0.67% yeast nitrogen base without amino acids, 0.5% casein amino acids, 2% glucose, and 0.01 mg/ml adenine and uracil. Curve labeled "Algal Hydrolysate" shows growth in medium containing 0.67% yeast nitrogen base without amino acids, 5-8% algal hydrolysate, 2% ethanol, and 0.01 mg/ml adenine and uracil. Curve labeled "Deuterated Algal Hydrolysate" shows growth in medium containing $^{2}H_{2}O$, 0.67% yeast nitrogen base without amino acids, 5-8% deuterated algal hydrolysate, 2% deuterated ethanol, 0.01 mg/ml adenine and uracil, and 0.5 mg/ml thiamine, pyrodoxine, and inositol.

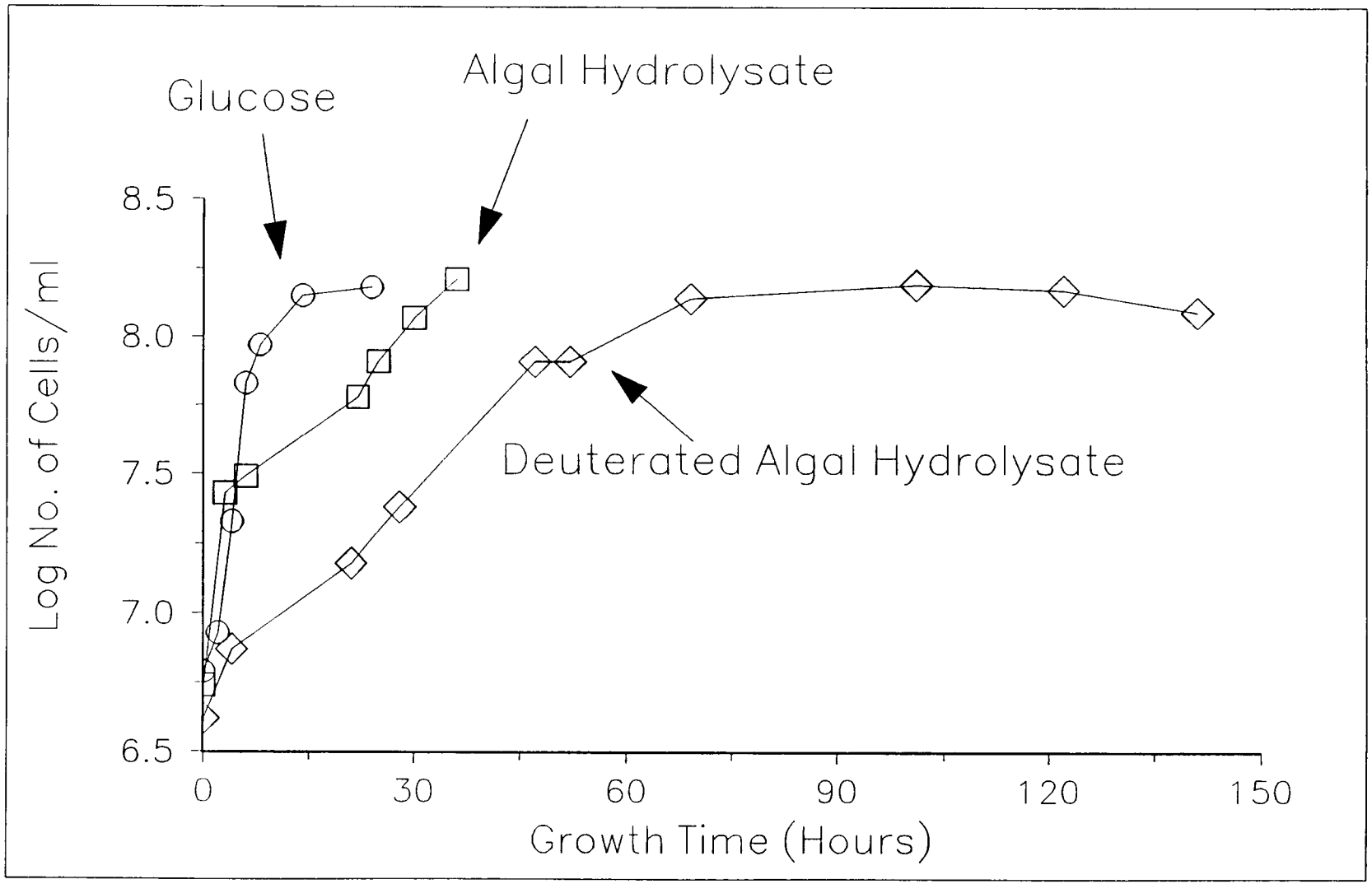
Glucose
Algal Hydrolysate
Deuterated Algal Hydrolysate
Log No. of Cells/ml
8.5
8.0
7.5
7.0
6.5
0
30
60
90
120
150
Growth Time (Hours)

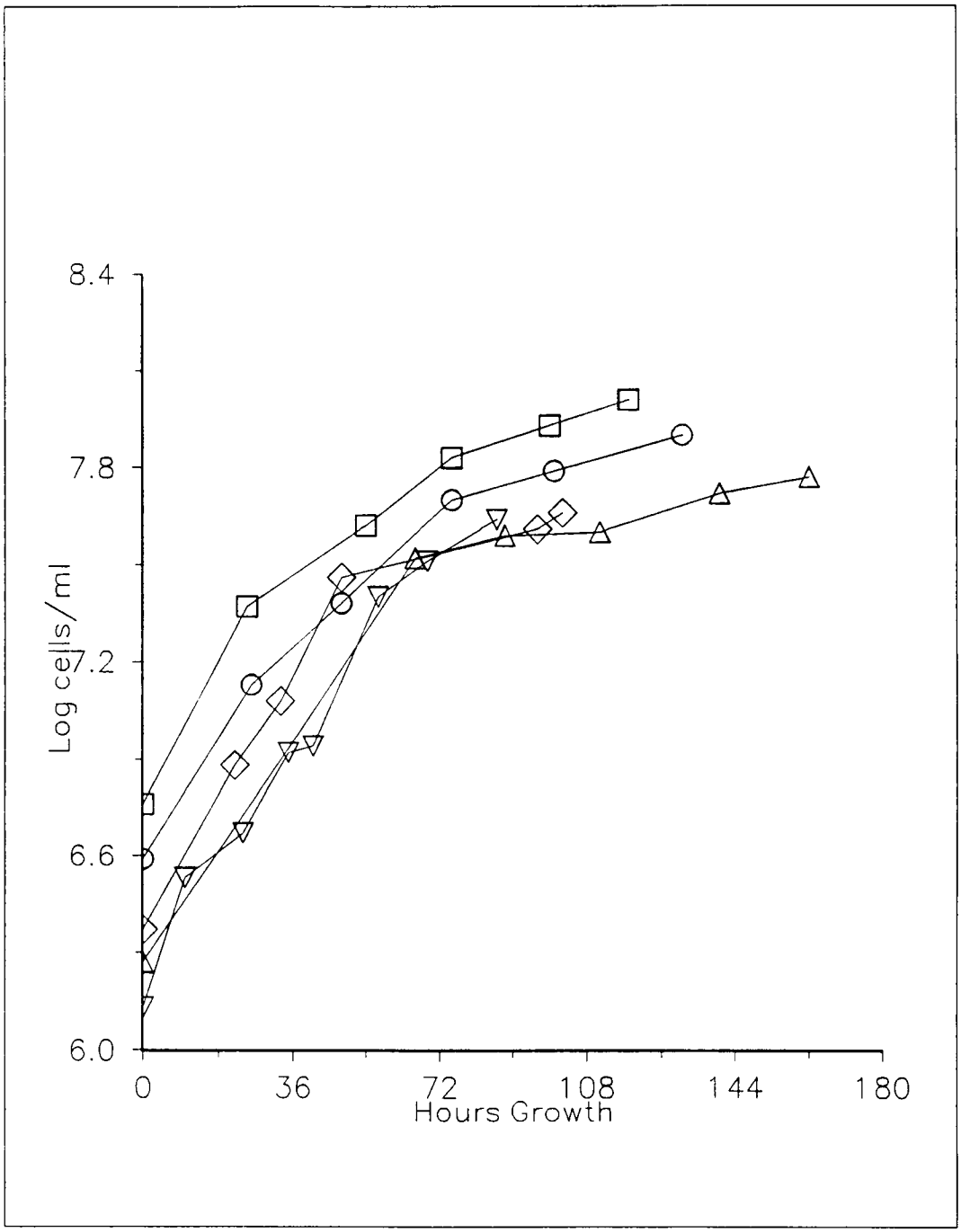

Figure 4. Yeast Growth for Deuterated PGK Purification. Several typical growth curves of yeast cultures grown for PGK preparation. Culture medium contained ^2H_2O, 0.67% yeast nitrogen base without amino acids, 5-8% deuterated algal hydrolysate, 2% deuterated ethanol, 0.01 mg/ml adenine and uracil, and 0.5 mg/ml thiamine, pyridoxine, and inositol.

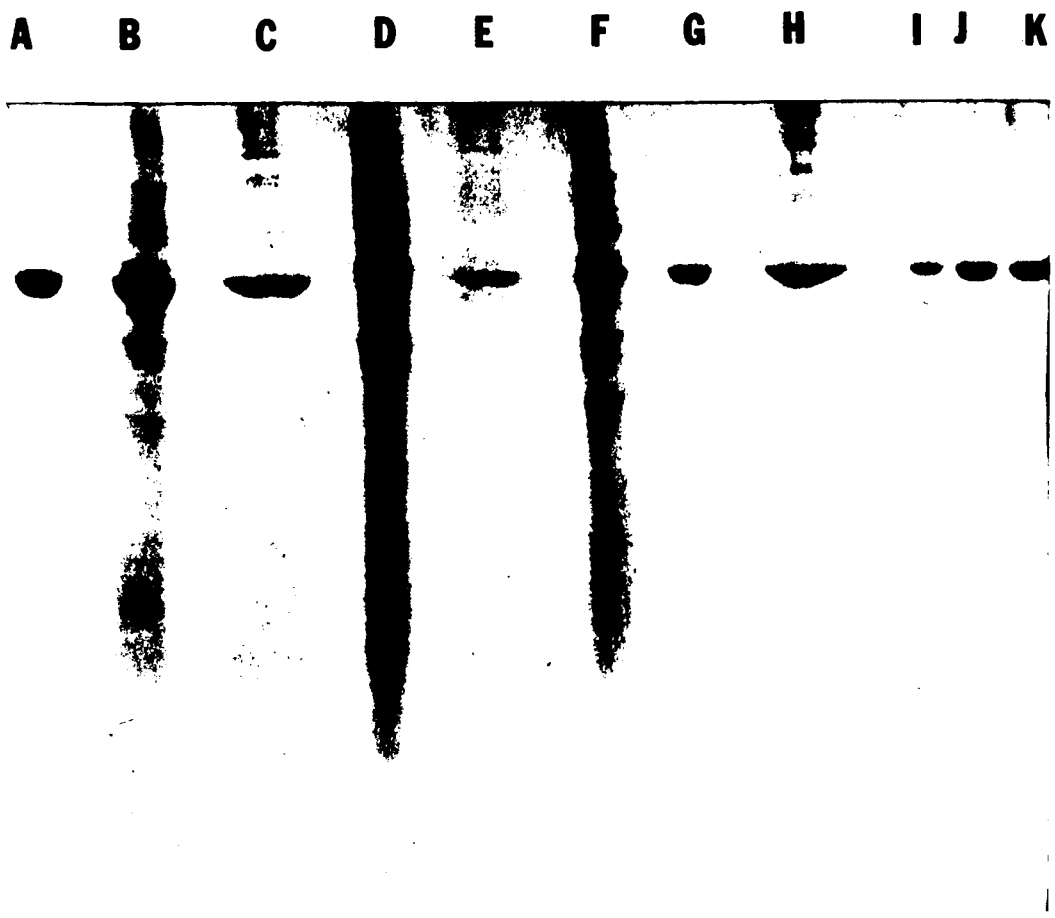

Figure 5. Deuterated PGK purification. Denaturing 10% SDS polyacrylamide gel of samples taken from each step of the purification of deuterated PGK. (A) PGK, 1μg. (B) Original cell extract. (C) Supernatant after first ammonium sulfate precipitation. (D) Pellet after first ammonium sulfate precipitation. (E) Supernatant after second ammonium sulfate precipitation. (F) Pellet after second ammonium sulfate precipitation. (G) Pellet containing precipitated dPGK after pH of second ammonium sulfate supernatant was lowered to 4.3. (H) Sample applied to Sephacryl HR200-S column. (I,J,K) Column fractions containing purified deuterated PGK.

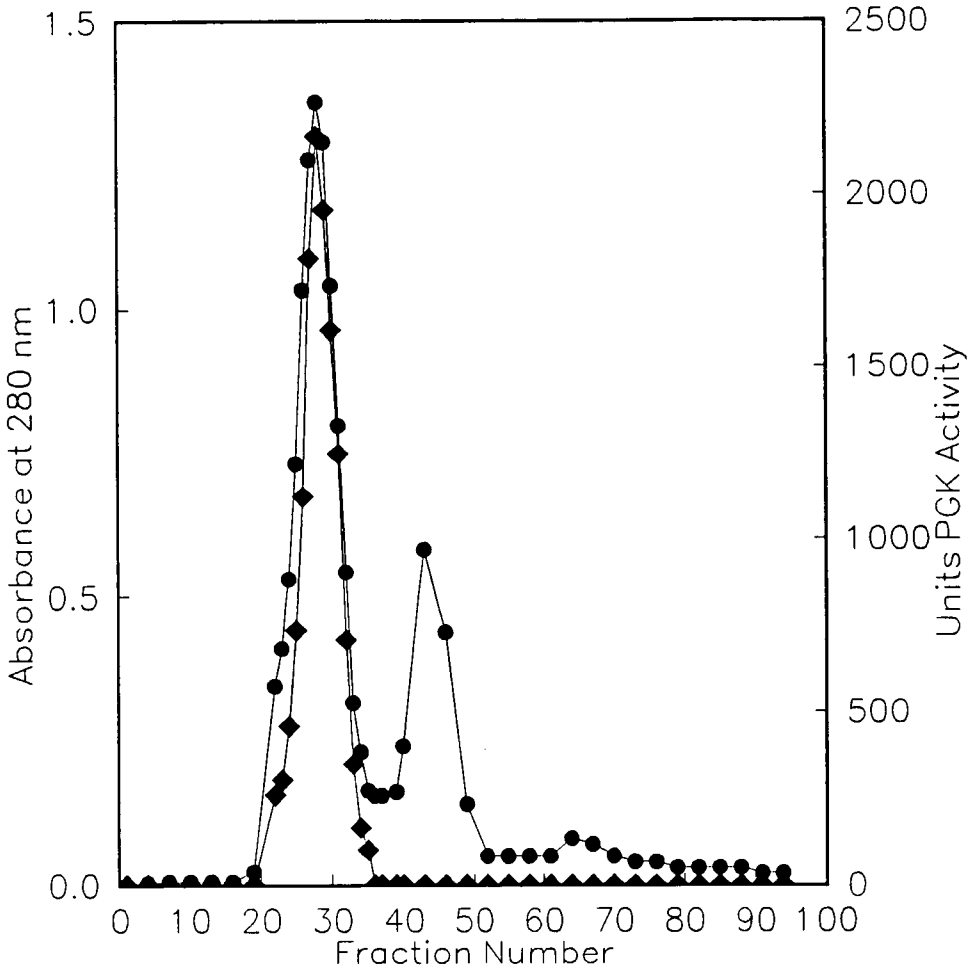

Figure 6. Elution Profile from Sephacryl HR-200S Column. The column was equilibrated in 10mM Tris-HCl, pH 7.5; the same buffer was used for elution. -•-•- Absorbance at 280 nm; -♦-♦- Units PGK activity.

Figure 7. ^{1}H NMR spectrum of normal and deuterated phosphoglycerate kinase.

Matched samples of normal and deuterated PGK were used with enzyme concentration of 622 μM in 40 mM deuterated Tris-^{2}HCl, pH 7.5. The spectrum was recorded on a Bruker AMX400 spectrometer at 27°C. Quadrature phase detection and a 60° observation pulse were used. 32K data points were collected for 2300 transients over a spectral width of 6024 Hz, with an acquisition time of 2.72 s and a relaxation delay of 12 s. Receiver gain setting for the normal enzyme was 256; for the deuterated enzyme it was 2K. Chemical shifts were determined relative to external DSS. Prior to Fourier transformation, an exponential multiplication function with a linebroadening factor of 1.0 Hz was applied. (A) Normal phosphoglycerate kinase. (B) Deuterated phosphoglycerate kinase.

^{1}H-NMR Spectrum of Normal PGK and Deuterated PGK

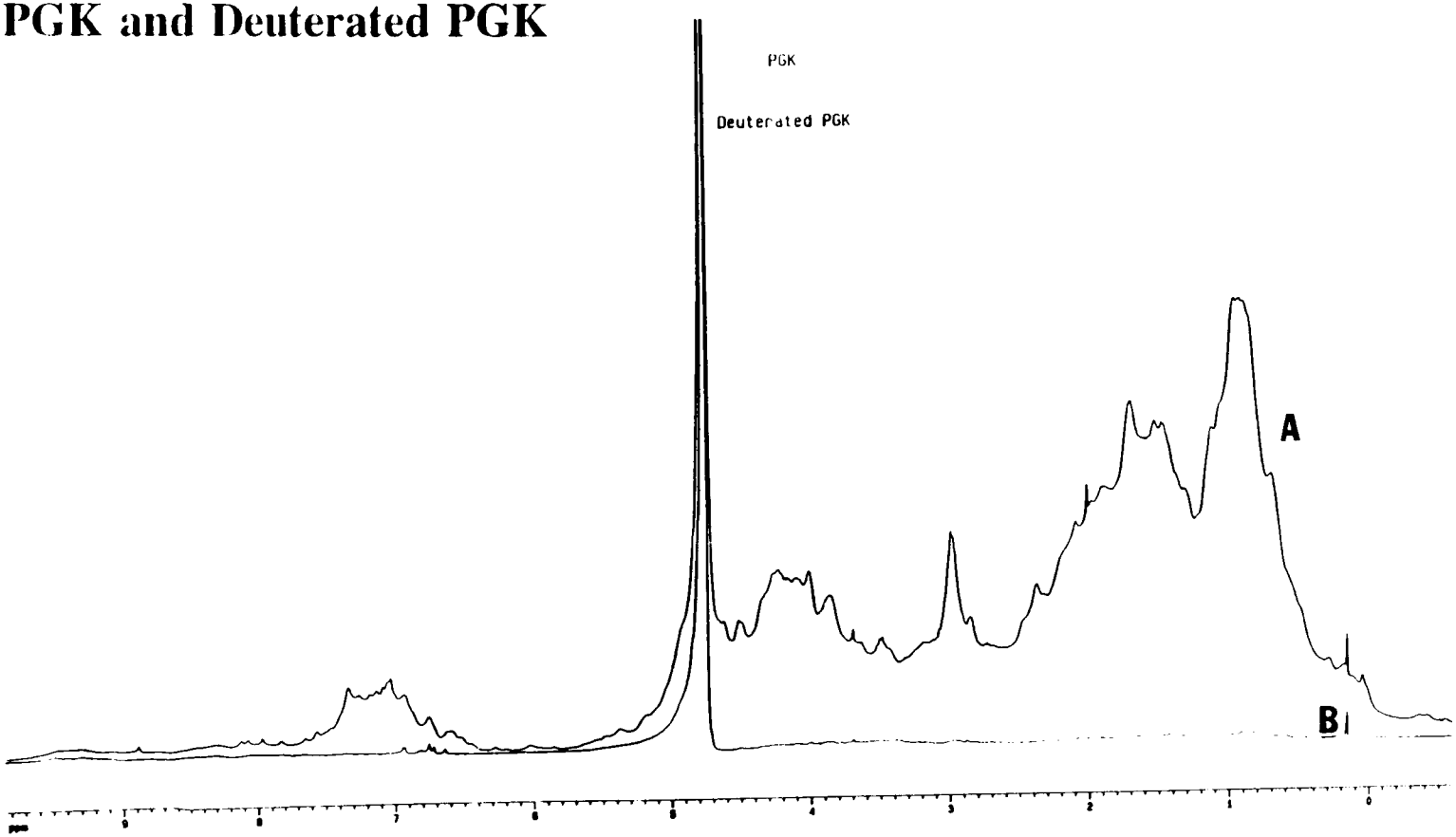

Figure 8. Kinetics of deuterated phosphoglycerate kinase with MgATP as the variable substrate.

A) Lineweaver-Burk plots of initial velocity *vs.* MgATP concentration. The assay mixture contained 50 mM Tris-HCl, pH 7.5, 150 mM NaCl, $MgCl_2$ in 1 mM excess of ATP concentration, and 0.2 mM NADH. Glyceraldehyde 3-phosphate dehydrogenase was used as the coupling enzyme; 100 μg was used per assay. The reaction in a total volume of 1 ml at 25°C was started by addition of 0.686 μg deuterated PGK per assay. MgATP concentration was varied between 0.047 mM and 1.21 mM at PGA concentrations of (from top to bottom): (○) 0.31 mM; (□) 0.52 mM; (△) 1.0 mM; (◇) 5.15 mM. (B) Secondary plot of $1/V_{max\ app}$ *vs.* 1/[PGA] for each of the curves in the primary plot. Extrapolation of this curve to the y-axis gives V_{max}.

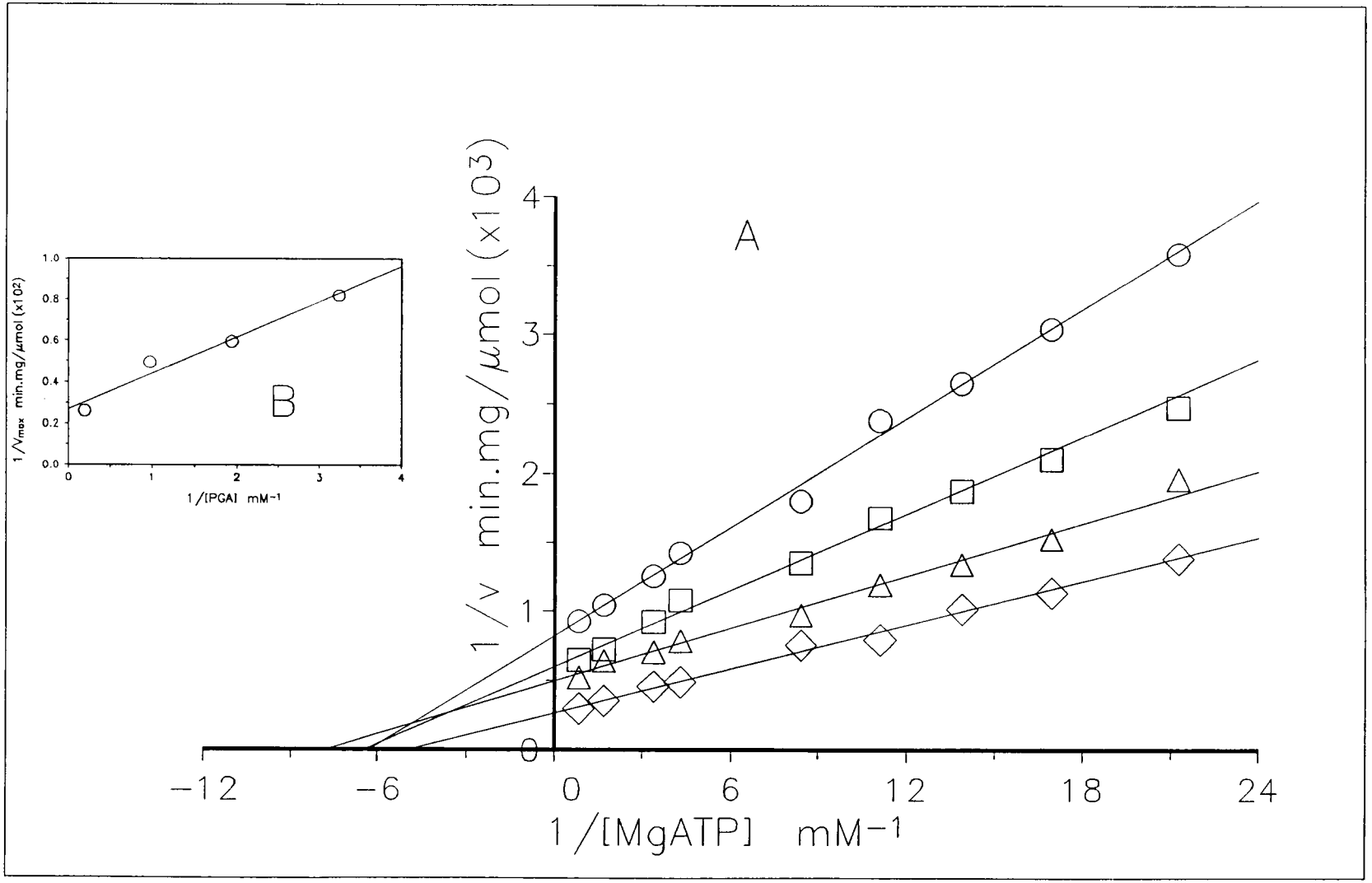
A
B
1/v min.mg/μmol (x103)
1/[MgATP] mM−1
−12
−6
0
6
12
18
24
0
1
2
3
4
1/Vmax min.mg/μmol (x102)
1/[PGA] mM−1
0.0
0.2
0.4
0.6
0.8
1.0

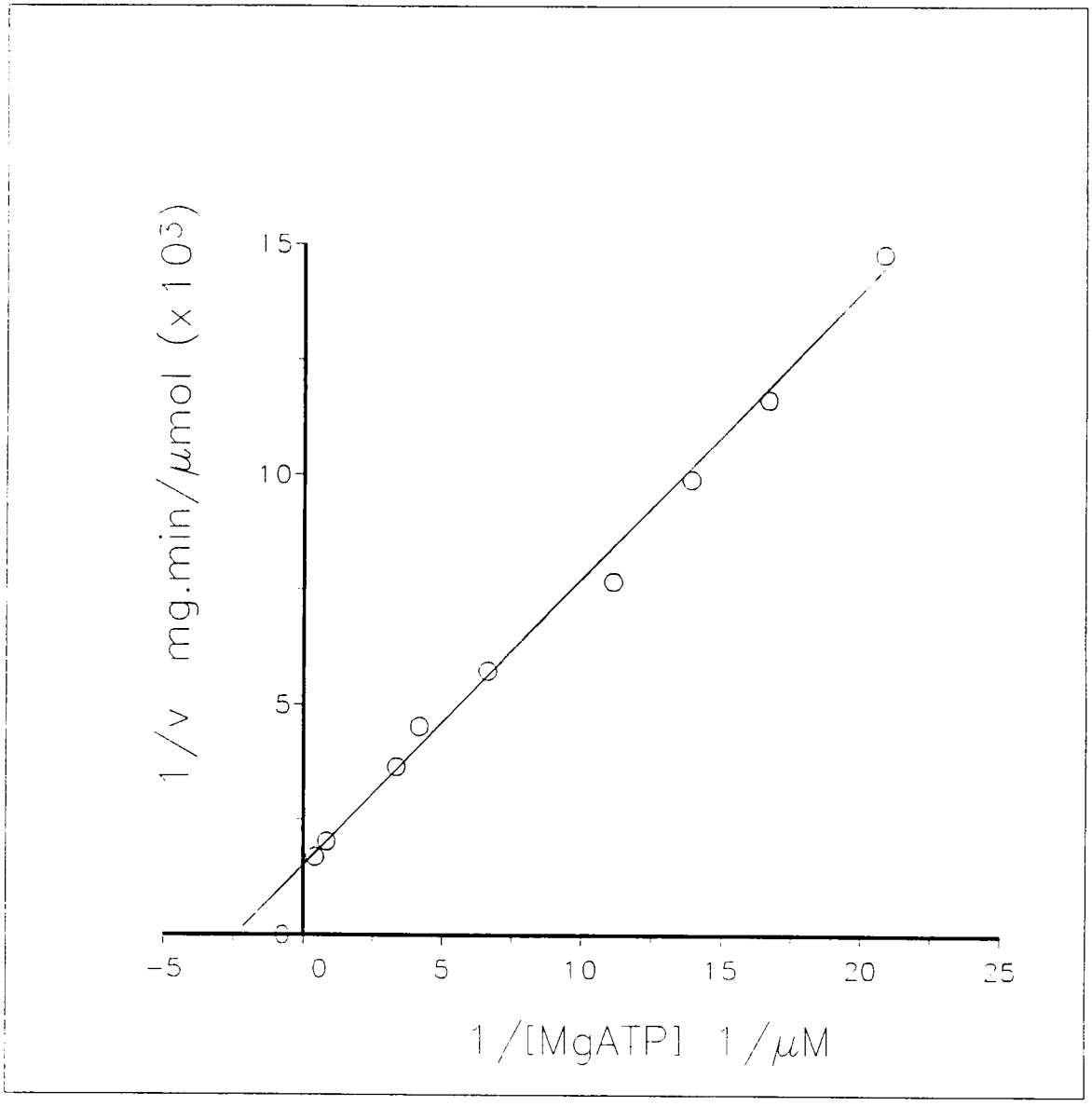

Figure 9. Kinetics of normal phosphoglycerate kinase with MgATP as the variable substrate. Double reciprocal plot of initial rates *vs*. MgATP concentration for normal PGK at pH 7.5. The assay mixture contained 50 mM Tris-HCl, pH 7.5, 150 mM NaCl, $MgCl_2$ in 1 mM excess of the ATP concentration, and 0.2 mM NADH. Glyceraldehyde 3-phosphate dehydrogenase was used as the coupling enzyme; 100 μg was used per assay. The reaction in a total volume of 1 ml at 25°C was started by addition of 0.25 μg PGK per assay. MgATP concentration was varied between 0.048 mM and 2.41 mM at a PGA concentration of 6.87 mM.

Figure 10. Kinetics of deuterated phospoglycerate kinase with PGA as the variable substrate.

(A) Lineweaver-Burk plots of initial rates vs. PGA concentration. The assay mixture contained 50 mM Tris-HCl, ph 7.5, 100 mM NaCl, $MgCl_2$ in 1mM excess of the ATP concentration, and 0.2 mM NADH. Glyceraldehyde 3-phosphate dehydrogenase was used as the coupling enzyme; 100 μg was used per assay. The reaction in a total volume of 1 ml at 25°C was started by adding 0.686 μg deuterated PGK per assay. The PGA concentration was varied between 0.10 mM and 5.15 mM at the following MgATP concentrations (from top to bottom): (O) 0.089 mM; (□) 0.18 mM; and (△) 0.42 mM. Curves were fit to the linear portion of the data, representing the high-affinity substrate binding site, to determine K_M. (B) Curves fit to the downward sloping portion of the data, representing the low-affinity substrate binding site. The y-intercept of each curve gives its $1/V_{max\ app}$. (C) Secondary plot of $1/V_{max\ app}$ for each curve plotted as a function of 1/MgATP concentration to determine V_{max}.

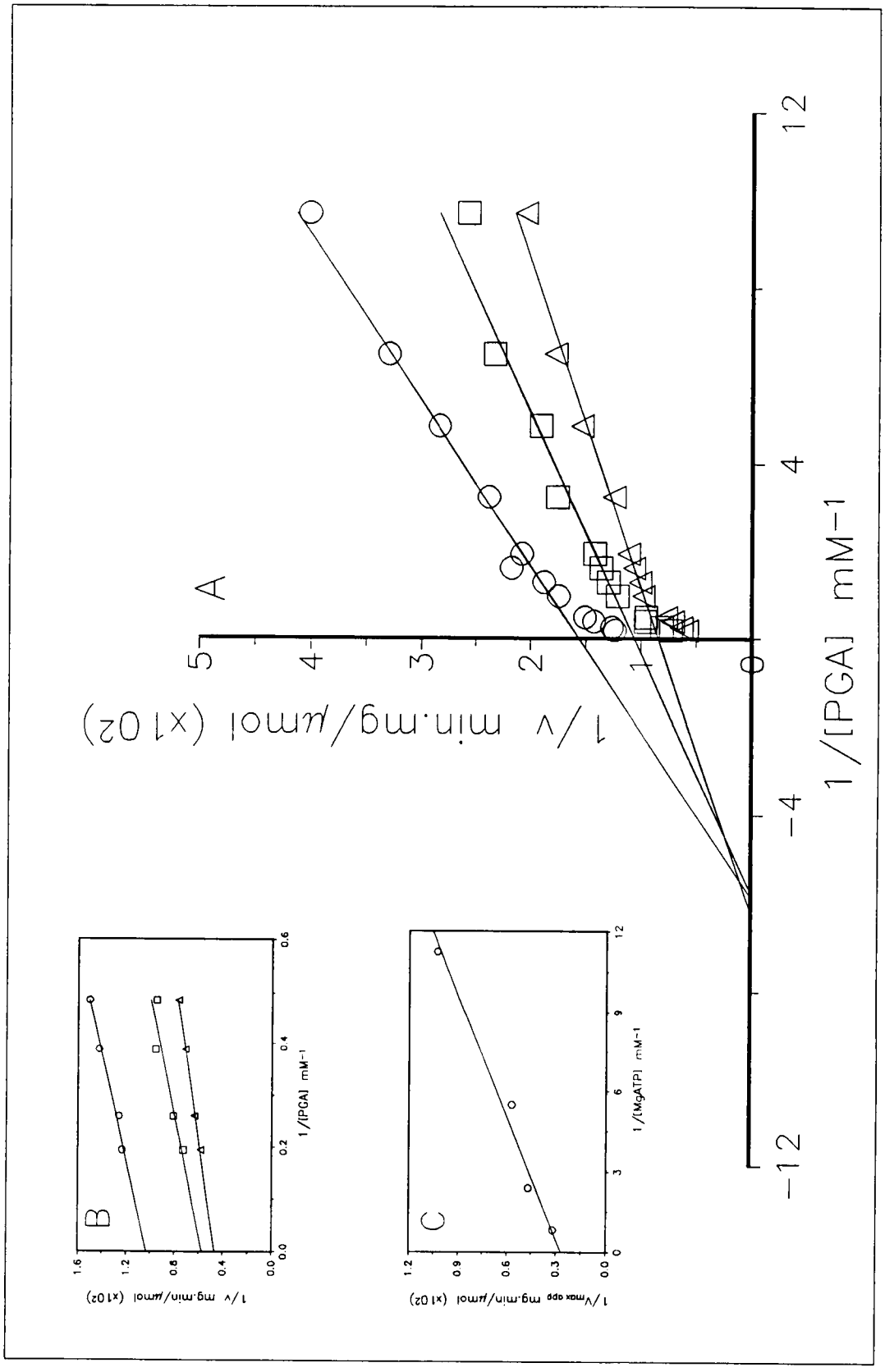
A
1/v min.mg/μmol (x102)
1/[PGA] mM-1
B
1/v mg.min/μmol (x102)
1/[PGA] mM-1
C
1/Vmax app mg.min/μmol (x102)
1/[MgATP] mM-1

Figure 11. Kinetics of normal phospoglycerate kinase with PGA as the variable substrate.

(A) Double-reciprocal plot of initial rates *vs.* PGA concentration. Assay mixture contained 50 mM Tris-HCl, ph 7.5, 100 mM NaCl, $MgCl_2$ in 1 mM excess of the ATP concentration, and 0.2 mM NADH. Glyceraldehyde 3-phosphate dehydrogenase was used as the coupling enzyme; 100 μg was used per assay. The reaction in a total volume of 1 ml at 25°C was started by adding 0.25 μg normal PGK per assay. The PGA concentration was varied between 0.098 mM and 4.91 mM at a saturating MgATP concentration of 4.11 mM. The curve was fit to the linear portion of the data, representing the high-affinity substrate binding site, to determine K_M. (B) Curve fit to the downward sloping portion of the data, representing the low-affinity substrate binding site, to determine V_{max}.

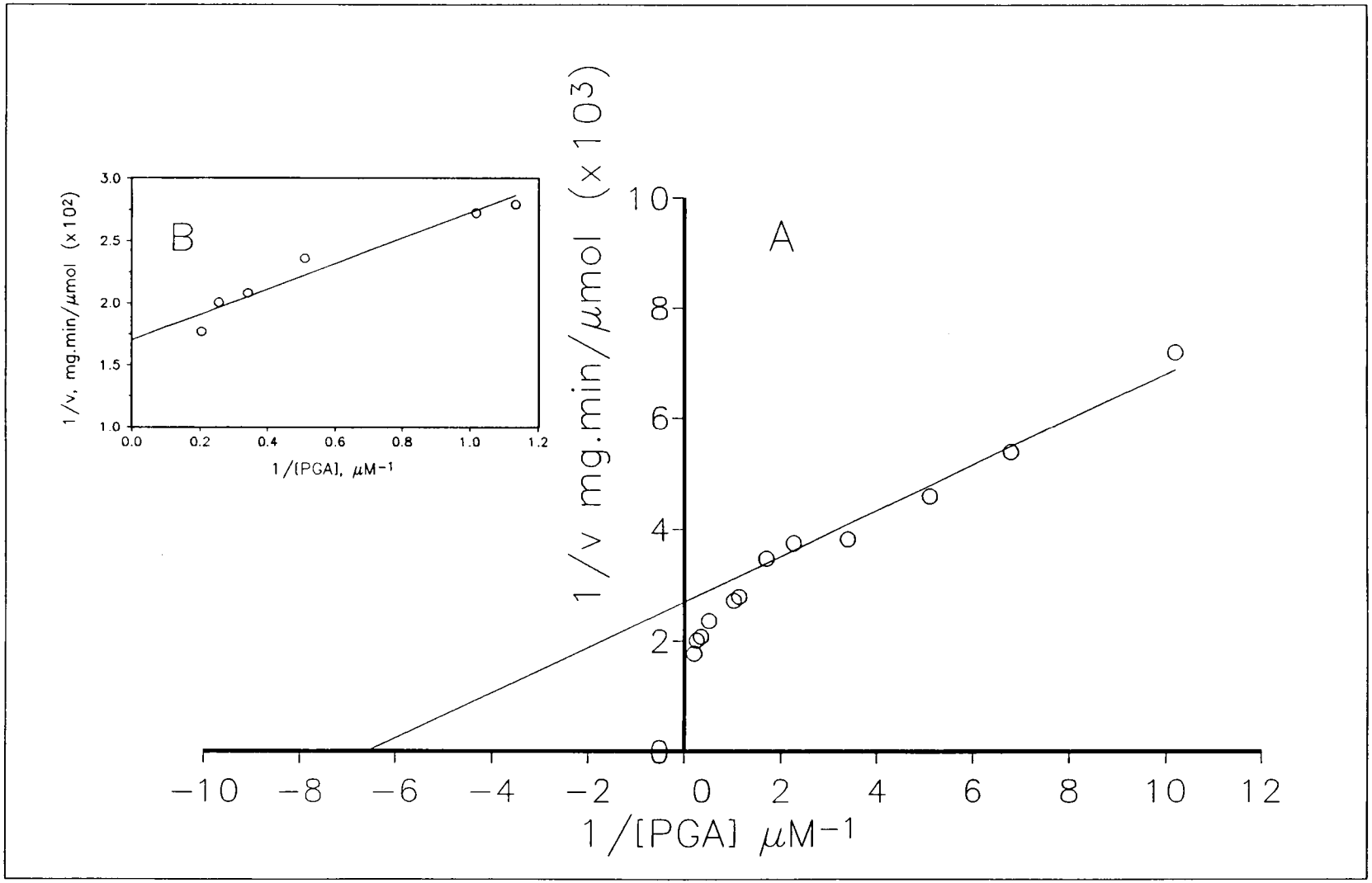
A
B
1/v mg.min/μmol (x103)
1/[PGA] μM−1
1/v, mg.min/μmol (x102)
1/[PGA], μM−1
10
8
6
4
2
0
−10
−8
−6
−4
−2
0
2
4
6
8
10
12
3.0
2.5
2.0
1.5
1.0
0.0
0.2
0.4
0.6
0.8
1.0
1.2

Figure 12. Kinetics of deuterated phosphoglycerate kinase with PGA as the variable substrate in the presence of 10 mM sulfate.

(A) Double-reciprocal plots of initial velocity *vs*. PGA concentration. Assay mix contained 50 mM Tris-HCl, ph 7.5, 0.2 mM NADH, $MgCl_2$ in 1 mM excess of the ATP concentration, and 10 mM Na_2SO_4. Glyceraldehyde 3-phosphate dehydrogenase was used as the coupling enzyme; 100 μg was used per assay. The reaction in a total volume of 1 ml at 25°C was started by adding 0.686 μg deuterated PGK per assay. The PGA concentration was varied between 0.10 mM and 5.15 mM at the following MgATP concentrations: (○) 0.087 mM; (□) 0.21 mM; and (△) 0.44 mM. (B) $1/V_{max_{app}}$ for each curve plotted as a function of 1/MgATP concentration to determine V_{max}.

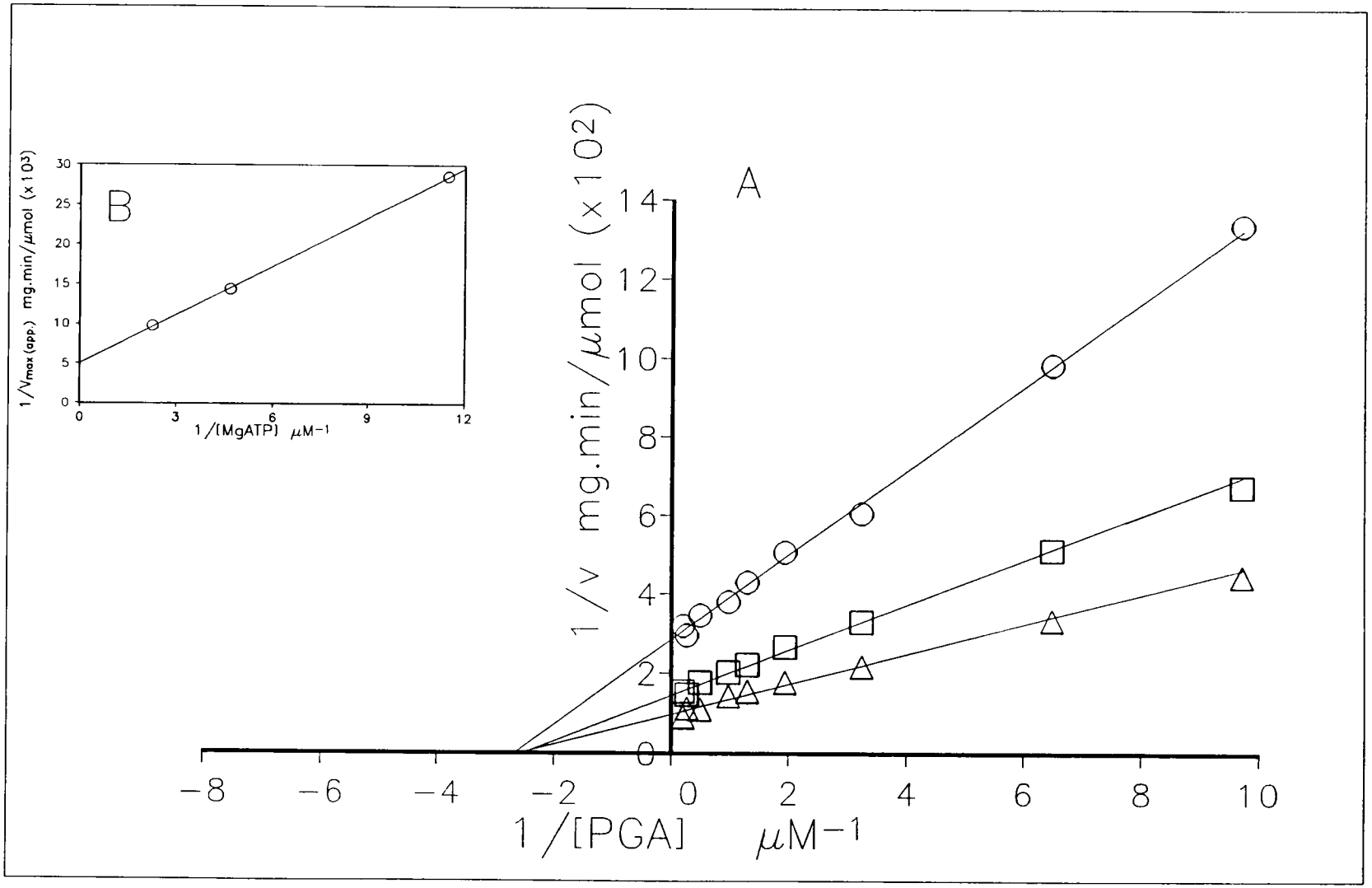
A
1/v mg.min/μmol (x102)
14
12
10
8
6
4
2
0
−8
−6
−4
−2
0
2
4
6
8
10
1/[PGA] μM−1
B
1/Vmax(app.) mg.min/μmol (x103)
30
25
20
15
10
5
0
0
3
6
9
12
1/[MgATP] μM−1

Figure 13. Inhibition of yeast phosphoglycerate kinase by D-glycerol-3-phosphate.

(A) Double reciprocal plot of initial velocity *vs.* PGA concentration. D,L-glycerol-3-phosphate concentrations were (from top to bottom) 3.64 mM (△), 1.56 mM (□), and 0.0 mM (○). The assay mixture also contained 50 mM Tris-HCl, pH 7.5, 0.26 mM ATP, 1.36 mM $MgCl_2$, 100 mM NaCl, and 0.2 mM NADH. Glyceraldehyde 3-phosphate dehydrogenase was used as the coupling enzyme; 100 μg was used per assay. The reaction in a total volume of 1 ml at 25°C was started by the addition of 0.25 μg PGK per assay. (B) Secondary plot of slopes *vs.* D,L-glycerol-3-phosphate concentration, to determine K_i.

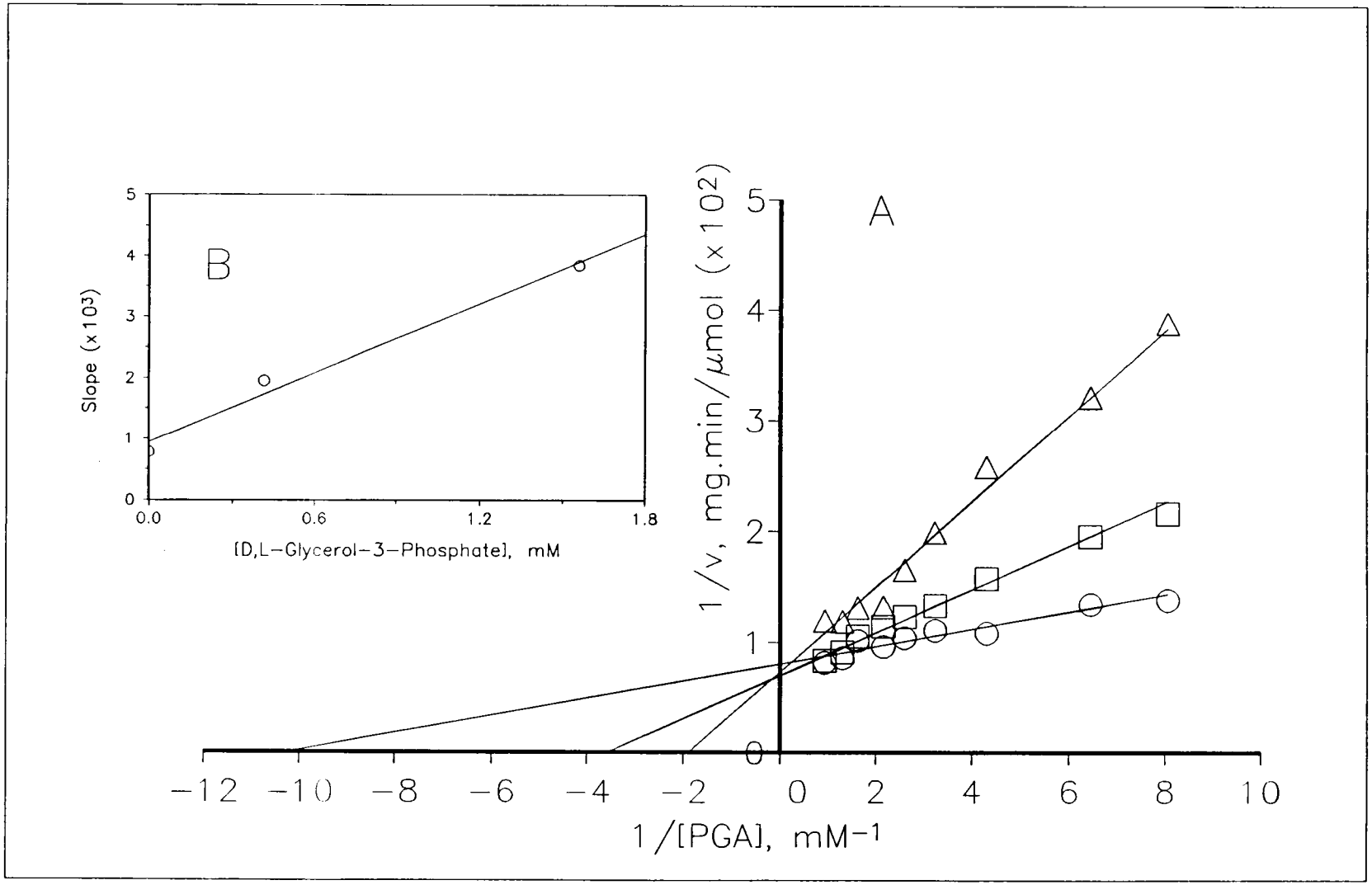
A
B
1/v, mg.min/μmol (x102)
1/[PGA], mM-1
Slope (x103)
[D,L-Glycerol-3-Phosphate], mM
0
1
2
3
4
5
6
8
10
-12
-10
-8
-6
-4
-2
0.0
0.6
1.2
1.8

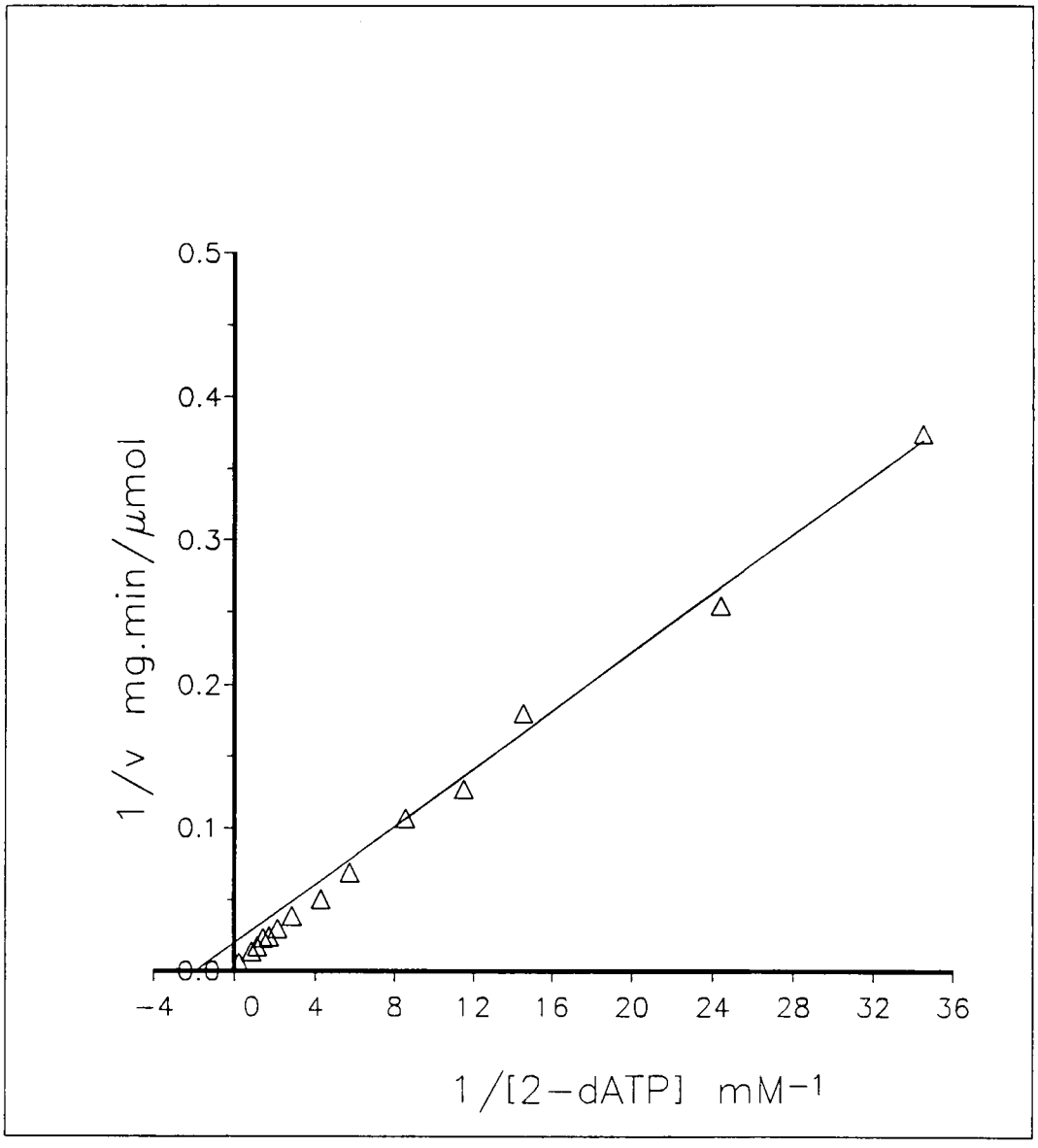

Figure 14. Kinetics of normal PGK with 2′-deoxyadenosine 5′-triphosphate as the variable substrate at saturating concentration of PGA. Double reciprocal plot of initial velocity vs. Mg-2′dATP concentration. The assay mixture contained 50 mM Tris-HCl, pH 7.5, 100 mM NaCl, 100 μg GAPDH, $MgCl_2$ in 1 mM excess of the 2′-dATP concentration, and 0.2 mM NADH. Concentration of Mg-2′dATP was varied between 0.029 mM and 1.17 mM at a PGA concentration of 7.37 mM. The reaction in a total volume of 1 ml at 25°C was started by addition of 0.254 μg PGK per assay.

Figure 15. Mn^{2+} binding to normal PGK.
(A) Titration of $MnCl_2$ with PGK, plotted as the double reciprocal of observed enhancement (ϵ^*) *vs.* enzyme concentration. $MnCl_2$ concentrations were (from top to bottom) 50.3 μM (◇), 75.3 μM (△), 150.5 μM (□), and 224.7 μM (○). Samples also contained 50 mM Tris-HCl, pH 7.5, and 100 mM NaCl. PGK was titrated into the samples up to a concentration of 513 μM. (B) Scatchard plot of Mn^{2+} binding to PGK. Additional points using $MnCl_2$ concentrations of 0.301 mM-3.5 mM at a PGK concentration of 272.5 μM were obtained to complete data required for the Scatchard plot.

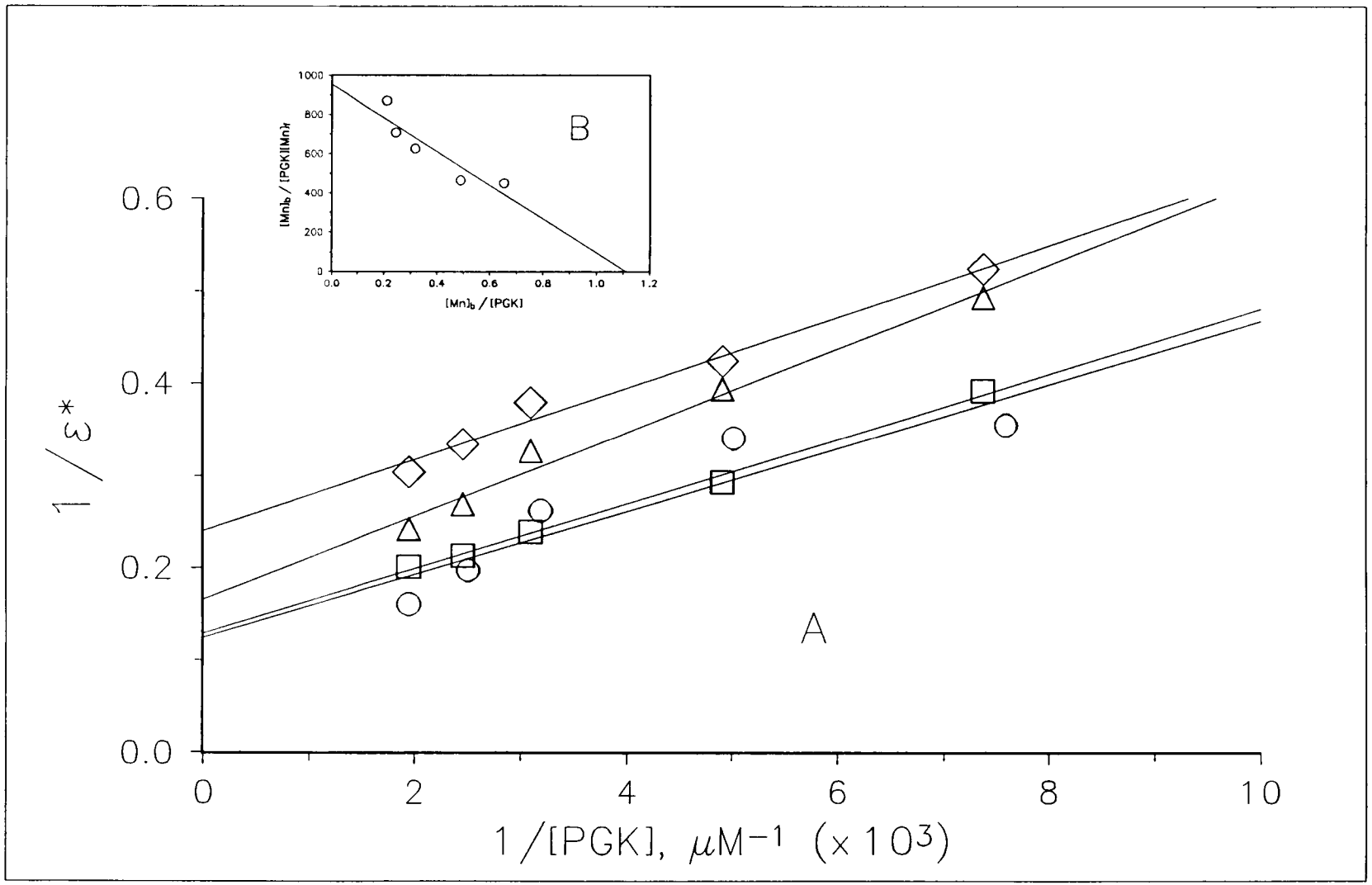
B
$[Mn]_b$ / [PGK][Mn]$_f$
$[Mn]_b$ / [PGK]
A
$1/\omega^*$
1/[PGK], μM^{-1} ($\times 10^3$)

Figure 16. Mn^{2+} binding to deuterated PGK.
(A) Titration of $MnCl_2$ with dPGK, plotted as the double reciprocal of observed enhancement (ϵ^*) *vs.* enzyme concentration. $MnCl_2$ concentration was 150.5 μM (O). Samples also contained 50 mM Tris-HCl, pH 7.5, and 100 mM NaCl. DPGK was titrated into the samples up to a concentration of 311 μM. (B) Scatchard plot of Mn^{2+} binding to dPGK. Additional points using $MnCl_2$ concentrations of 1.3 mM-3.5 mM at a dPGK concentration of 249 μM were obtained to complete data required for the Scatchard plot.

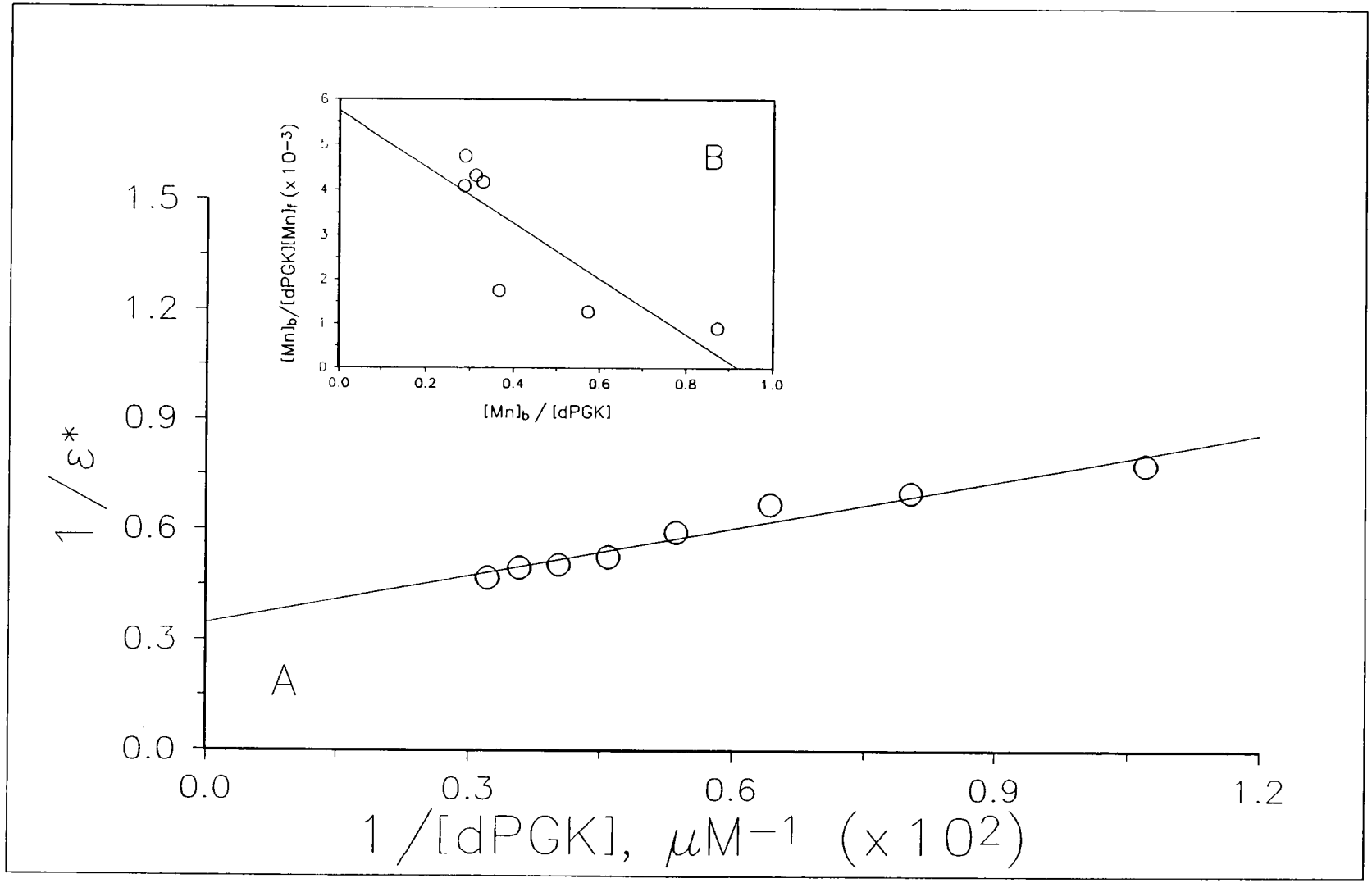
1.5
1.2
0.9
0.6
0.3
0.0
1/ω*
A
0.0
0.3
0.6
0.9
1.2
1/[dPGK], μM⁻¹ (x 10²)
B
[Mn]b/[dPGK][Mn]f (x 10⁻³)
[Mn]b / [dPGK]
0.0
0.2
0.4
0.6
0.8
1.0

Figure 17. Titration to determine ϵ_T for PGK-Mn^{2+}-ATP complex.

(A) Titration of PGK-Mn^{2+} complex with ATP, plotted as the double reciprocal of observed enhancement (ϵ^*) *vs.* ATP concentration. All titrations were done at a $MnCl_2$ concentration of 50.5 μM; PGK concentrations were 131.7 μM (○), 199.3 μM (□), 313.2 μM (△), 398.7 μM (◇), and 512.6 μM (▽). Samples also contained 50 mM Tris-HCl, pH 7.5, and 100 mM NaCl. Curves are fit to the linear portion of the data, representing ternary complex formation; at higher ATP concentrations, metal dissociates from the enzyme to form the binary metal-ATP complex which has a lower enhancement than the ternary complex. Extrapolated values of enhancement to infinite ATP concentration for each PGK concentration are designated ϵ_c^*. (B) Secondary double-reciprocal plot of ϵ_c^* *vs.* PGK concentration for each curve in plot (A). Extrapolation of this curve to infinite enzyme concentration gives ϵ_T.

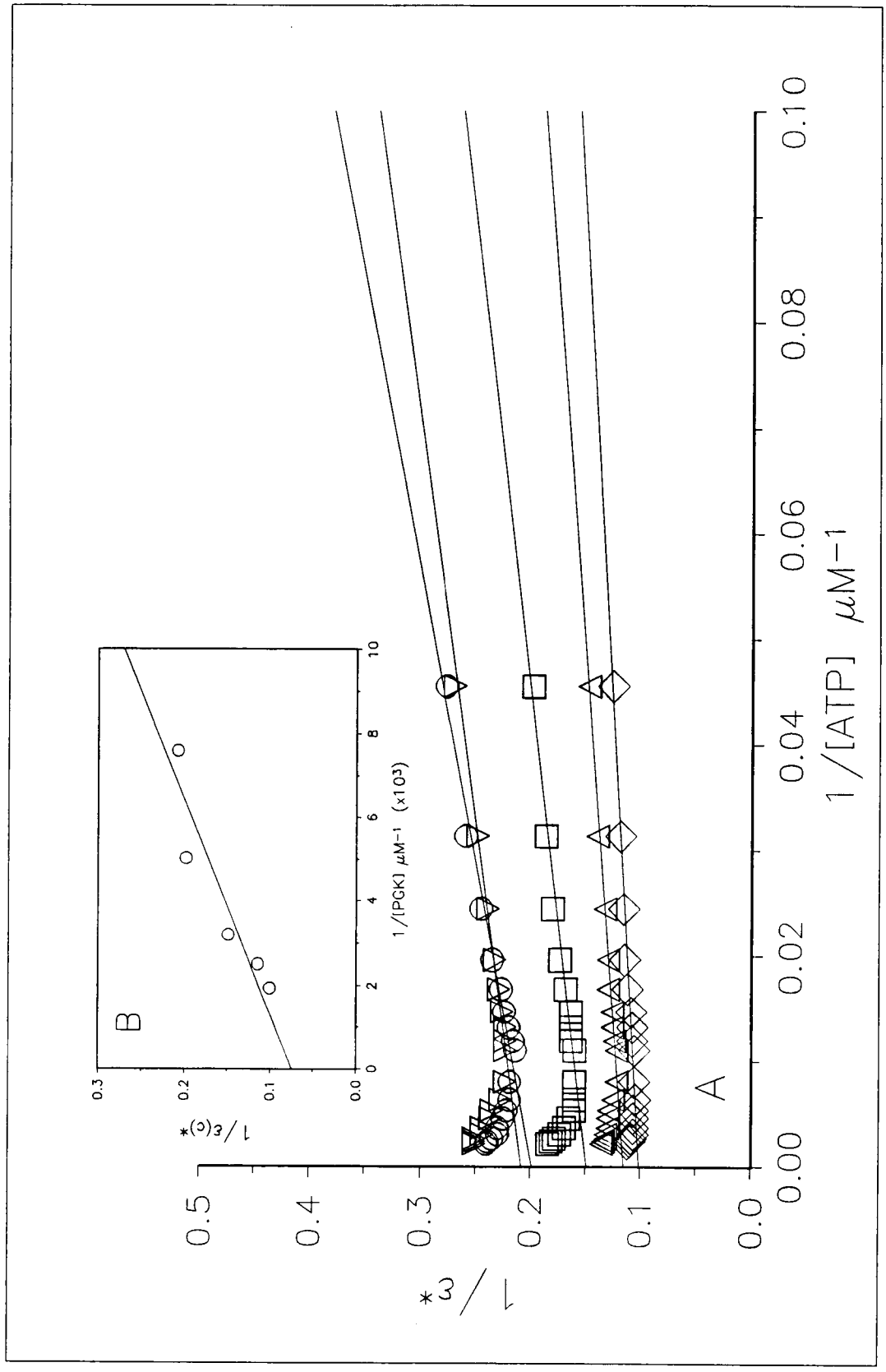
A
B
1/ε*
1/[ATP] μM−1
0.0
0.1
0.2
0.3
0.4
0.5
0.00
0.02
0.04
0.06
0.08
0.10
1/ε(c)*
1/[PGK] μM−1 (x10³)
0.0
0.1
0.2
0.3
0
2
4
6
8
10

Figure 18. ATP binding to PGK and deuterated PGK.
Titration of the enzyme-metal complex with ATP, showing the changes in the observed enhancement (ϵ^*) of the paramagnetic effects of Mn^{2+} on $1/T_1$ of coordinated water protons. Normal PGK concentration was 131.7 μM with $MnCl_2$ concentrations of 100.6 μM (O) and 150.9 μM (□). Deuterated PGK concentration was 124.4 μM with $MnCl_2$ concentration of 100.9 μM (△). Samples also included 50 mM Tris-HCl, pH 7.5, and 100 mM NaCl.

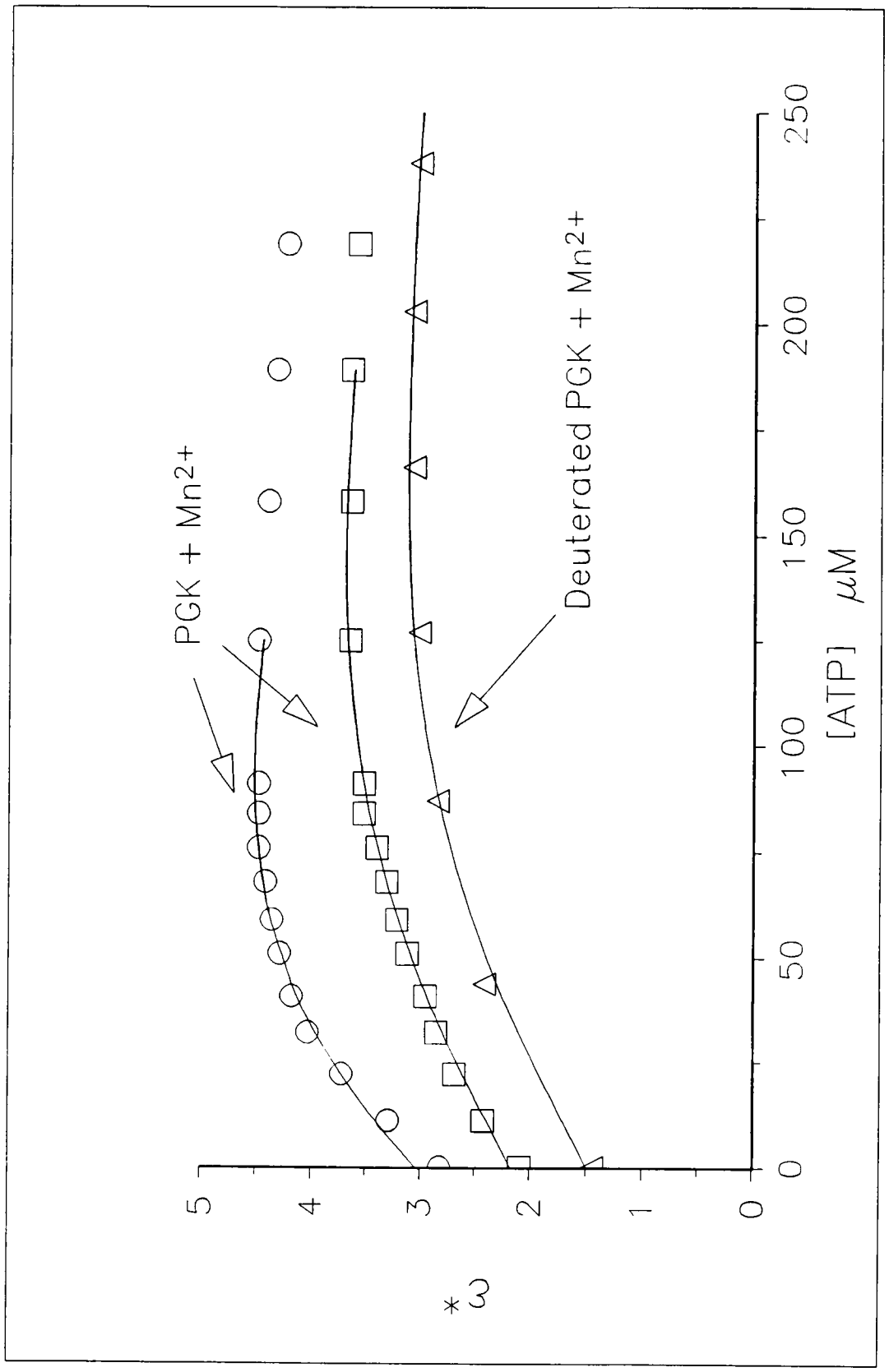
PGK + Mn2+
Deuterated PGK + Mn2+
[ATP] μM
*ω
0
50
100
150
200
250
0
1
2
3
4
5

Figure 19. Quaternary complex formation with normal PGK and deuterated PGK.

Titration of the enzyme-metal-ATP complex with glycerol-3-phosphate, a phosphoglycerate analogue, showing changes in the observed enhancement (ϵ^*) of the paramagnetic effects of Mn^{2+} on coordinated water protons. The titration with the normal enzyme (O) was carried out with 100.9 μM $MnCl_2$, 120.2 μM PGK, 181.3 μM ATP, and glycerol-3-phosphate concentrations up to 10.0 mM. The titration with the deuterated enzyme (□) was carried out with 100.6 μM $MnCl_2$, 132.6 μM dPGK, 181.3 μM ATP, and glycerol-3-phosphate concentrations up to 10.7 mM. All samples also contained 50 mM Tris-HCl, pH 7.5, and 100 mM NaCl.

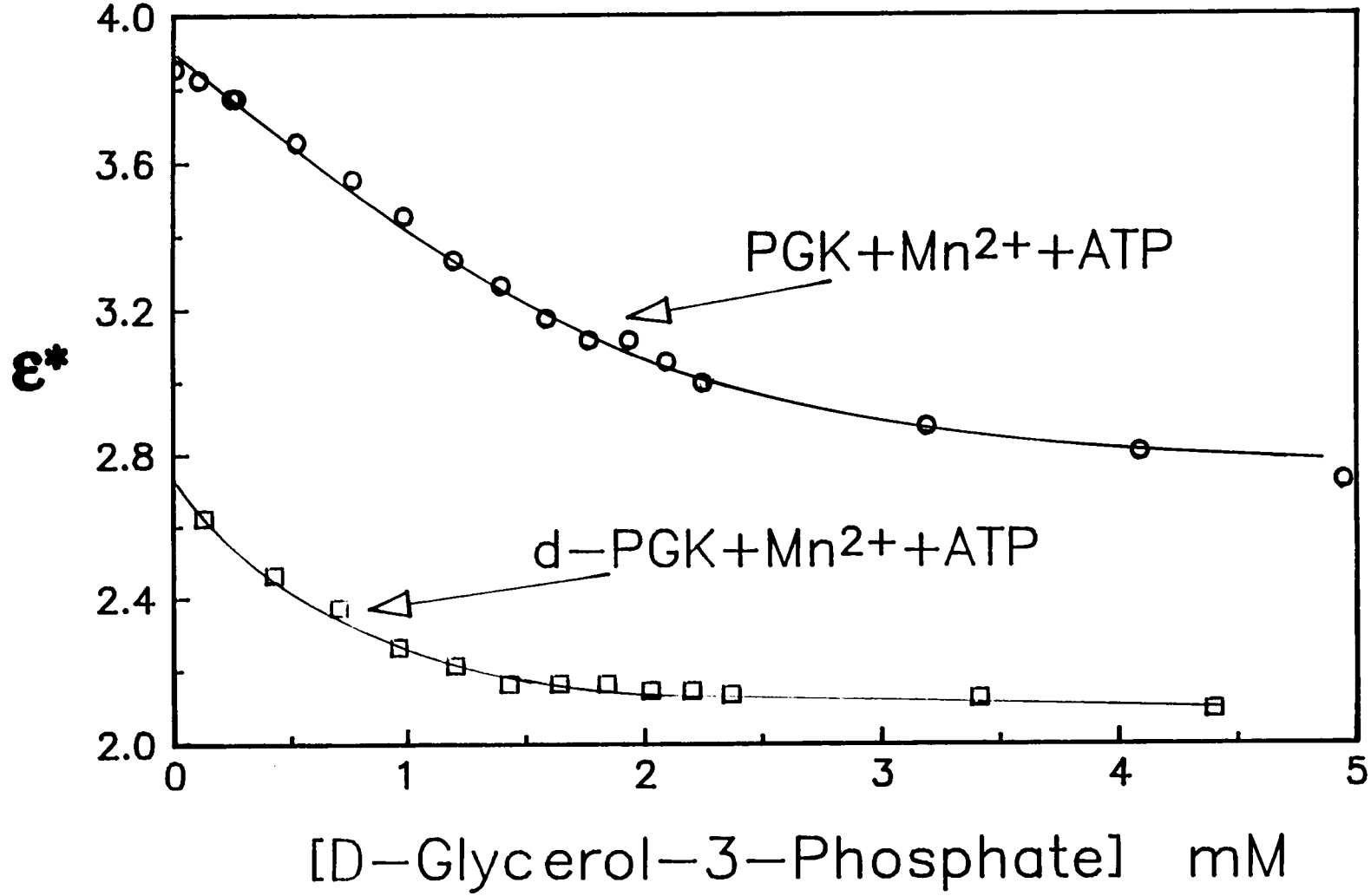
4.0
3.6
3.2
2.8
2.4
2.0
ε*
0
1
2
3
4
5
PGK+Mn2++ATP
d−PGK+Mn2++ATP
[D−Glycerol−3−Phosphate] mM

Figure 20. ^{1}H NMR spectrum of free 2′-deoxyadenosine 5′-triphosphate (2′-dATP).

The concentration of the 2′-dATP sample was 19.14 mM in $^{2}H_2O$ (99.96 atom %). The spectrum was recorded on a Bruker AMX400 spectrometer at 27°C. Quadrature phase detection and a 60° observation pulse were used. 32K data points were collected for 128 transients over a spectral width of 6024 Hz, with an acquisition time of 2.72 s and a relaxation delay of 6 s. Chemical shifts were determined relative to external DSS. Prior to Fourier transformation, an exponential multiplication function with a linebroadening factor of 1.0 Hz was applied to the free induction decays.

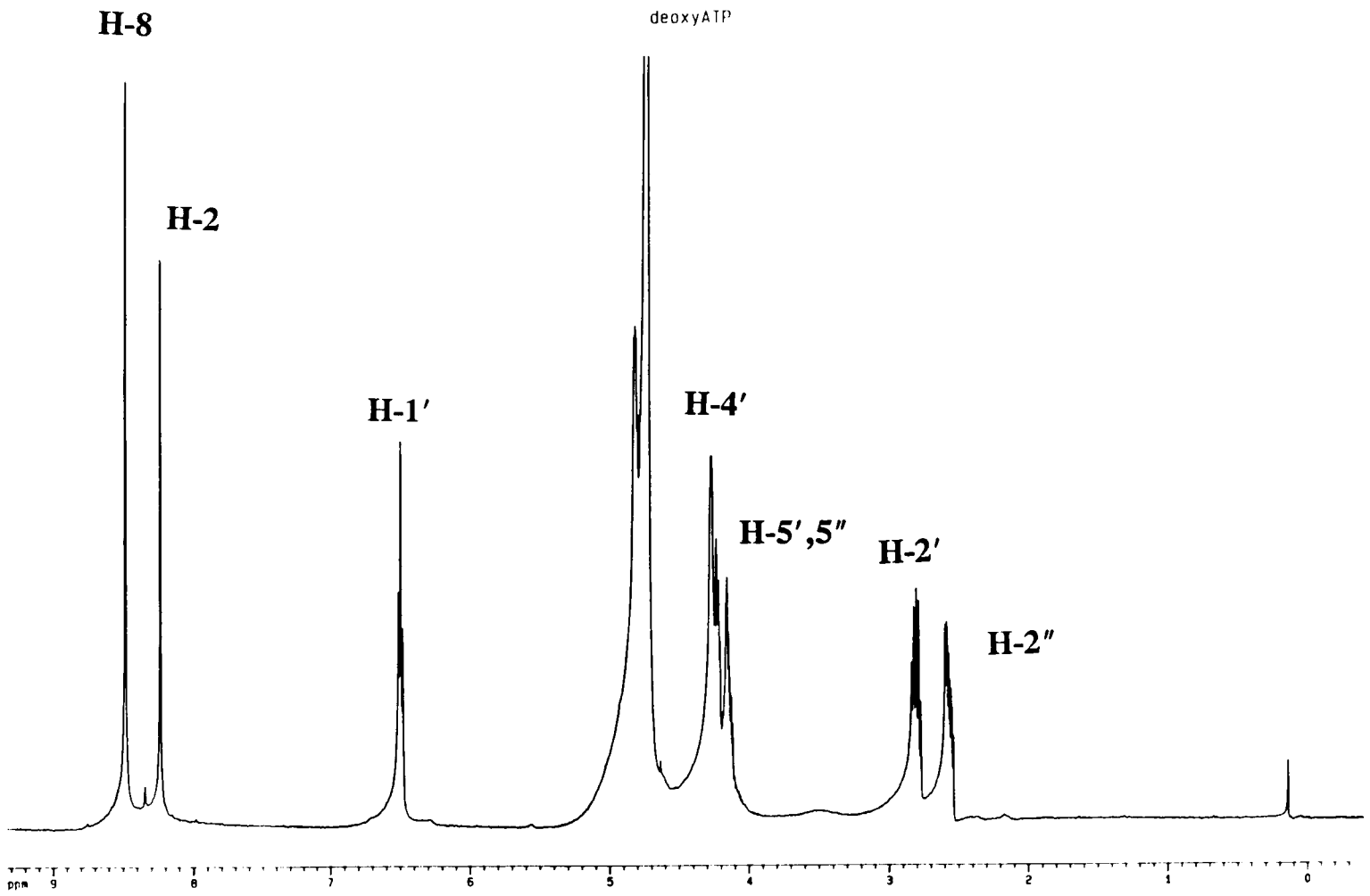
deoxyATP
H-8
H-2
H-1′
H-4′
H-5′,5″
H-2′
H-2″
ppm 9
8
7
6
5
4
3
2
1
0

Figure 21. ^{1}H NMR spectrum of 2′-deoxyadenosine 5′-triphosphate (2′-dATP) bound to normal phosphoglycerate kinase.

The concentration of the 2′-dATP sample was 4.78 mM in $^{2}H_2O$ (99.96 atom %), with 458.5 μM PGK, 5.73 μM $MgCl_2$, and 100 mM NaCl. The spectrum was recorded on a Bruker AMX400 spectrometer at 27°C. Quadrature phase detection and a 60° observation pulse were used. 32K data points were collected for 128 transients over a spectral width of 6024 Hz, with an acquisition time of 2.72 s and a relaxation delay of 12 s. Chemical shifts were determined relative to external DSS. Prior to Fourier transformation, an exponential multiplication function with a linebroadening factor of 1.0 Hz was applied to the free induction decays. (A) Region upfield of the $^{1}HO^{2}H$ resonance. (B) Region downfield of the $^{1}HO^{2}H$ resonance.

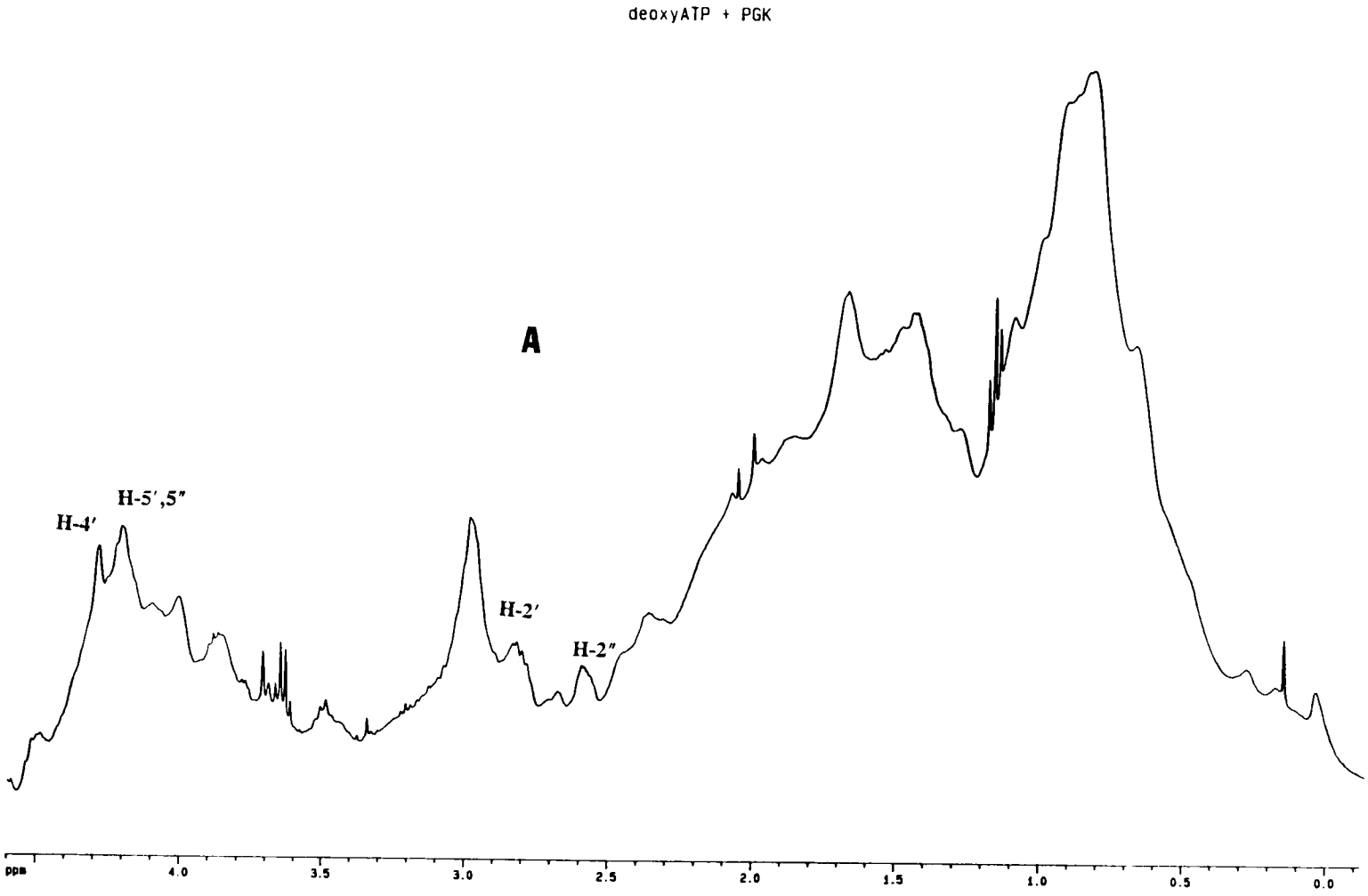
deoxyATP + PGK
A
H-4′
H-5′,5″
H-2′
H-2″
ppm
4.0
3.5
3.0
2.5
2.0
1.5
1.0
0.5
0.0

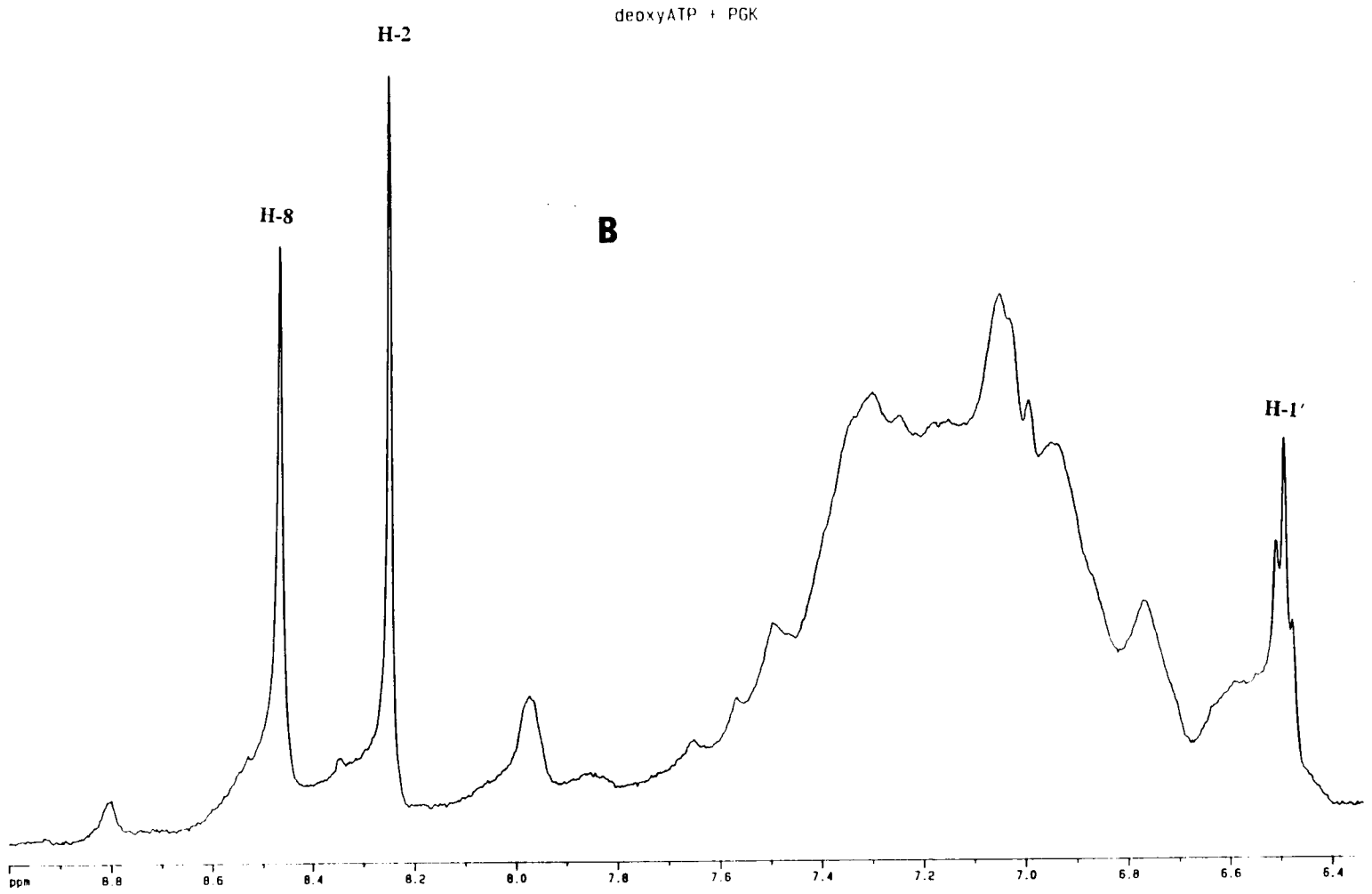
deoxyATP + PGK
H-2
H-8
B
H-1'
ppm
8.8
8.6
8.4
8.2
8.0
7.8
7.6
7.4
7.2
7.0
6.8
6.6
6.4

Figure 22. ^{1}H NMR spectrum of 2′-deoxyadenosine 5′-triphosphate (2′-dATP) bound to deuterated phosphoglycerate kinase.

The concentration of the 2′-dATP sample was 4.78 mM in $^{2}H_2O$ (99.96 atom %), with 452.5 μM dPGK, 5.73 μM $MgCl_2$, and 100 mM NaCl. The spectrum was recorded on a Bruker AMX400 spectrometer at 27°C. Quadrature phase detection and a 60° observation pulse were used. 32K data points were collected for 128 transients over a spectral width of 6024 Hz, with an acquisition time of 2.72 s and a relaxation delay of 12 s. Chemical shifts were determined relative to external DSS. Prior to Fourier transformation, an exponential multiplication function with a linebroadening factor of 1.0 Hz was applied to the free induction decays. (A) Region upfield of the $^{1}HO^{2}H$ resonance. (B) Region downfield of the $^{1}HO^{2}H$ resonance.

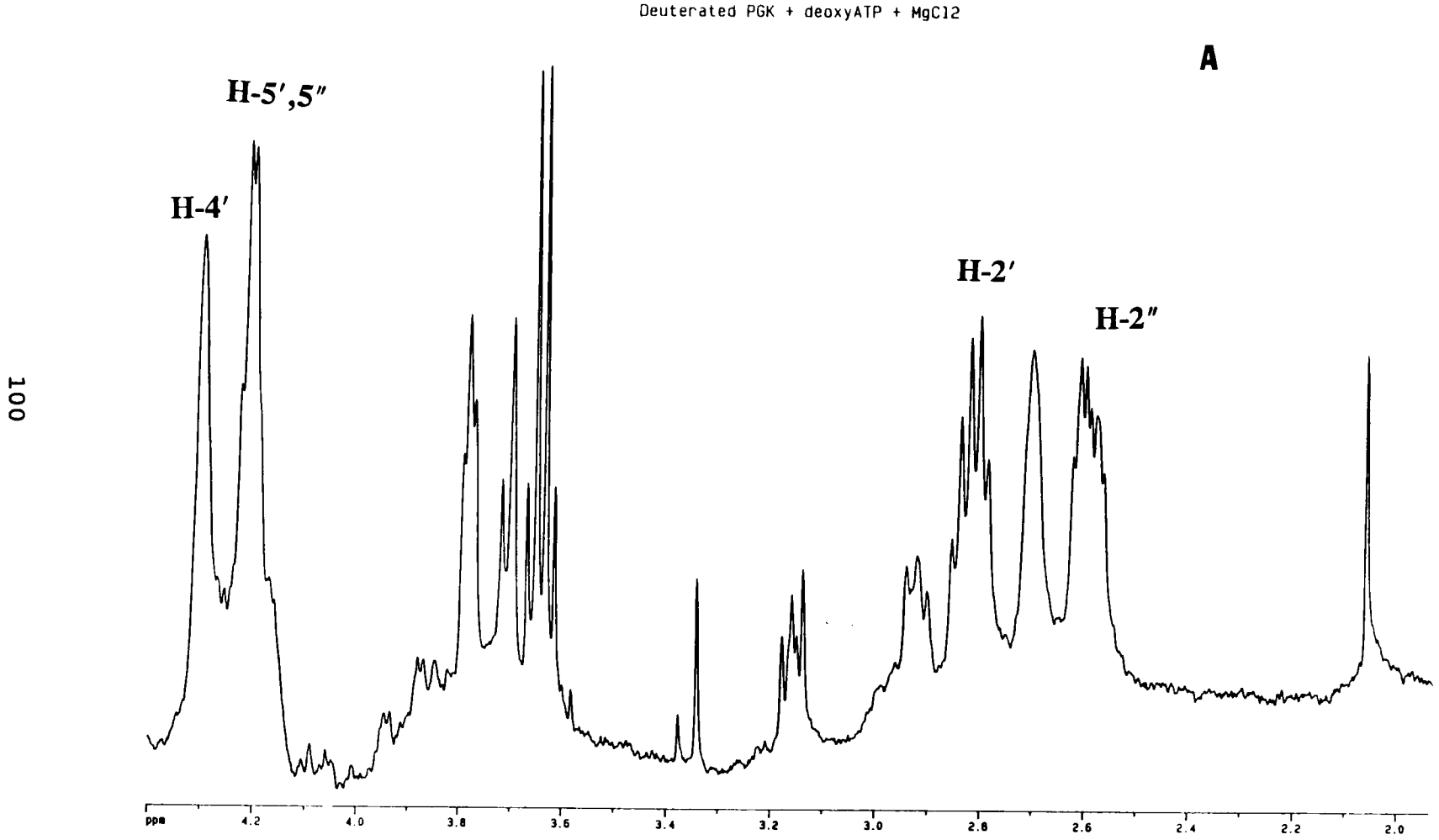
Deuterated PGK + deoxyATP + MgCl2
A
H-5′,5″
H-4′
H-2′
H-2″
100
ppm
4.2
4.0
3.8
3.6
3.4
3.2
3.0
2.8
2.6
2.4
2.2
2.0

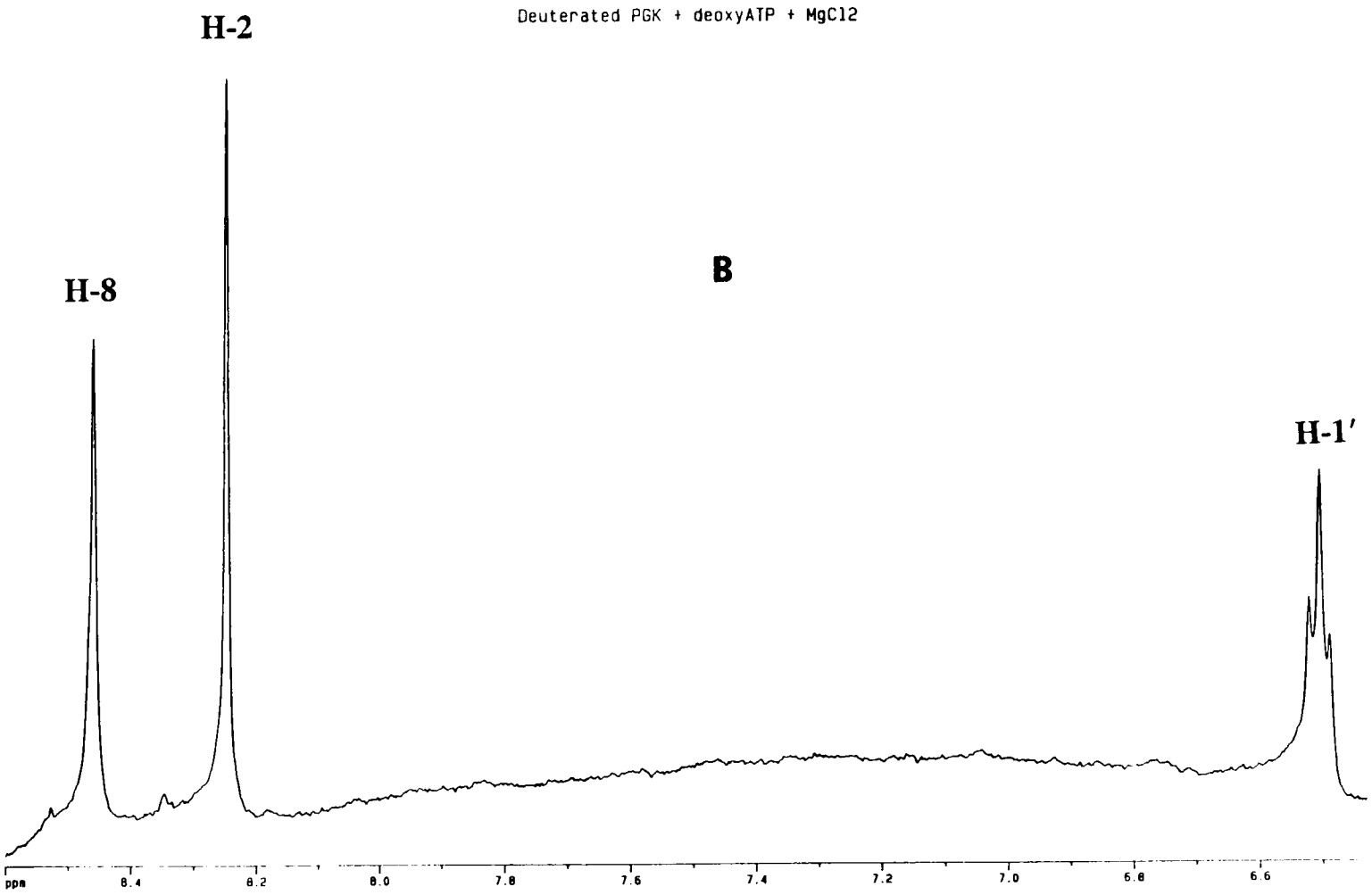
Deuterated PGK + deoxyATP + MgCl2
H-2
H-8
B
H-1′
ppm
8.4
8.2
8.0
7.8
7.6
7.4
7.2
7.0
6.8
6.6

Figure 23. ^{1}H NMR contour plot of 2′-deoxyadenosine 5′-triphosphate (2′-dATP) bound to normal phosphoglycerate kinase, mixing time 30 ms.

NOESY experiment with mixing time of 30 ms carried out on a 4.78 mM sample of 2′-dATP in $^{2}H_{2}O$ (99.96 atom %) with 399.7 μM PGK, 5.73 mM $MgCl_{2}$, 100 mM NaCl, and 40 mM deuterated Tris-^{2}HCl, pH 7.5. The spectrum was recorded on a Bruker AMX400 spectrometer at 30°C. Data were collected in the phase sensitive mode using the TPPI method. The transmitter offset was placed on the $HO^{2}H$ resonance, which was irradiated during the relaxation delay of 1.0 s to suppress the water signal. Mixing time was randomly varied up to ± 5% in order to eliminate COSY cross-peaks. 2K data points were collected over a spectral width of 4032.26 Hz in t_{2} for each t_{1} value, with 128 transients per free induction decay. The data were zero-filled to 2K points in t_{1} and were multiplied by a $\sin^{2}$ window function in both dimensions before Fourier transformation. (A) Full spectrum, with visible substrate crosspeaks 2′→ 1′, 2″→ 1′, 2′→ 8. (B) Enlargement of region around the substrate crosspeaks.

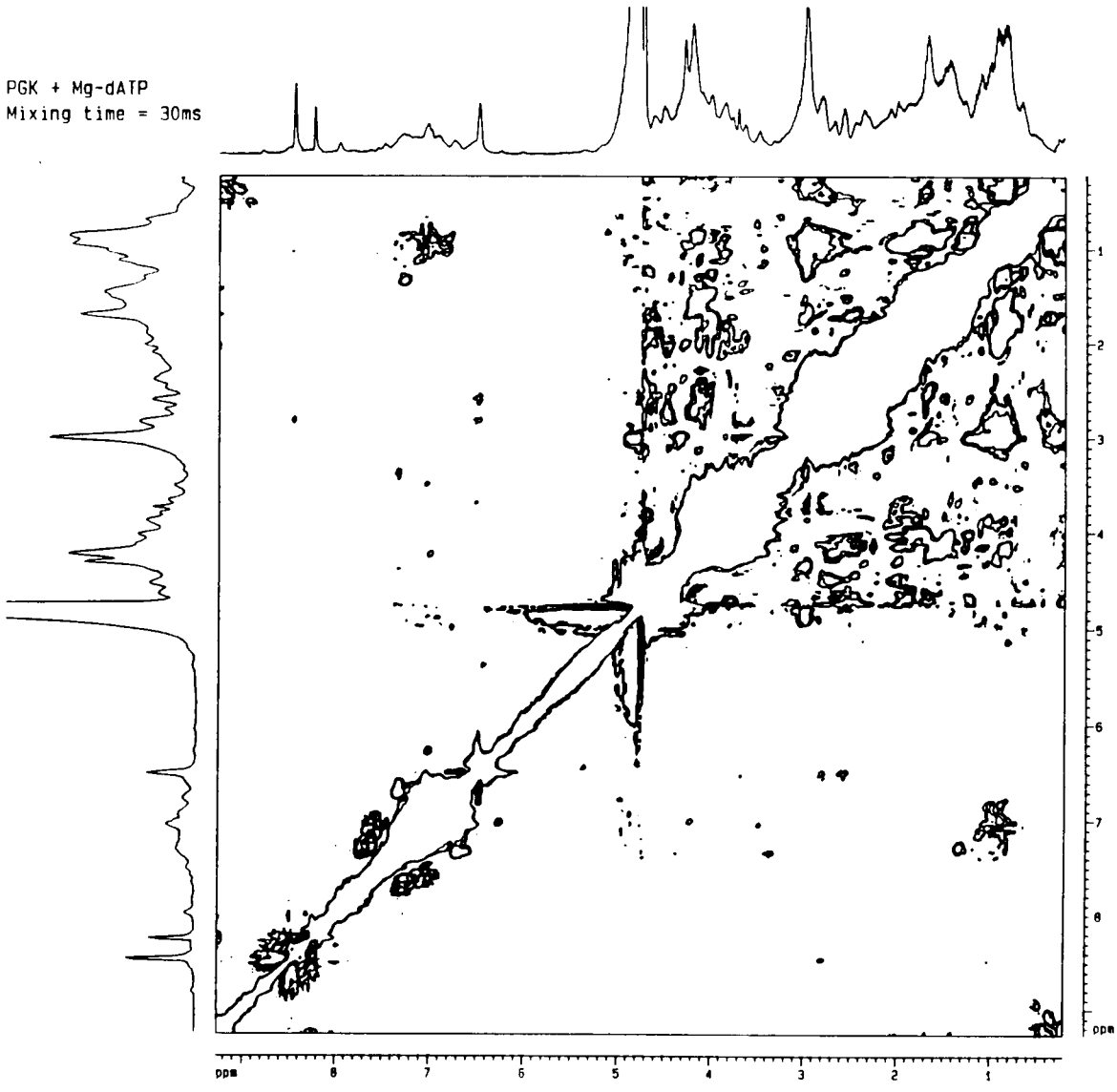

A

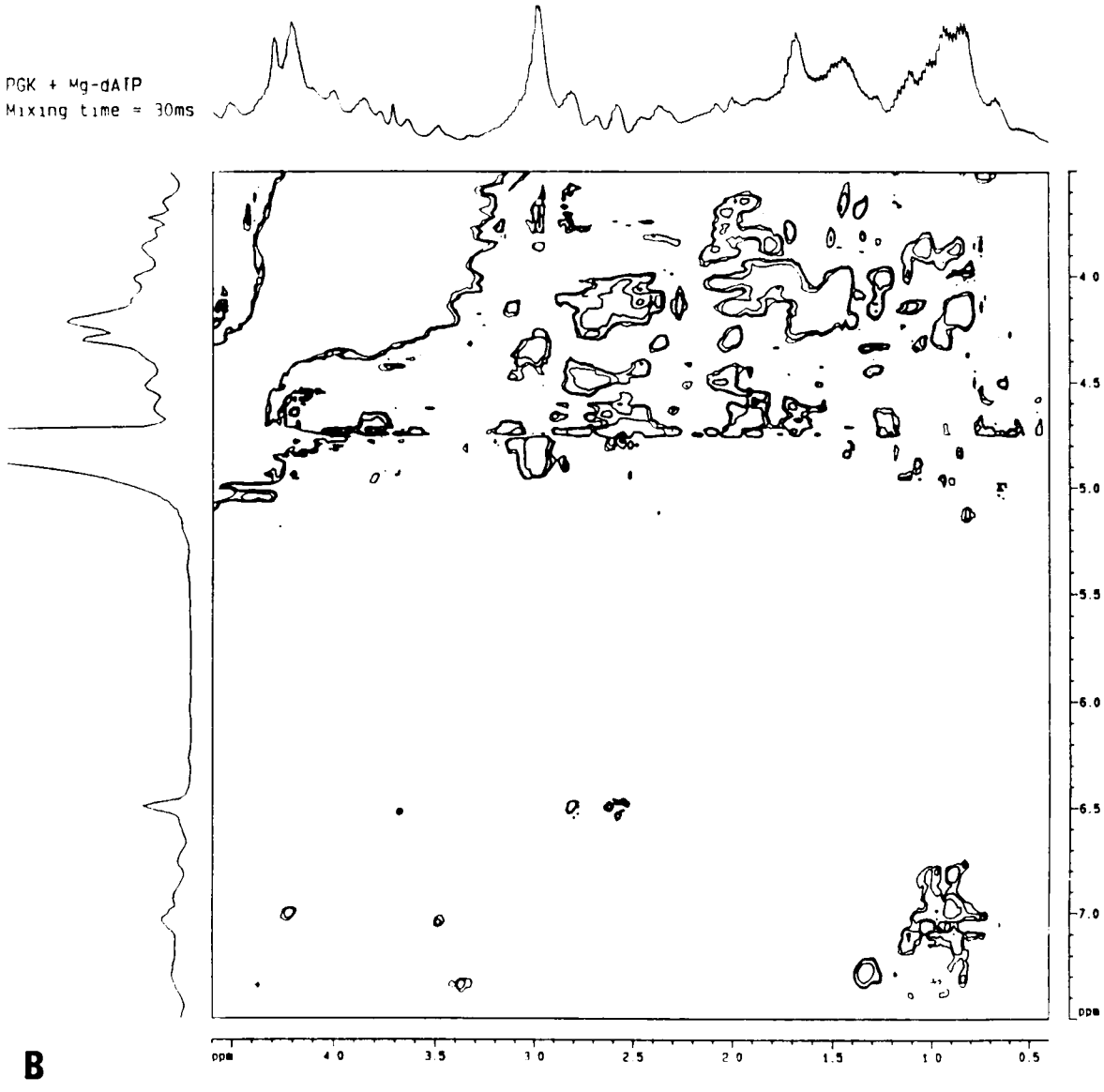
PGK + Mg-dATP
Mixing time = 30ms
4.0
4.5
5.0
5.5
6.0
6.5
7.0
ppm
ppm
4.0
3.5
3.0
2.5
2.0
1.5
1.0
0.5

B

Figure 24. ^{1}H NMR contour plot of 2′-deoxyadenosine 5′-triphosphate (2′-dATP) bound to deuterated phosphoglycerate kinase, mixing time 30 ms.

NOESY experiment with mixing time of 30 ms carried out on a 4.78 mM sample of 2′-dATP in $^{2}H_2O$ (99.96 atom %) with 400.7 μM PGK, 5.73 mM $MgCl_2$, 100 mM NaCl, and 40 mM deuterated Tris-^{2}HCl, pH 7.5. The spectrum was recorded on a Bruker AMX400 spectrometer at 30°C. Data were collected in the phase sensitive mode using the TPPI method. The transmitter offset was placed on the $HO^{2}H$ resonance, which was irradiated during the relaxation delay of 1.0 s to suppress the water signal. Mixing time was randomly varied up to ± 5% in order to eliminate COSY cross-peaks. 2K data points were collected over a spectral width of 4032.26 Hz in t_2 for each t_1 value, with 128 transients per free induction decay. The data were zero-filled to 2K points in t_1 and were multiplied by a $\sin^2$ window function in both dimensions before Fourier transformation. (A) Full spectrum, with visible substrate crosspeaks 2′→ 1′, 2″→ 1′, 2′→ 3′, and 2″→ 3′. (B) Enlargement of region around the substrate crosspeaks.

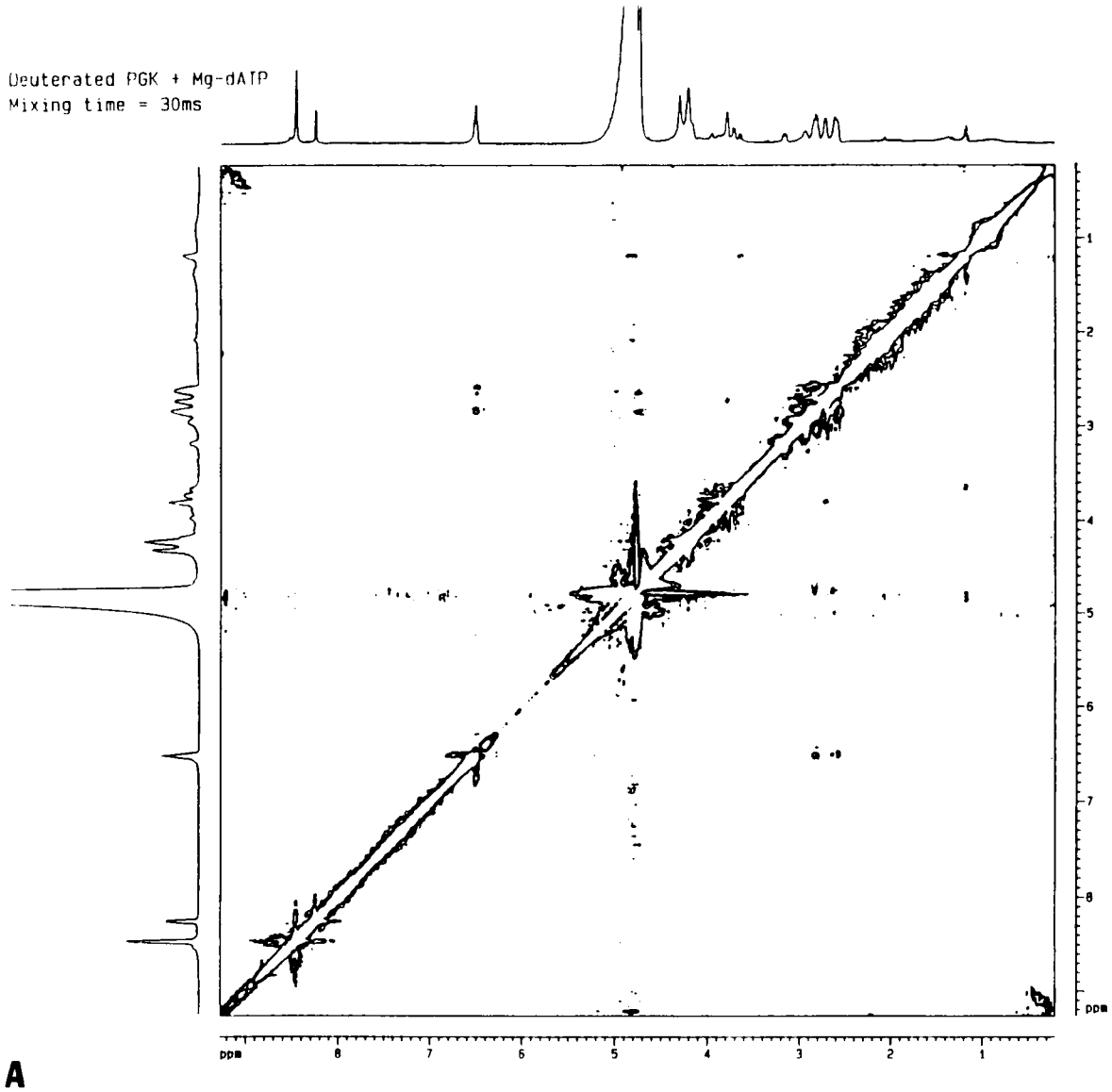

A

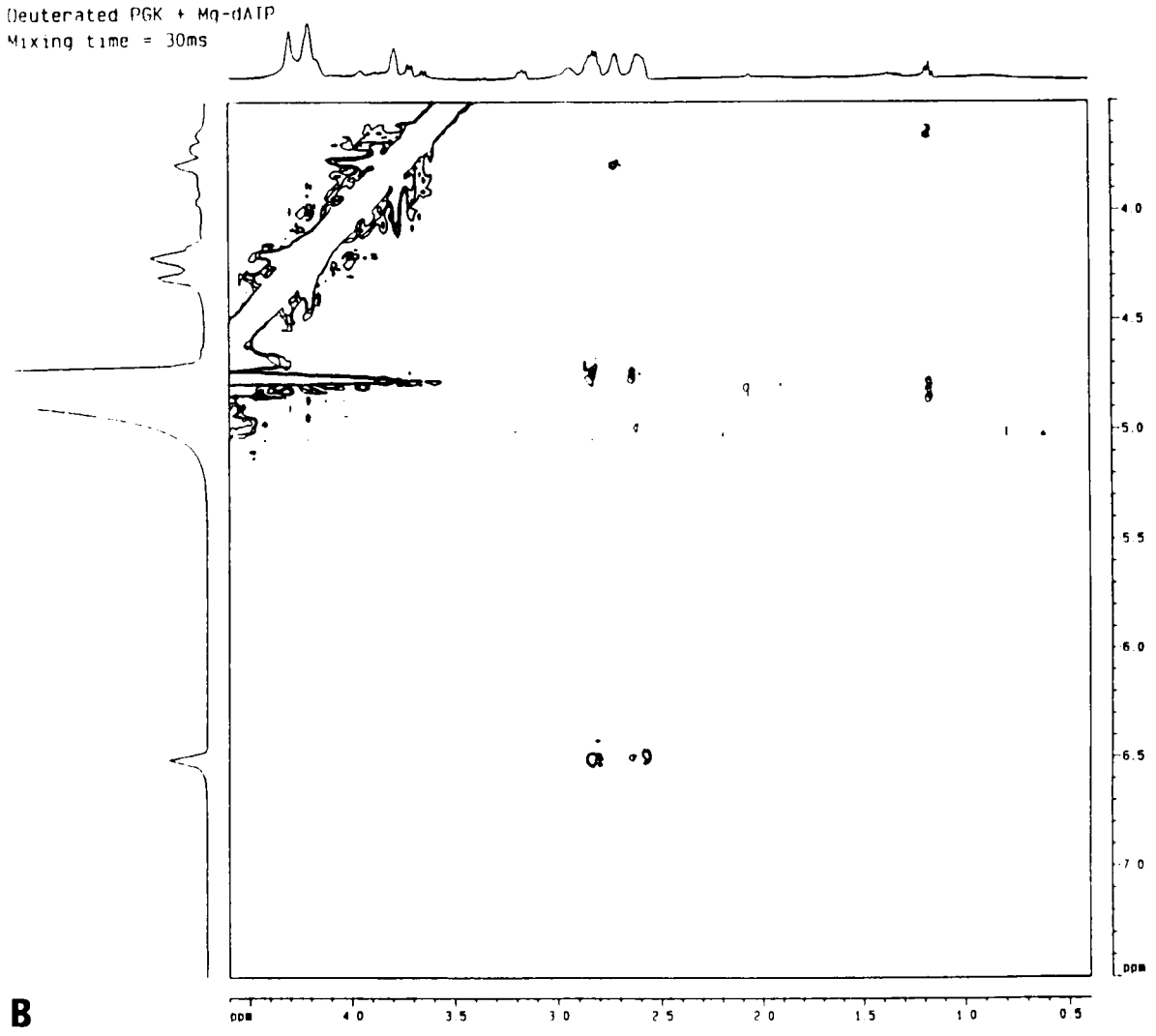
Deuterated PGK + Mg-dATP
Mixing time = 30ms
4.0
4.5
5.0
5.5
6.0
6.5
7.0
ppm
ppm
4.0
3.5
3.0
2.5
2.0
1.5
1.0
0.5

B

Figure 25. ^{1}H NMR contour plot of 2′-deoxyadenosine 5′-triphosphate (2′-dATP) bound to normal phosphoglycerate kinase, mixing time 200 ms.

NOESY experiment with mixing time of 200 ms carried out on a 4.78 mM sample of 2′-dATP in $^{2}H_2O$ (99.96 atom %) with 399.7 μM PGK, 5.73 mM $MgCl_2$, 100 mM NaCl, and 40 mM deuterated Tris-^{2}HCl, pH 7.5. The spectrum was recorded on a Bruker AMX400 spectrometer at 30°C. Data were collected in the phase sensitive mode using the TPPI method. The transmitter offset was placed on the $HO^{2}H$ resonance, which was irradiated during the relaxation delay of 1.0 s to suppress the water signal. Mixing time was randomly varied up to ± 5% in order to eliminate COSY cross-peaks. 2K data points were collected over a spectral width of 4032.26 Hz in t_2 for each t_1 value, with 128 transients per free induction decay. The data were zero-filled to 2K points in t_1 and were multiplied by a $\sin^2$ window function in both dimensions before Fourier transformation. (A) Full spectrum, with visible substrate crosspeaks 2′→ 1′, 2″→ 1′, 2′→ 3′, 2″→ 3′, 2′→ 8, and 4′→ 1′. (B) Enlargement of region around the substrate crosspeaks.

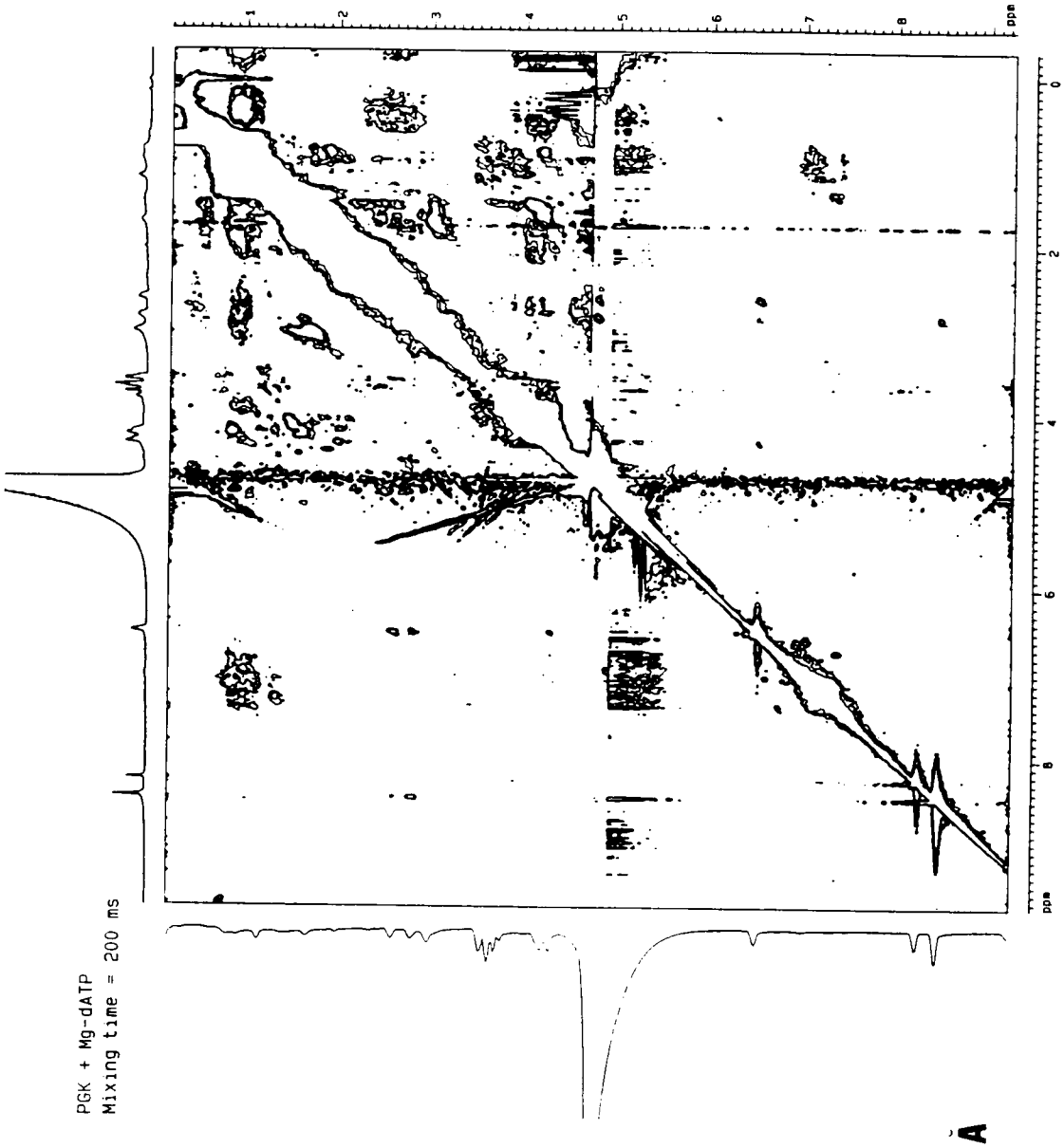
PGK + Mg-dATP
Mixing time = 200 ms
A

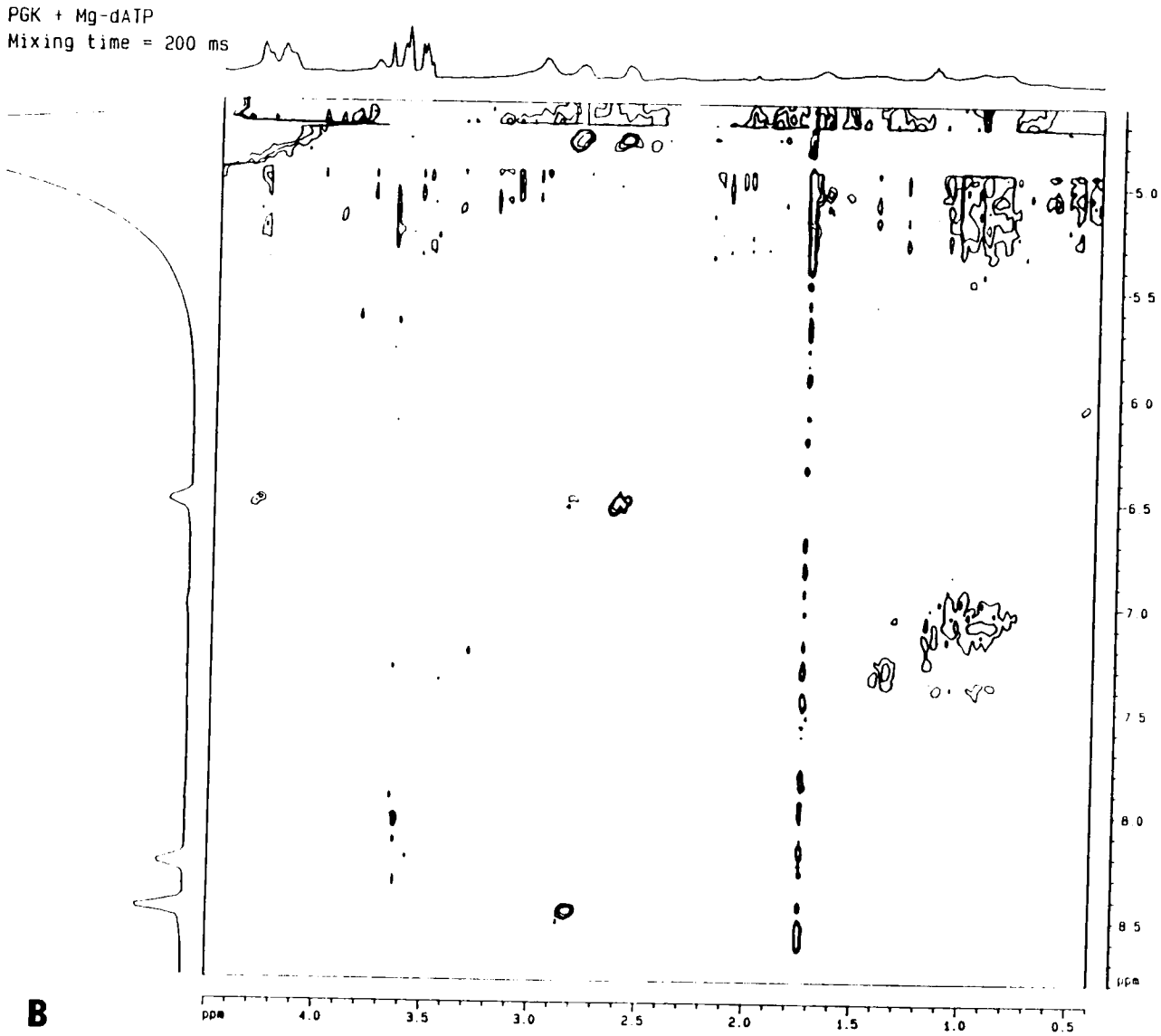
PGK + Mg-dATP
Mixing time = 200 ms
5.0
5.5
6.0
6.5
7.0
7.5
8.0
8.5
ppm
ppm
4.0
3.5
3.0
2.5
2.0
1.5
1.0
0.5

B

Figure 26. ^{1}H NMR contour plot of 2′-deoxyadenosine 5′-triphosphate (2′-dATP) bound to deuterated phosphoglycerate kinase, mixing time 200 ms.

NOESY experiment with mixing time of 200 ms carried out on a 4.78 mM sample of 2′-dATP in $^{2}H_{2}O$ (99.96 atom %) with 400.7 μM PGK, 5.73 mM $MgCl_{2}$, 100 mM NaCl, and 40 mM deuterated Tris-^{2}HCl, pH 7.5. The spectrum was recorded on a Bruker AMX400 spectrometer at 30°C. Data were collected in the phase sensitive mode using the TPPI method. The transmitter offset was placed on the $HO^{2}H$ resonance, which was irradiated during the relaxation delay of 1.0 s to suppress the water signal. Mixing time was randomly varied up to ± 5% in order to eliminate COSY cross-peaks. 2K data points were collected over a spectral width of 4032.26 Hz in t_{2} for each t_{1} value, with 128 transients per free induction decay. The data were zero-filled to 2K points in t_{1} and were multiplied by a $\sin^{2}$ window function in both dimensions before Fourier transformation. (A) Full spectrum, with visible substrate crosspeaks 2′→ 1′, 2″→ 1′, 2′→ 3′, 2″→ 3′, 2′→ 8, and 4′→ 1′. (B) Enlargement of region around the substrate crosspeaks.

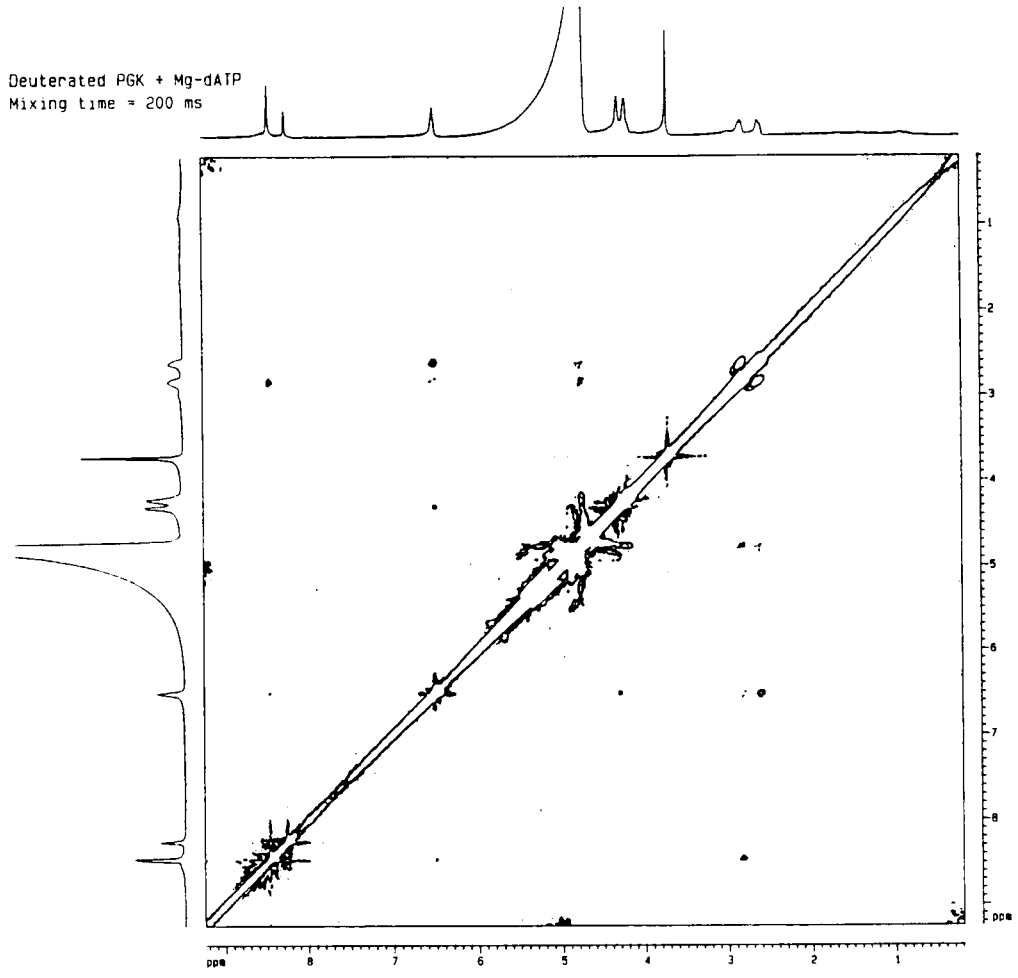

A

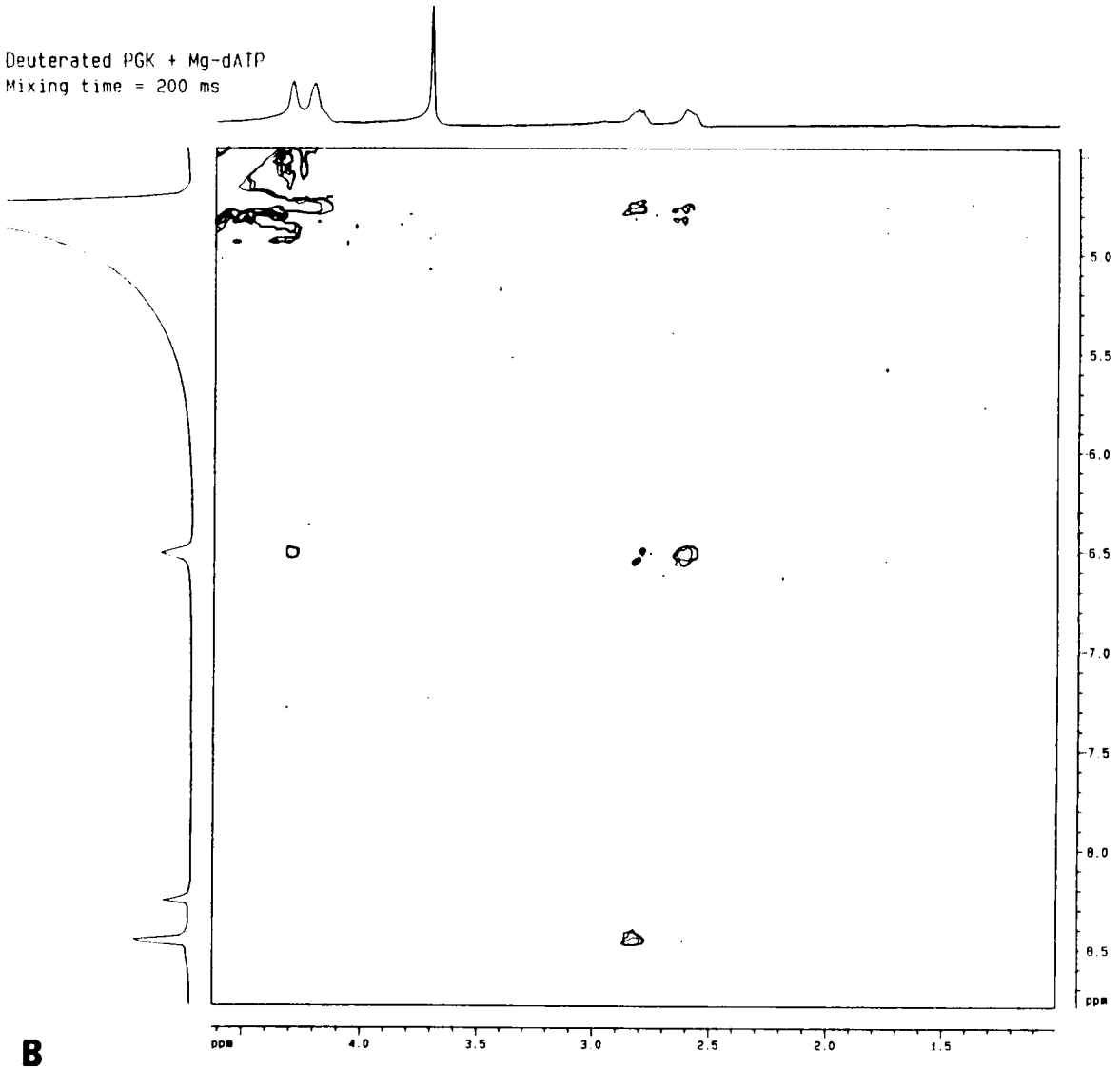
Deuterated PGK + Mg-dATP
Mixing time = 200 ms
5.0
5.5
6.0
6.5
7.0
7.5
8.0
8.5
ppm
ppm
4.0
3.5
3.0
2.5
2.0
1.5

B

TABLE 1

PURIFICATION DATA FOR DEUTERATED PHOSPHOGLYCERATE KINASE

Purification Step	Total Units PGK	%Recovery
Original Extract	23,751	100
Protamine Sulfate	21,151	89
1st Ammonium Sulfate Supernatant	23,628	99
1st Ammonium Sulfate Pellet	296	---
2nd Ammonium Sulfate Supernatant	14,011	59
2nd Ammonium Sulfate Pellet	2049	---
pH 4.3 Supernatant	283	---
pH 4.3 Pellet	5761	24
Sephacryl HR-200S	12,984	55

TABLE 2

ASSAY OF SEPHACRYL HR200-S COLUMN

Fraction Number	A_{280}	mg/ml	Total Protein (mg)	Units	Spec. Act. (units/mg
22	0.3452	0.69	1.04	260	251
23	0.4104	0.82	1.23	303	246
24	0.5296	1.06	1.59	458	288
25	0.7308	1.46	2.19	737	336
26	1.0332	2.07	3.10	1123	362
27	1.2628	2.53	3.79	1812	478
28	1.3633	2.73	4.09	2166	529
29	1.2906	2.58	3.87	1952	504
30	1.0431	2.09	3.13	1606	513
31	0.7973	1.60	2.39	1247	521
32	0.5421	1.08	1.63	708	435
33	0.3162	0.63	0.95	348	367
34	0.2301	0.46	0.69	164	238
35	0.1635	0.33	0.49	100	204
Total	---	---	30.18	12,984	430

TABLE 3

KINETIC DATA FOR NORMAL AND DEUTERATED PGK

Constant	Normal PGK	Deuterated PGK
K_m^{MgATP}, μM	409 ± 30	162 ± 20
K_m^{PGA}, μM (high affinity)	152 ± 22	168 ± 25
K_m^{PGA}, mM (low affinity)	0.604 ± 0.11	1.27 ± 0.45
K_m^{PGA}, μM (+10 mM Na_2SO_4)	---	385 ± 47
K_m^{dATP} (μM) (high affinity)	522 ± 365	---
K_m^{dATP} (mM) (low affinity)	3.54 ± 0.55	---
V_{max} (ATP) (μmol/min.mg)	623 ± 16	373 ± 60
V_{max} (PGA) (μmol/min.mg)	588 ± 29	371 ± 59
V_{max}, μmol/min.mg (+10 mM Na_2SO_4)	---	199.4 ± 9.9
V_{max} (dATP) (μmol/min.mg)	303 ± 41	---
$K_i^{D\text{-Glycerol-3-P}}$, μM	248.9 ± 31	---

TABLE 4

BINDING DATA FOR NORMAL AND DEUTERATED PGK

Constant	Normal PGK	Deuterated PGK
ϵ_b (Titration)	7.31 ± 2.5	2.91 ± 0.20
ϵ_b (Curve fit)	7.45 ± 2.3	2.98 ± 0.13
n (Mn^{2+})	1.11 ± 0.34	0.923 ± 0.24
ϵ_T (Titration)	13.38 ± 3.6	---
ϵ_T (Curve fit)	13.10 ± 0.2	11.4 ±0.50
K_D^{Mn2+} (μM) (Scatchard Plot)	1160 ± 38	160.3 ± 24
K_D^{Mn2+} (μM) (Curve fit)	500 ± 100	300 ± 13.2
K_S (μM)	117 ± 80	97.8 ± 4.3
K_2 (μM)	273.3 ± 30	279.4 ± 17.6
K_A' (μM)	45 ± 15	40 ± 1.8

VITA

Celeste Geron Shibata was born in Birmingham, Alabama, on August 2, 1952. She grew up in Birmingham and in Decatur, Alabama, where she attended Decatur High School until 1969. She enrolled at Birmingham Southern College in Birmingham, Alabama in 1969. She was elected to Phi Beta Kappa in December, 1972, and received a Bachelor of Arts degree, *magna cum laude,* in English in May, 1973. She then enrolled as a graduate student at Vanderbilt University during 1973-1974. She taught high school English and French for nine years thereafter in Birmingham, Montgomery, and Athens, Alabama, and in Brookfield, Wisconsin. In 1981 she received a Master of Arts degree in English from Vanderbilt University in Nashville, Tennessee. In 1985 she began taking classes in science and mathematics at the University of Alabama in Huntsville. In 1989 she enrolled as a full-time graduate student at the University of Tennessee, Knoxville, and was awarded a Master of Science degree in Biochemistry in December, 1992.